

**DIVERSIFICATION OF 4-ALKYL PYRIDINES:
MINING FOR REACTIVITY WITH ALKYLIDENE DIHYDROPYRIDINES**

BRIAN DOAN

A THESIS SUBMITTED TO THE FACULTY OF GRADUATE STUDIES
IN PARTIAL FULFILLMENT OF THE REQUIREMENTS
FOR THE DEGREE OF MASTER OF SCIENCE

GRADUATE PROGRAM IN CHEMISTRY
YORK UNIVERSITY
TORONTO, ONTARIO

JULY 2022

© BRIAN DOAN, 2022

Abstract

Pyridines are valued structures in pharmaceutical development. Using a soft enolization approach, we can diversify alkyl pyridines under mild conditions via alkylidene dihydropyridines (ADHPs). Recent work in our group has demonstrated the utility of ADHPs in palladium-catalyzed reactions. However, the fundamental reactivity of ADHPs remains largely unexplored, with only scattered reports in the literature. We seek to further explore the reactivity of these electron-rich intermediates in different contexts, as new transformations can provide useful synthetic tools for pharmaceutical discovery. Herein we describe our investigations in this area, including the development of two new synthetic methods. Specifically, we describe the oxidation of ADHPs to the corresponding pyridylic ketones under mild conditions, and the iridium-catalyzed asymmetric alkylation of alkylidene dihydropyridines branch-allylated alkyl pyridines.

Acknowledgements

For my mother, father, sister, and partner Sandra. My success and opportunities in life are built on your love and support. Thank you for everything, always.

My supervisor Art, thank you for your guidance and support over these last few years. You have been a leader during these difficult times, and I thank you for all that you have taught me in my professional career so-far.

My friends and mentors Nour and Ashik have been an integral part of my development as a chemist, scientist, and professional. I am thankful for having the opportunity to learn from you both.

Past and current members of the Orellana group, thank you for your support, chemistry discussions, and friendship. Especially Faizan, Anmol and Samira, your friendship and support through difficult times I will always remember.

Special thanks to Dr. Arturo Orellana, Dr. Christopher Caputo, and Dr. Gino Lavoie for their support in the next stage of my career.

Dr. Howard Hunter for his assistance with NMR experiments and trouble shooting. Thank you for always providing your time and expertise.

I would like to thank the members of my thesis committee, Dr. Christopher Caputo, Dr. Christine Le, and Dr. William van Wijngaarden.

York University Dalton Pharma/Douglas Butler, and Natural Sciences and Engineering Research Council (NSERC) Canada are thanked for funding over the course of my graduate research.

TABLE OF CONTENTS

ABSTRACT.....	II
ACKNOWLEDGEMENTS.....	III
TABLE OF CONTENTS.....	IV
LIST OF SCHEMES.....	VI
LIST OF TABLES.....	VIII
LIST OF FIGURES.....	IX
LIST OF SYMBOLS AND ABBREVIATIONS.....	X
CHAPTER I: INTRODUCTION.....	1
1.1 IMPORTANCE OF PYRIDINES IN PHARMACEUTICALS.....	1
1.2 DIVERSIFICATION OF 4-ALKYL PYRIDINES VIA ALKYLIDENE DIHYDROPYRIDINES.....	2
1.3 MINING FOR REACTIVITY WITH ALKYLIDENE DIHYDROPYRIDINES.....	3
CHAPTER II: I DEVELOPMENT OF THE SUSTAINABLE SYNTHESIS OF 4-ACETYL PYRIDINES.....	4
2.1 OXIDATION OF ALKYLIDENE DIHYDROPYRIDINES TO PYRIDYLIC KETONES.....	4
2.2 MILD OXIDATION OF 4-BENZYL PYRIDINE ADHP TO 4-BENZOYL PYRIDINE.....	8
2.3 ADHP OXIDATION IS SELECTIVE FOR THE 4-PYRIDYLIC POSITION.....	9
2.4 REACTION OPTIMIZATION.....	11
2.4.1 IDENTIFICATION OF BY-PRODUCTS.....	11
2.4.2 SCREENING ADDITIVES.....	12
2.4.3 SCREENING SOLVENTS.....	14
2.4.4 SCREENING TEMPERATURE.....	15
2.4.5 INVESTIGATING 1-POT OXIDATION CONDITIONS.....	16
2.4.6 SCREENING RATES OF ETHYL CHLOROFORMATE ADDITION.....	17
2.5 CONCLUSIONS AND FUTURE WORK.....	18
CHAPTER III: DEVELOPMENT OF THE IRIIDIUM-CATALYZED ALKYLATION OF 4-METHYL PYRIDINES.....	19
3.1 IRIIDIUM-CATALYZED ASYMMETRIC-ALKYLATION.....	19
3.2 IRIIDIUM-CATALYZED ALLYLATION OF ALKYLIDENE DIHYDROPYRIDINES.....	21
3.3 PROOF OF CONCEPT.....	23
3.4 REACTION OPTIMIZATION.....	26
3.5 METHOD REPRODUCIBILITY.....	27
3.6 EFFECT OF BORON TRIFLUORIDE ETHERATE.....	28
3.7 ALTERNATIVE ADHP ALLYLATION STRATEGIES.....	28
3.8 CONCLUSIONS AND FUTURE WORK.....	31
4.0 EXPERIMENTAL.....	32
4.1.1 CHAPTER 2 EXPERIMENTAL.....	32
4.1.2 CHAPTER 2 GENERAL PROCEDURES.....	33

4.1.3 PYRIDYLIC KETONES (2-2, 2-4, 2-15).....	35
4.1.4 BY-PRODUCT SYNTHESIS (2-11, 2-12, 2-13).....	39
4.2.1 CHAPTER 3 EXPERIMENTAL	46
4.2.2 STARTING MATERIAL SYNTHESIS (S1, 3-1, 3-2, 3-3).....	47
4.2.3 IRIDIUM-CATALYZED ALLYLATION OF ADHPS GENERAL PROCEDURE.....	60
4.2.4 OPTIMIZATION EXPERIMENTS HPLC TRACE.....	65
REFERENCES	72

List of Schemes

SCHEME 1.1 PREPARATION OF ALKYLIDENE DIHYDROPYRIDINES FROM 4-ALKYL PYRIDINES.	2
SCHEME 1.2 PALLADIUM-CATALYZED A) ALLYLATION OF 4-ALKYL PYRIDINES, AND B) DEHYDROGENATION OF 4-ALKYL PYRIDINES VIA ADHPs.	2
SCHEME 1.3 PYRIDYLIC AND HOMOPYRIDYLIC STEREOGENIC CENTERS FOUND IN ALKYL PYRIDINE PHARMACEUTICALS.	3
SCHEME 1.4 A) OXIDATION OF ADHPs TO 4-ACETYL PYRIDINES B) IRIIDIUM-CATALYZED ALLYLATION OF ADHPs.	3
SCHEME 2.1 A) ADHP OXIDATION REPORTED BY PIGGE. B) OUR OBSERVED ADHP OXIDATION.	4
SCHEME 2.2 NICOLAOU'S OXIDATION OF ALKYL PYRIDINES WITH IBX.	4
SCHEME 2.3 MAES'S DIRECT, CATALYTIC OXIDATION OF BENZYL PYRIDINES.	5
SCHEME 2.4 MAES'S IRON-CATALYZED CHEMOSELECTIVE OXIDATION OF THE METHYLENE HETEROARENE POSITION.	5
SCHEME 2.5 COPPER CATALYZED OXIDATION OF ALKYL-PYRIDINES MECHANISM BY MAES.	6
SCHEME 2.6 ZHUO AND LEI'S ETHYL CHLOROACETATE PROMOTED, COPPER-CATALYZED OXIDATION OF ALKYL PYRIDINES.	6
SCHEME 2.7 VAN HUMBECK'S DUAL-CATALYTIC SITE-SELECTIVE OXIDATION OF BENZYLIC AND PYRIDYLIC POSITIONS.	7
SCHEME 2.8 WU & CO-WORKERS TRANSITION METAL FREE HETEROBENZYLIC OXIDATION.	7
SCHEME 2.9 PROPOSED OXIDATION MECHANISM BY WU & CO-WORKERS.	7
SCHEME 2.10 OXIDATION OF 4-BENZYL PYRIDINE TO 4-BENZOYL PYRIDINE.	8
SCHEME 2.11 PROPOSED MECHANISM OF ADHP AUTO-OXIDATION TO 4-BENZOYL PYRIDINE.	9
SCHEME 2.12 REGIOSELECTIVE PYRIDYLIC OXIDATION OF 5,6,7,8-TETRAHYDROISOQUINOLINE ADHP.	9
SCHEME 2.13 CHEMOSELECTIVE OXIDATION OF ADHP IN THE PRESENCE OF DIPHENYL METHYLENE.	9
SCHEME 2.14 UNSUCCESSFUL 2-PYRIDYLIC OXIDATION OF 5,6,7,8-TETRAHYDROQUINOLINE, AND 2- BENZYL PYRIDINE.	10
SCHEME 2.15 UNSUCCESSFUL OXIDATION OF ADHP BEARING AN ADJACENT BENZYLIC POSITION. ..	11
SCHEME 2.16 PROPOSED BY-PRODUCT FORMATION MECHANISM.	11
SCHEME 2.17 SYNTHESIS OF PYRIDYLIC ALCOHOL 2-11 AND CARBONATE 2-12.	11
SCHEME 2.18 SYNTHESIS OF PYRIDONE 2-13.	11
SCHEME 2.19 PROPOSED MECHANISM FOR THE FORMATION OF 2-13.	12
SCHEME 2.20 PROPOSED MECHANISM FOR THE FORMATION OF 2-11 AND 2-12.	12
SCHEME 2.21 1-POT OXIDATION OF 4-ALKYL PYRIDINES TO 4-ACETYL PYRIDINES.	18

SCHEME 3.1 A) FIRST REPORTED IR-CATALYZED ALLYLIC ALKYLATION BY KASHIO AND TAKEUCHI. B) MECHANISM DETERMINED BY HELMCHEN.....	19
SCHEME 3.2 FIRST ENANTIOSELECTIVE IRIIDIUM-CATALYZED ALLYLATION BY HELMCHEN AND JANSEN.	20
SCHEME 3.3 HARTWIG'S SYNTHESIS OF FERINGA LIGAND BASED IRIDACYCLIC COMPLEX.	20
SCHEME 3.4 CARREIRA'S IRIIDIUM-CATALYZED SYNTHESIS OF PRIMARY ALLYLIC AMINES.....	20
SCHEME 3.5 SURVEY OF NUCLEOPHILES APPLIED IN CARREIRA'S IRIIDIUM-CATALYZED ASYMMETRIC ALKYLATION.....	20
SCHEME 3.6 PROPOSED MECHANISM OF CARREIRA'S IR-CATALYZED ASYMMETRIC ALLYLATION METHOD.	21
SCHEME 3.7 ADHP ADDITION TO CATIONIC ALLYL-PALLADIUM.	22
SCHEME 3.8 ADHP AS SOFT NUCLEOPHILES.	22
SCHEME 3.9 ADHPs AS NUCLEOPHILES IN CARREIRA'S IRIIDIUM-CATALYZED ALLYLATION PROTOCOL.	22
SCHEME 3.10 SYNTHESIS OF ADHP 3-1 AND BRANCHED ALLYL PARTNERS 3-2, 3-3.	23
SCHEME 3.11 PROPOSED MECHANISM FOR THE IRIIDIUM-CATALYZED ALLYLATION OF ADHPs.	25
SCHEME 3.12 A) BEST OPTIMIZATION CONDITIONS B) BEST REPRODUCED RESULTS.	27
SCHEME 3.13 UNSUCCESSFUL ALLYLATION OF 3-6.	29
SCHEME 3.14 UNSUCCESSFUL SYNTHESIS OF ADHP 3-7.	30
SCHEME 3.15 IRIIDIUM-CATALYZED ENANTIOSELECTIVE ALLYLATION OF 4-ALKYL PYRIDINES VIA ADHPs.....	31

List of Tables

TABLE 2.1. EFFECT OF ADDITIVES ON ADHP OXIDATION. CND = COULD NOT DETERMINE. QUANTITATIVE NMR YIELDS.....	13
TABLE 2.2. EFFECT OF SOLVENT AND REACTION CONCENTRATION ON ADHP OXIDATION. QUANTITATIVE NMR YIELDS.....	14
TABLE 2.3. EFFECT OF TEMPERATURE ON ADHP OXIDATION.....	15
TABLE 2.4. SCREENING 1-POT 4-ALKYL PYRIDINE OXIDATION CONDITIONS. QUANTITATIVE NMR YIELDS.	16
TABLE 2.5 EFFECT OF CHLOROFORMATE ADDITION RATE ON 1-POT 4-ALKYL PYRIDINE OXIDATION. QUANTITATIVE NMR YIELDS.....	17
TABLE 3.1 PROOF OF CONCEPT REACTIONS SUMMARY.....	24
TABLE 3.2 SUMMARY OF OPTIMIZATION EXPERIMENTS.	26
TABLE 3.3 IMPACT OF $\text{BF}_3 \cdot \text{OEt}_2$ QUALITY ON PRODUCT YIELD.	28
TABLE 3.4 EFFECT OF $\text{BF}_3 \cdot \text{OEt}_2$ ON PRODUCT YIELD.	28
TABLE 3.5 IRIIDIUM-CATALYZED ALLYLATION OF ALLYL-ADHPs, PROOF OF CONCEPT.....	29

List of Figures

FIGURE 1.1 FREQUENCY OF PYRIDINES IN U.S. FDA APPROVED SMALL-MOLECULE DRUGS.	1
---	---

List of Symbols and Abbreviations

α	1,2 relative positions
β	1,3 relative positions
Ac	Acetyl
ACS	American Chemical Society
ADHP	Alkylidene Dihydropyridine
API	Active Pharmaceutical Ingredient
Ar	Aromatic Group
b	Branched
cod	1,5 Cyclooctadiene
DCM	Dichloromethane
δ	Chemical shift
DFT	Density Functional Theory
DMA	<i>N,N</i> -dimethyl acetylide
DMF	<i>N,N</i> -dimethyl formamide
DMP	Dess-Martin Periodinane
DMSO	Dimethyl sulfoxide
ee	Enantiomeric excess
EPR	Electronic paramagnetic resonance
Equiv.	Equivalents
Et	Ethyl
FG	Functional Group
GC-MS	Gas chromatography-mass spectrometry
HPLC	High performance-liquid chromatography
Hz	Hertz (s^{-1})
i-Pr	Isopropyl
IBX	2-Iodoxybenzoic acid
<i>in situ</i>	In the reaction mixture
<i>in vacuo</i>	Under vacuum
Ir	Iridium
<i>J</i>	Coupling constant

Ln	Ligands
Me	Methyl
MeCN	Acetonitrile
<i>n</i> -BuLi	Butyl lithium
NMP	N-Methyl-2-pyrrolidone
NMR	Nuclear magnetic resonance
O/N	Overnight
<i>p</i>	<i>Para</i>
Pd	Palladium
Ph	Phenyl
ppm	Parts per million
r.t.	Room temperature
RDS	Rate determining step
SET	Single electron transfer
TLC	Thin layer-chromatography

CHAPTER I: Introduction

1.1 Importance of Pyridines in Pharmaceuticals

In 2014, Vitaku conducted a structural analysis of small-molecule drugs approved by the U.S. Food and Drug Administration (FDA) and found that nitrogen-heterocycles were the most frequent structural motif, appearing in 60% of all small-molecule drugs (figure 1.1).^[1] Of these heterocycles, pyridine was found to be the most frequent six-membered aromatic nitrogen heterocycle. Because of their prevalence in pharmaceuticals, research in our group has focused on developing synthetic methods towards alkyl-pyridines. With their ubiquity in pharmaceutically active ingredients, natural products, and agrochemicals, synthetic diversification of alkyl-pyridines would provide immense value to the pharmaceutical industry.^[2]

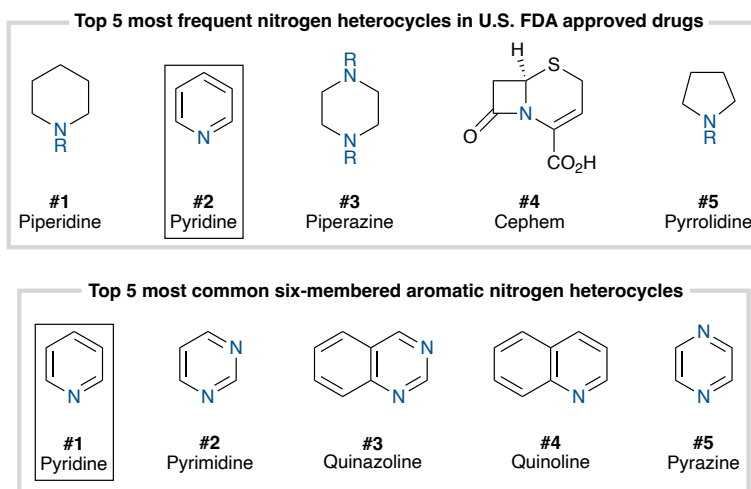
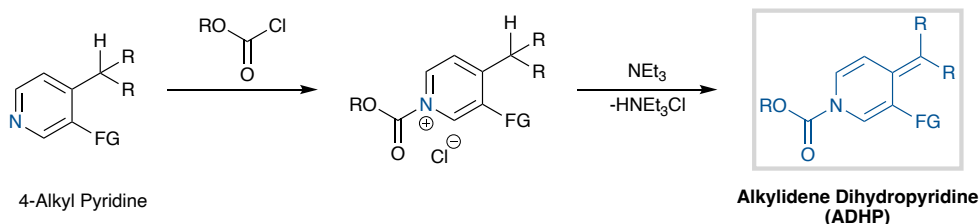


Figure 1.1 Frequency of pyridines in U.S. FDA approved small-molecule drugs.

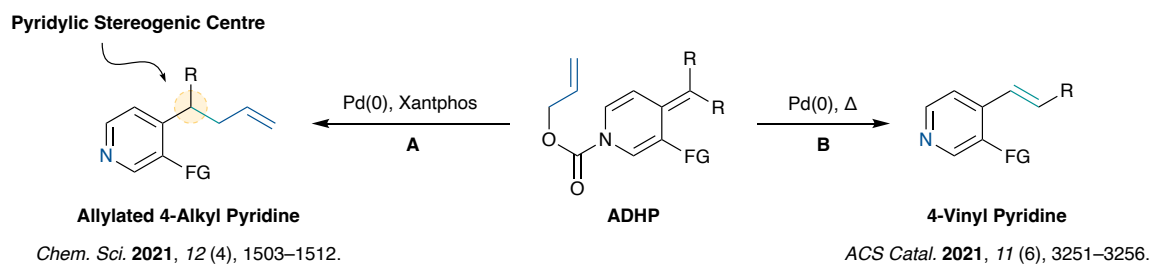
1.2 Diversification of 4-Alkyl Pyridines via Alkylidene Dihydropyridines

An underutilized approach to alkyl pyridine diversification utilizes alkylidene dihydropyridines (ADHP) intermediates. ADHPs are de-aromatized 4-alkyl pyridines, prepared through a *soft enolization* approach (scheme 1.1).^[3] Activation of the pyridine by nucleophilic acyl substitution to a chloroformate acidifies the pyridylic protons, allowing for deprotonation by a mild amine base to form the semi-stable ADHP. To our knowledge, use of ADHPs in synthetic transformations has been scarcely reported, and their fundamental reactivity has not been studied or exploited.^[4–6]

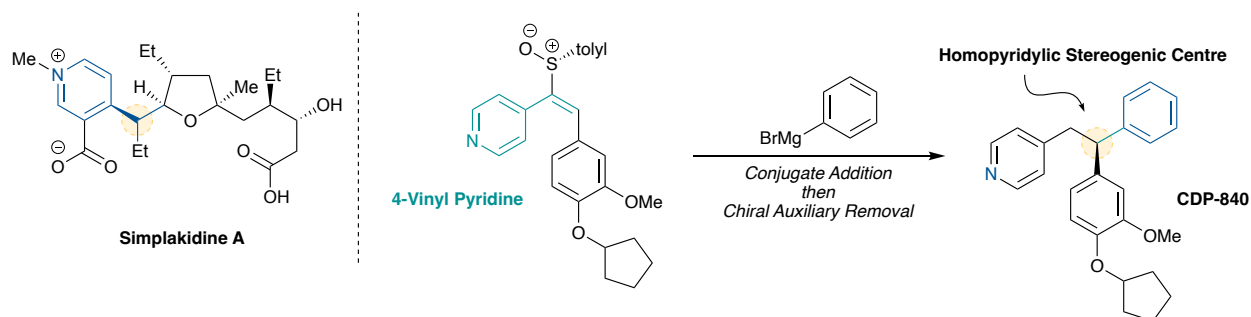


Scheme 1.1 Preparation of alkylidene dihydropyridines from 4-alkyl pyridines.

Recently, we have developed a decarboxylative allylation approach toward diverse 4-alkyl pyridines via ADHPs (scheme 1.2).^[7–9] ADHPs prepared from allyl chloroformate and 4-alkyl pyridines can undergo palladium-catalyzed decarboxylative allylation, forming 4-allylated alkyl pyridines bearing a new stereogenic at the pyridylic position (scheme 1.2, **A**). In particular, 4-alkyl pyridines with stereogenic centres at the pyridylic or homopyridylic positions are privileged motifs in medicinal chemistry (scheme 1.3).^[10,11] Alternatively, these ADHPs can form 4-vinyl pyridines (scheme 1.2, **B**), well-regarded intermediates towards diverse alkyl pyridine scaffolds (scheme 1.3).



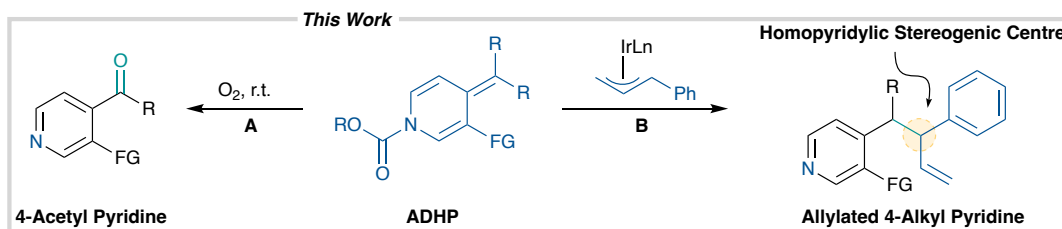
Scheme 1.2 Palladium-catalyzed A) allylation of 4-alkyl pyridines, and B) dehydrogenation of 4-alkyl pyridines via ADHPs.



Scheme 1.3 Pyridylic and homopyridylic stereogenic centers found in alkyl pyridine pharmaceuticals.

1.3 Mining for Reactivity with Alkylidene Dihydropyridines.

Over the course of our investigation of ADHPs as synthetic intermediates, we observed their decomposition under aerobic conditions to 4-acyl pyridines (scheme 1.4, **A**). Acyl pyridines (pyridylic ketones) are versatile functional groups that can be transformed into a diverse array of intermediates and are key compounds in pharmaceutical development.^[12,13] Strikingly, the auto-oxidation of ADHPs proceeds under exceptionally mild conditions. In contrast to existing methods, the auto-oxidation of ADHPs is exclusive for 4-alkyl pyridines. In **chapter 2**, we report the development of the selective oxidation of 4-alkyl pyridines to 4-pyridylic ketones via ADHPs.



Scheme 1.4 A) Oxidation of ADHPs to 4-acetyl pyridines B) Iridium-catalyzed allylation of ADHPs.

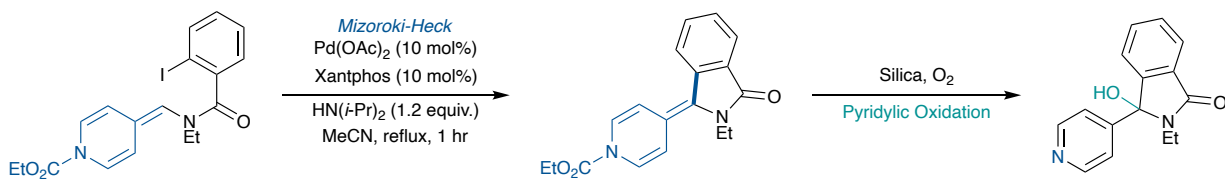
Shown previously, we established pyridylic stereogenic centres can be accessed via palladium-catalysis (scheme 1.2, **A**). Currently, our group is investigating ADHPs as in enantioselective allylations to access homopyridylic stereogenic centers. This can be accomplished using ADHPs and branched allylic electrophiles under iridium-catalysis (scheme 1.4, **B**).^[14] In **chapter 3**, we investigate the application of ADHPs in direct iridium-catalyzed asymmetric alkylations to form branch allylated 4-alkyl pyridines.

CHAPTER II: I Development of the Sustainable Synthesis of 4-Acetyl Pyridines

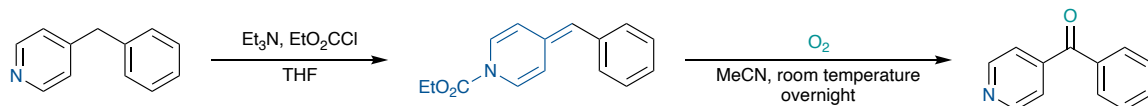
2.1 Oxidation of Alkylidene Dihydropyridines to Pyridylic Ketones

In 2016, Pigge reported alkylidene dihydropyridines as substrates in Mizoroki—Heck cyclization (scheme 2.1, A).^[4] During column chromatography purification of the cyclized alkylidene dihydropyridine, they observed oxidation at the pyridylic position. In our investigation of ADHPs as mild synthetic intermediates, we observed the facile oxidation of monosubstituted ADHPs to 4-pyridylic ketones under aerobic conditions (scheme 2.1, B). Pyridylic ketones are versatile intermediates in the preparation of activate pharmaceutical ingredients (APIs) and natural products.^[13] We believe this mild oxidation of ADHPs to 4-pyridylic ketones could be a sustainable alternative over existing methods that rely on transition metals, additives, and elevated temperatures.^[15]

A) Pigge 2016

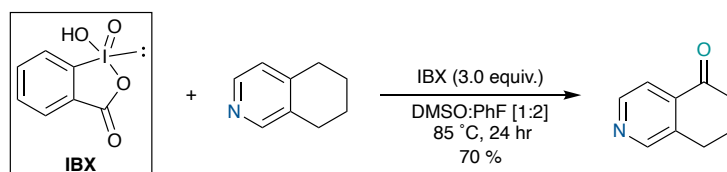


B) Our Observation



Scheme 2.1 A) ADHP oxidation reported by Pigge. B) Our observed ADHP oxidation.

Traditionally, direct oxidation of alkyl pyridines to pyridylic ketones has been accomplished with stoichiometric oxidants and elevated temperatures. In 2002, Nicolaou reported several applications of hypervalent iodine oxidants *o*-iodylbenzoic acid (IBX) and Dess-Martin periodinane (DMP), in the oxidation of benzylic, pyridylic and alpha-carbonyl positions (scheme 2.2).^[16,17]

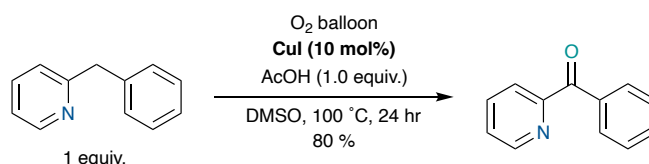


Scheme 2.2 Nicolaou's oxidation of alkyl pyridines with IBX.

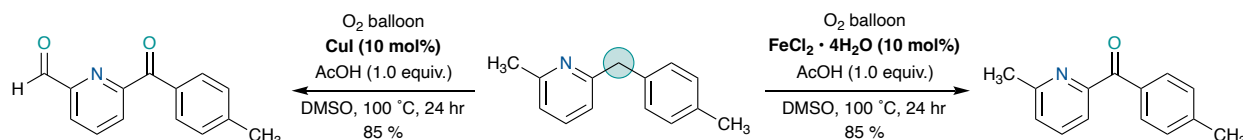
This work highlighted the broad utility of this class of oxidants, however, these oxidations required super-stoichiometric amounts of oxidant, elevated temperatures, and had poor

overall atom economy.^[18] Since this work, pyridylic and benzylic oxidations have been developed with sustainability in mind, specifically, using oxygen as the terminal oxidant, earth abundant transition metal catalysts, and recyclable additives. Over the last decade, a number of methods for pyridylic oxidation have been established,^[15,19–22] however they generally exhibit poor chemoselectivity.

In 2012, Maes reported the aerobic oxidation of 2-benzyl pyridine to 2-benzoyl pyridine with catalytic copper and acetic acid (scheme 2.3).^[23] In their investigations into chemoselectivity, they found different levels of site-selectivity were achieved when using copper or iron transition metal catalysts (scheme 2.4).

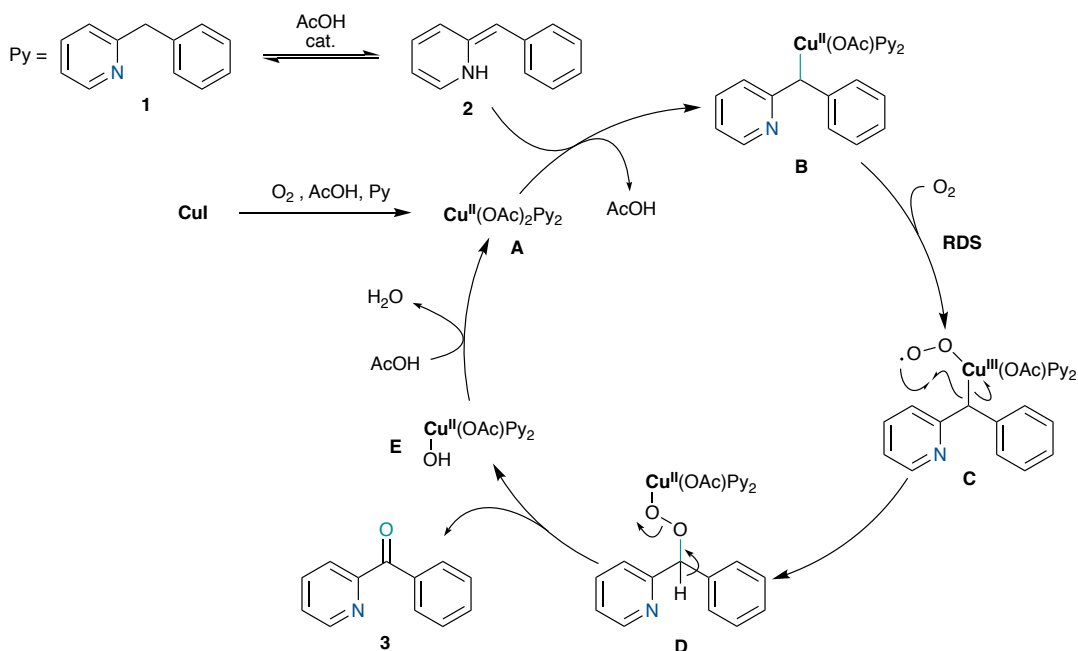


Scheme 2.3 Maes's direct, catalytic oxidation of benzyl pyridines.



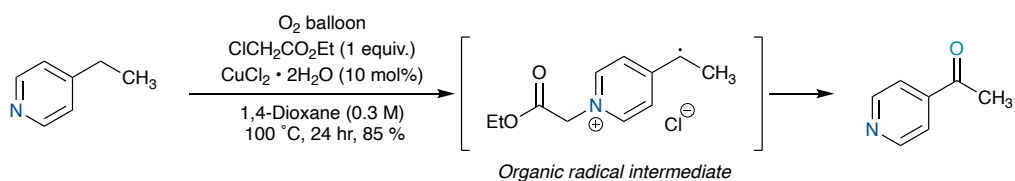
Scheme 2.4 Maes's iron-catalyzed chemoselective oxidation of the methylene heteroarene position.

In 2016, mechanistic studies conducted by Maes uncovered the role of copper and oxygen (scheme 2.5).^[24] The active copper catalyst **A** is formed from copper iodide by oxygen oxidation, ligation by 2-benzyl pyridine **1** and acetic acid. Catalyst **A** is intercepted by the enamine pyridine tautomer **2**, forming pyridylic copper complex **B**. Oxidation of complex **B** with molecular oxygen is proposed to be the rate determining step, forming the short-lived copper (III) complex **C**, which rearranges to the organic copper (II) peroxide **D**. Heterolytic cleavage of the pyridylic protons form 2-benzoyl pyridine **3**, and copper (II) hydroxide **E**.



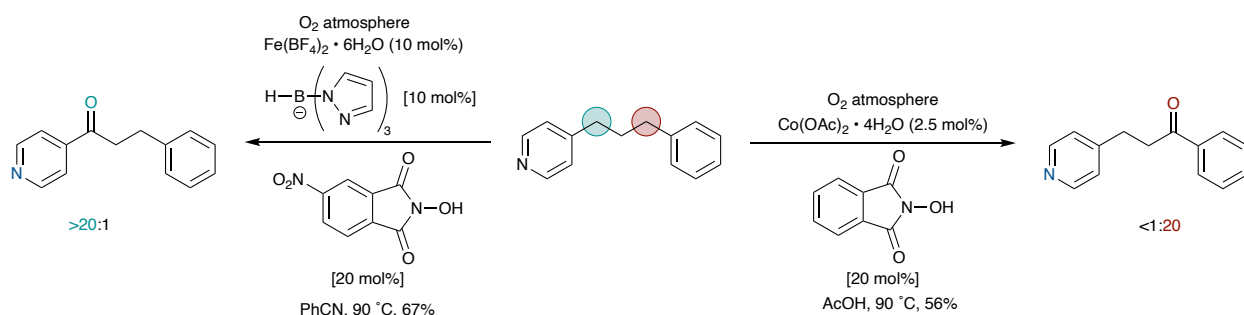
Scheme 2.5 Copper catalyzed oxidation of alkyl-pyridines mechanism by Maes.

A broader oxidation substrate scope was reported by Zhuo and Lei in 2015, demonstrating selective oxidation of heterobenzylic methylenes and alkanes by α -chloroacetate promoted copper catalysis (scheme 2.6).^[25] Density functional theory (DFT) calculations suggested stronger activation of the pyridylic position is achieved with α -chloroacetate compared to acetic acid. Based on gas chromatography-mass spectrometry (GC-MS) and electron paramagnetic resonance (EPR) experiments, the authors proposed the oxidation proceeds through an organic radical intermediate.



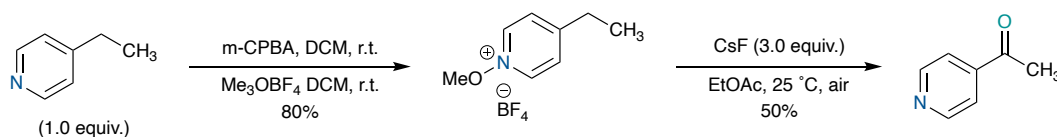
Scheme 2.6 Zhuo and Lei's ethyl chloroacetate promoted, copper-catalyzed oxidation of alkyl pyridines.

Although sustainable transition metals and oxidants are used in both Maes, Zhuo, and Lei's reports, they also require stoichiometric activating agents. In 2018, Van Humbeck reported the dual-catalytic, site-selective oxidation of benzylic and pyridylic azaheterocycles without stoichiometric activating agents (scheme 2.7).^[26] Depending on the desired site of oxidation, a suitable catalyst system can achieve benzylic or pyridylic oxidation with excellent chemoselectivity.



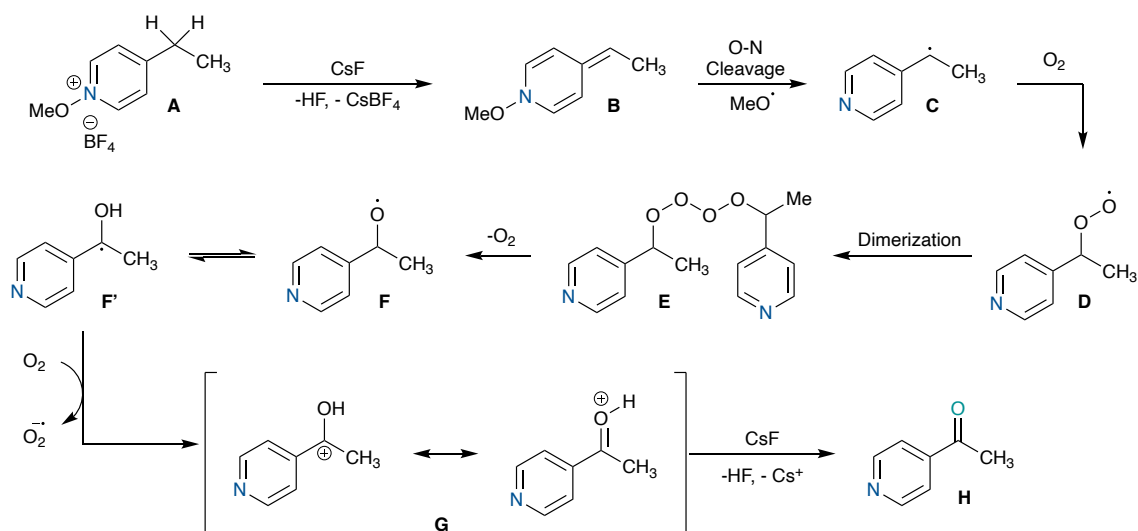
Scheme 2.7 Van Humbeck's dual-catalytic site-selective oxidation of benzylic and pyridylic positions.

In 2019, Wu & co-workers reported the transition metal-free oxidation of heterobenzylic C-H bonds (scheme 2.8).^[27]



Scheme 2.8 Wu & co-workers transition metal free heterobenzylic oxidation.

This exceptionally mild oxidation conducted under ambient atmosphere is believed to proceed through a pyridylic radical **C**, generated by O-N homolytic cleavage of ADHP **B** (scheme 2.9, **A** to **C**). Following a heterobenzylic oxidation pathway proposed by Ingold, Carlo and Jiao,^[28–30] radical **C** combines with molecular oxygen to form **D**, dimerizing and fragmenting to the pyridylic hydroxy radical **F**. Solvent assisted equilibration of **F** to **F'** and single electron oxidation by molecular oxygen forms oxocarbenium **G**.

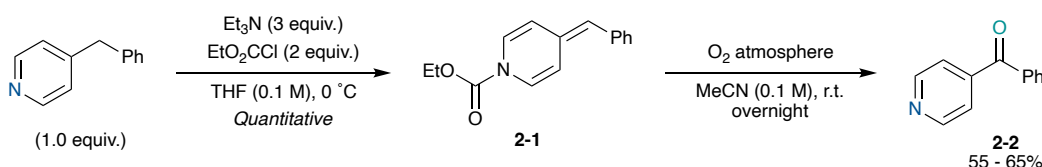


Scheme 2.9 Proposed oxidation mechanism by Wu & co-workers.

Despite the advancements in pyridylic oxidation, there is still room to develop more sustainable methods. Specifically, development towards a metal-free, site-selective, and mild oxidation of alkyl pyridines would provide a sustainable pathway to prepare valuable pharmaceuticals.^[18]

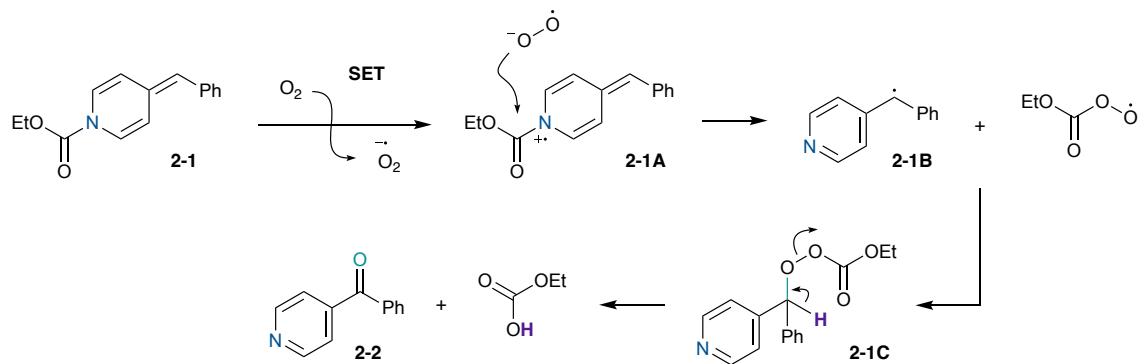
2.2 Mild Oxidation of 4-Benzyl Pyridine ADHP to 4-Benzoyl Pyridine

In a solution of acetonitrile under oxygen atmosphere, the ADHP **2-1** prepared from 4-benzyl pyridine, oxidized to 4-benzoyl pyridine (scheme **2.10**). After concentration of the reaction mixture, ¹H-NMR analysis showed crude 4-benzoyl pyridine **2-2** as the major product. Using oxygen and room temperature conditions, this ADHP oxidation to 4-benzoyl pyridine is exceptionally mild in comparison to existing methods.^[19,22]



Scheme 2.10 Oxidation of 4-benzyl pyridine to 4-benzoyl pyridine.

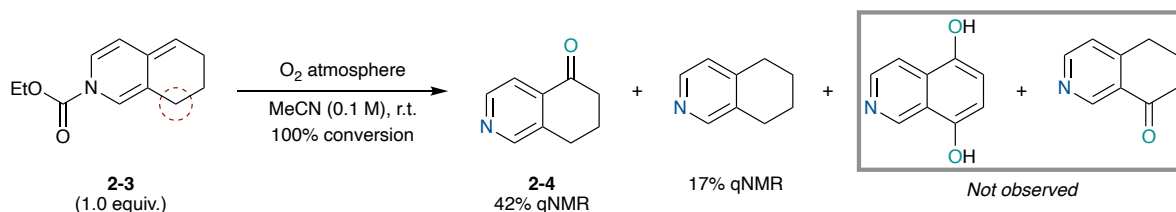
The free-base 4-benzoyl pyridine obtained without additional workup is speculated to form by the following mechanism (scheme **2.11**). Single electron-transfer (SET) oxidation of ADHP **2-1** gives radical cation **2-1A**. Superoxide displaces the acyl pyridinium, forming the heterobenzylic radical **2-1B**, which could oxidize to ketone **2-2** following the mechanism proposed by Wu (scheme **2.9**).^[28–30] Alternatively, radical **2-1B** combines with the ethoxy carbonyl peroxide radical, forming peroxide **2-1C**. Following a similar mechanistic step proposed by Maes (scheme **2.5, D to 3**),^[24] heterolytic deprotonation of peroxide **2-1C** forms 4-benzoyl pyridine **2-2** and ethyl carbonic acid.



Scheme 2.11 Proposed mechanism of ADHP auto-oxidation to 4-benzoyl pyridine.

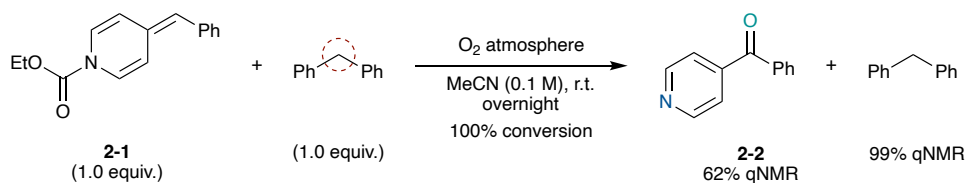
2.3 ADHP Oxidation is Selective for the 4-Pyridylic Position

To expand the utility of this reaction, we investigated the chemoselectivity of the ADHP oxidation by adding additives or using substrates with competing oxidation sites. To demonstrate pyridylic chemoselectivity, we prepared the ADHP **2-3** from 5,6,7,8-tetrahydroisoquinoline for oxidation (scheme **2.12**). The reaction gave oxidation exclusively at the 4-pyridylic position (**2-4**). This is in contrast to existing methods, which are not selective when competing pyridylic and benzylic positions are present.^[15]



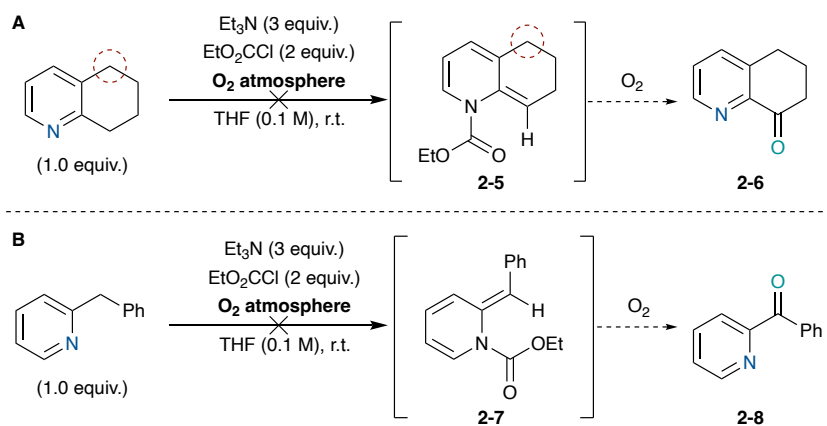
Scheme 2.12 Regioselective pyridylic oxidation of 5,6,7,8-tetrahydroisoquinoline ADHP.

We investigated benzylic chemoselectivity by introducing diphenyl methylene into a solution of 4-benzyl pyridine ADHP **2-1** prior to oxidation (scheme **2.13**). After the reaction was complete, quantitative ¹H-NMR analysis gave diphenyl methylene in 99%.



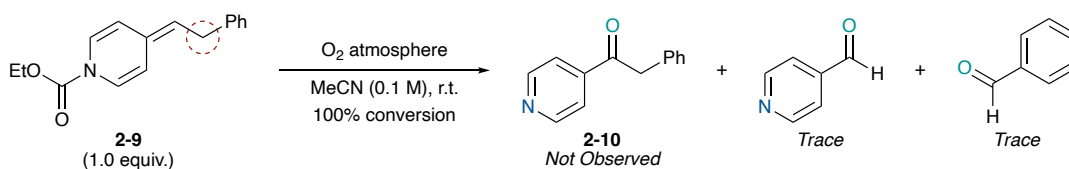
Scheme 2.13 Chemoselective oxidation of ADHP in the presence of diphenyl methylene.

In our previous work, we established that 2-alkyl pyridines could not form the corresponding ADHP due to the steric clash between the 2-alkyl substituent and the alkoxy carbonyl.^[7,31] To investigate the possibility of 2-pyridylic oxidation in the presence of a 3-pyridylic position, 5,6,7,8-tetrahydroquinoline, excess triethyl amine and ethyl chloroformate was stirred under an oxygen atmosphere (scheme **2.14, A**). If trace amounts of ADHP formed during the reaction, we believed oxidation could occur to give ketone, driving the ADHP equilibrium to completion. However, we did not observe 2-pyridylic ketone or ADHP by ¹H-NMR analysis. A similar result was obtained when 2-benzoyl pyridine was subjected to the same conditions (scheme **2.14, B**). These results suggest the ADHP oxidation cannot be applied to 2-alkyl pyridines.

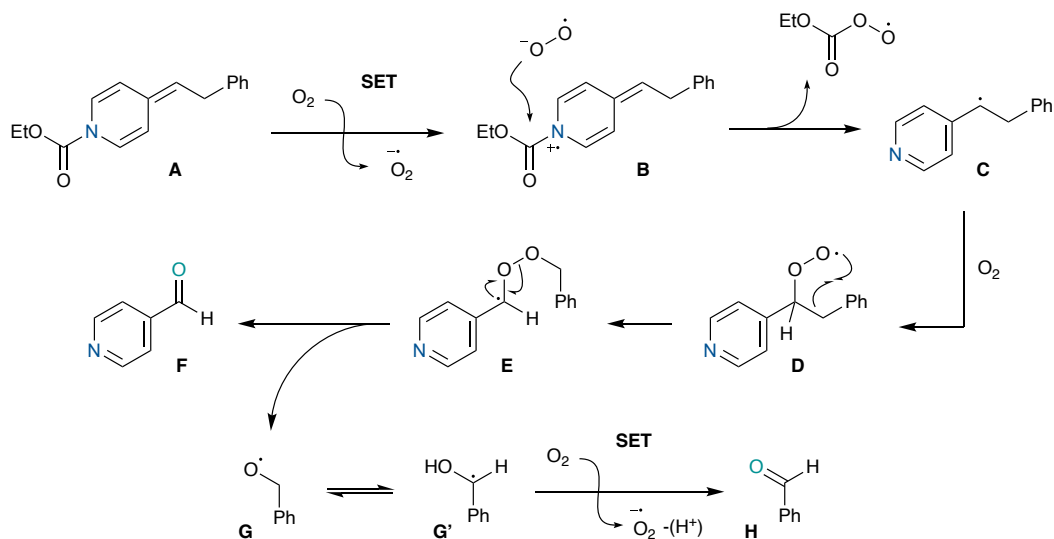


Scheme 2.14 Unsuccessful 2-pyridylic oxidation of 5,6,7,8-tetrahydroquinoline, and 2-benzyl pyridine.

A peculiar result in our chemoselectivity experiments arose from the oxidation of ADHP **2-9** bearing an adjacent benzylic site (scheme **2.15**). We believed selective oxidation of the pyridylic position would occur over the benzylic position. Upon oxidation, we observed complete conversion of the ADHP (consistent mass balance) to unknown decomposition products and trace amounts of aldehyde by-products. However, we did not observe ketone product **2-10**. By-products 4-pyridinecarboxyaldehyde and benzaldehyde could be attributed to internal C-C homolytic cleavage of **D** (scheme **2.16**), forming pyridylic radical peroxide **E**. Homolytic O-O cleavage of **E** forms 4-pyridine carboxaldehyde **F**, and benzyl radical **G'**. Auto-oxidation of **G'** following the mechanism proposed by Ingold provides benzaldehyde **H**.^[29]



Scheme 2.15 Unsuccessful oxidation of ADHP bearing an adjacent benzylic position.

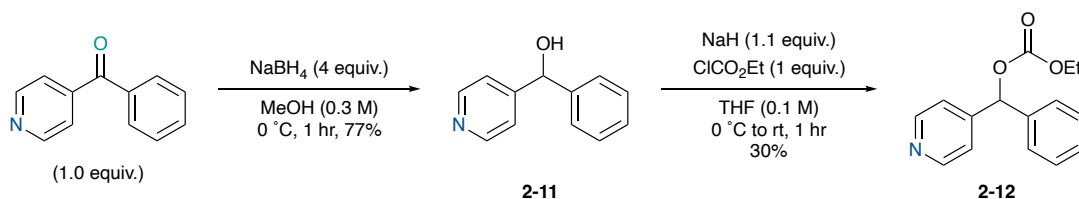


Scheme 2.16 Proposed by-product formation mechanism.

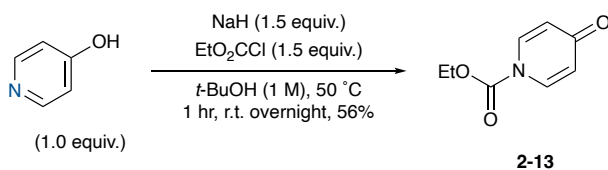
2.4 Reaction Optimization

2.4.1 Identification of By-products

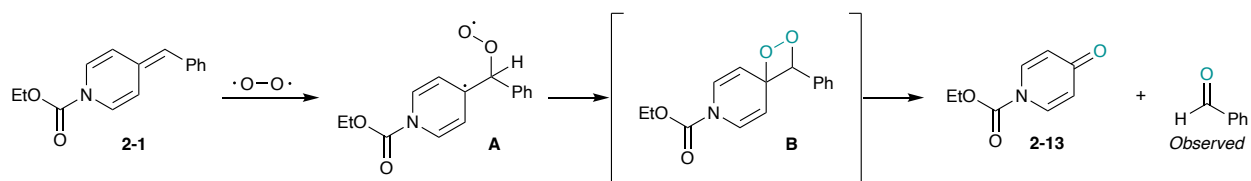
Over the course of our investigation, we synthesized and characterized commonly observed semi-oxidation by-products (scheme 2.17, 2-11, 2-12). Notably, pyridone by-product 2-13 (scheme 2.18) is observed in all oxidations in trace-amounts, potentially formed by intramolecular fragmentation of 2-1 (scheme 2.19).



Scheme 2.17 Synthesis of pyridylic alcohol 2-11 and carbonate 2-12.

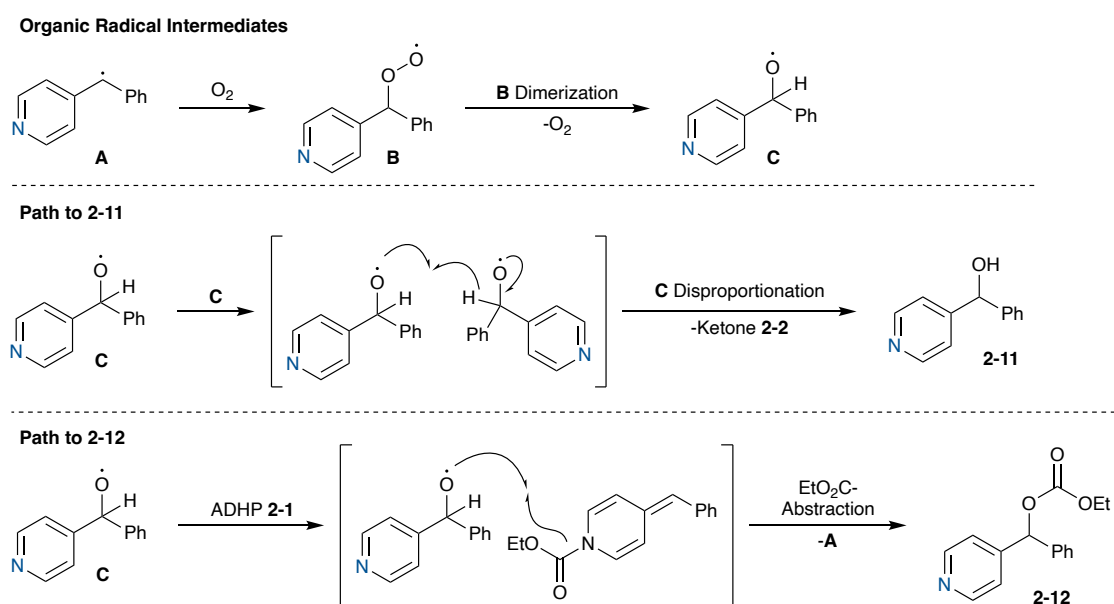


Scheme 2.18 Synthesis of pyridone 2-13.



Scheme 2.19 Proposed mechanism for the formation of 2-13.

Semi-oxidation by-products **2-11** and **2-12** could potentially be formed by intermolecular side-reactions between ADHP **2-1** and organic radical intermediates formed following Wu's proposed mechanism (scheme **2.20**).^[27]

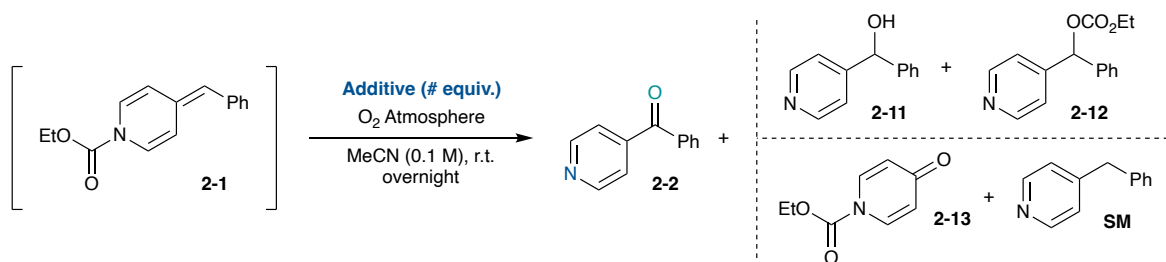


Scheme 2.20 Proposed mechanism for the formation of 2-11 and 2-12.

2.4.2 Screening Additives

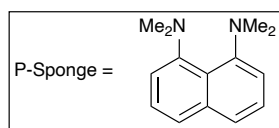
Based on our proposed mechanism (scheme **2.11**), we believed a basic additive would neutralize ethyl carbonic acid formed during the reaction. This transient acid could protonate the ADHP **2-1**, leading to starting material 4-benzyl pyridine **SM**. If this were correct, it is reasonable to expect that stoichiometric base should result in increased yields of ketone by preventing undesired decomposition of the ADHP. Therefore, stoichiometric amounts of additives were investigated (table **2.1**), however none were found to give a meaningful increase in ketone yield **2-2**.

Table 2.1 Effect of additives on ADHP oxidation. Cnd = could not determine. Quantitative NMR yields.



Entry	Additive	Equiv.	2-1 Conv. (%)	2-2 (%)	2-11 (%)	2-12 (%)	2-13 (%)	SM (%)
1	None	-	100	56	9	0	2	<i>cnd</i>
2	Et ₃ N	1	94	58	<i>cnd</i>	<i>cnd</i>	<i>cnd</i>	<i>cnd</i>
3	P-Sponge	1	51	19	0	0	0	<i>cnd</i>
4	K ₂ CO ₃	1	100	55	<i>cnd</i>	<i>cnd</i>	3	<i>cnd</i>
5	K ₂ CO ₃	3	100	60	<i>cnd</i>	<i>cnd</i>	3	<i>cnd</i>
6	K ₂ CO ₃	5	100	57	<i>cnd</i>	<i>cnd</i>	1	<i>cnd</i>
7	K ₂ CO ₃	10	100	61	<i>cnd</i>	<i>cnd</i>	4	<i>cnd</i>
8	Na ₂ CO ₃	1	100	60	<i>cnd</i>	<i>cnd</i>	2	<i>cnd</i>
9	NaHCO ₃	1	100	59	<i>cnd</i>	<i>cnd</i>	2	<i>cnd</i>
10	Na ₂ SO ₄	1	100	58	<i>cnd</i>	<i>cnd</i>	2	<i>cnd</i>
11	MgSO ₄	1	100	59	<i>cnd</i>	<i>cnd</i>	2	<i>cnd</i>
12	CS ₂ CO ₃	1	100	53	3	5	<i>cnd</i>	<i>cnd</i>
13	CS ₂ CO ₃	3	100	54	2	10	<i>cnd</i>	<i>cnd</i>
14	CS ₂ CO ₃	5	93	23	<i>cnd</i>	<i>cnd</i>	<i>cnd</i>	<i>cnd</i>
15	CS ₂ CO ₃	10	86	32	<i>cnd</i>	14	<i>cnd</i>	<i>cnd</i>

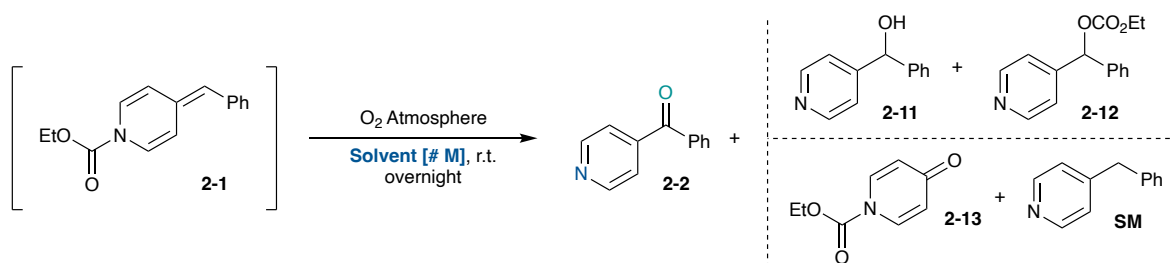
Conditions: **2-1** prepared from 4-benzyl pyridine (50 mg, 0.295 mmol). Percentages based on ¹H-NMR qNMR analysis with *p*-anisaldehyde. *Cnd* = (Could not determine).



2.4.3 Screening Solvents

From qualitative observations in our group, we found that ADHP **2-1** conversion to **2-2** under aerobic conditions was solvent dependent. In general, non-polar solvents (hexanes, heptanes, toluene, diethyl ether) and polar organic solvents (DMSO, 1,4-dioxane, DMF, DMA) gave poor conversion of ADHP **2-1** to **2-2**. Additionally, polar protic solvents (alkyl alcohols, aqueous solvents) gave poor conversion of ADHP **2-1** (data not included).¹ After thorough screening of various solvents, we investigated polar-aprotic solvents known to give complete conversion of ADHP **2-1** (table **2.2**). Acetone (entry **4**) gave the cleanest oxidation with minimal side products. To avoid potential intermolecular side-reactions (scheme **2.20**), we investigated the oxidation at a lower concentration (entry **5**), noting no meaningful difference in yield or reduction of side products compared to 0.1 molar dilution (entry **4**).

Table 2.2 Effect of solvent and reaction concentration on ADHP oxidation. Quantitative NMR yields.



Entry	Solvent	Conc. [mol/L]	2-1 Conv. (%)	2-2 (%)	2-11 (%)	2-12 (%)	2-13 (%)	SM (%)
1	MeCN	0.1	100	56	9	0	2	<i>cmd</i>
2	EtOAc	0.1	100	55	3	10	3	<i>cmd</i>
3	EtOAc	0.01	100	54	2	10	4	<i>cmd</i>
4	Acetone	0.1	100	78	3	0	<i>trace</i>	<i>cmd</i>
5	Acetone	0.01	100	74	0	0	<i>trace</i>	0
6	THF	0.1	100	44	4	3	4	0
7	1,2-DME	0.1	100	46	8	8	1	0
8	DCM	0.1	100	54	<i>cmd</i>	4	2	0

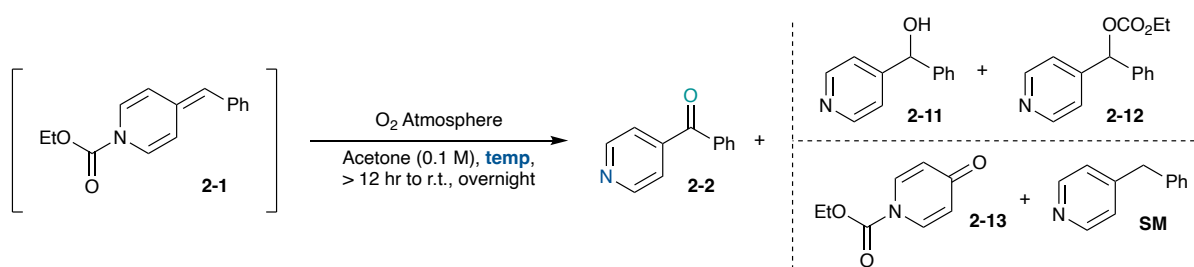
Conditions: **2-1** prepared from 4-benzyl pyridine (50 mg, 0.295 mmol). Percentages based on ¹H-NMR qNMR analysis with *p*-anisaldehyde. *Cnd* = (Could not determine).

¹ Solvent effects on ADHP **2-1** conversion observed by Matthew Puzhitsky.

2.4.4 Screening Temperature

A brief temperature screen suggested 23 °C as the optimal temperature (table 2.3, entry 1). At reflux (entry 2), ADHP conversion is poor compared to entry 1, likely due to the elevated reaction temperatures reducing the concentration of oxygen in solution. At 0 °C over 12 hours (entry 3), ADHP conversion is improved compared to reflux, however more side products were observed. When entries 1 and 3 (table 2.3) were returned to room temperature and left standing for 18 hours under oxygen atmosphere, we observed complete conversion of ADHP 2-1.

Table 2.3 Effect of temperature on ADHP oxidation.



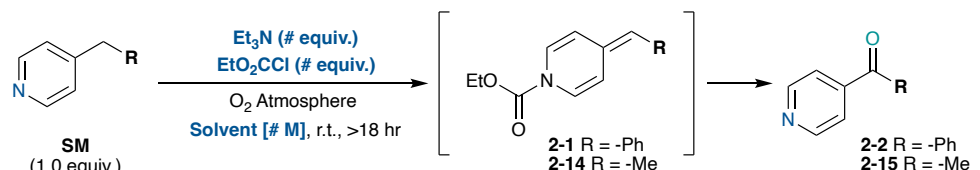
Entry	Temp (°C)	2-1 Conv. (%)	2-2 (%)	2-11 (%)	2-12 (%)	2-13 (%)	SM (%)
1	23	100	78	3	0	trace	cnd
2	Reflux	24	12	0	0	0	0
3	0 °C	78	46	11	cnd	2	11

Conditions: 2-1 is prepared from 4-benzyl pyridine (50 mg, 0.295 mmol). Percentages based on ¹H-NMR qNMR analysis with *p*-anisaldehyde. Cnd = (Could not determine).

2.4.5 Investigating One-Pot Oxidation Conditions

To simplify the oxidation procedure, we proposed that under an oxygen atmosphere, ADHP formed from 4-alkyl pyridine **SM** would oxidize *in situ* to give ketone (table 2.4). Under 1-pot conditions, we found the systematic reduction of triethylamine and ethyl chloroformate improved the conversion of ADHP **2-14** and formation of product **2-15** (entries 3-5). With near stoichiometric equivalents of triethyl amine and ethylchloroformate, the 1-pot oxidation of 4-benzyl pyridine (entry 6) gave comparable results to the 2-step protocol (table 2.2, entry 4). Interestingly, a ten-fold dilution of the reaction solution for the oxidation of 4-ethyl pyridine ADHP **2-14** (entry 7) reduced by-product formation, and improved ketone **2-15** formation compared to 0.1 molar (entry 5). In comparison, the oxidation of ADHP **2-1** at 0.01 molar gave similar yields to 0.1 molar (table 2.2, entry 5 vs 4). We speculated that 4-ethyl pyridine experiences more intermolecular side reactions compared to 4-benzyl pyridine. This could be due to difference electronic effects of the **-R** group on ADHP and radical intermediate stability. This difference is observed in early 1-pot optimization experiments, where ADHP **2-14** conversion is greater compared to ADHP **2-1** (table 2.4, entry 2 vs 1).

Table 2.4 Screening 1-pot 4-alkyl pyridine oxidation conditions. Quantitative NMR yields.



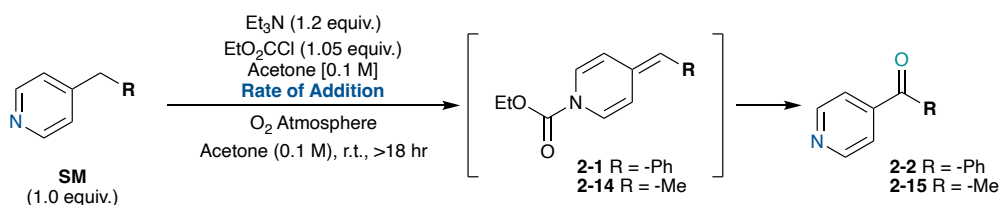
Entry	SM -R, (%)	Conv. -R, (%)	Solvent [mol/L]	Et ₃ N (equiv.)	EtO ₂ CCl (equiv.)	ADHP (%)	Ketone (%)
1	-Ph (96)		THF [0.1]	3	2	2-1 (42)	2-2 (24)
2	-Me (100)		THF [0.1]	3	2	2-14 (0)	2-15 (56)
3	-Me (98)		Acetone [0.1]	3	2	2-14 (43)	2-15 (26)
4	-Me (96)		Acetone [0.1]	3	1.05	2-14 (17)	2-15 (43)
5	-Me (92)		Acetone [0.1]	1.2	1.05	2-14 (0)	2-15 (54)
6	-Ph (100)		Acetone [0.1]	1.2	1.05	2-1 (0)	2-2 (78)
7	-Me (89)		Acetone [0.01]	1.2	1.05	2-14 (0)	2-15 (69)

Conditions: **2-1** prepared from 4-benzyl pyridine (50 mg, 0.295 mmol). **2-14** prepared from 4-ethyl pyridine (50 mg, 0.467 mmol). Percentages based on ¹H-NMR qNMR analysis with *p*-anisaldehyde.

2.4.6 Screening Rates of Ethyl Chloroformate Addition

To obtain a low reaction concentration and avoid potential intermolecular side reactions (scheme 2.20), we proposed the gradual addition of ethyl chloroformate would generate a low concentration of ADHP **2-14**, oxidizing *in situ* to form ketone **2-15** (table 2.5). We found that a dilute chloroformate solution (0.1 M in acetone) added gradually over 1 hour improved conversion of 4-ethyl pyridine and ketone **2-15** formation (entry 3). However, when 4-benzyl pyridine was subjected to the slowed rate of chloroformate addition (entry 5), we observed poorer conversion of intermediate ADHP **2-1** and less ketone **2-2** formation compared to a rapid rate of addition (entry 4).

Table 2.5 Effect of chloroformate addition rate on 1-pot 4-alkyl pyridine oxidation. Quantitative NMR yields.

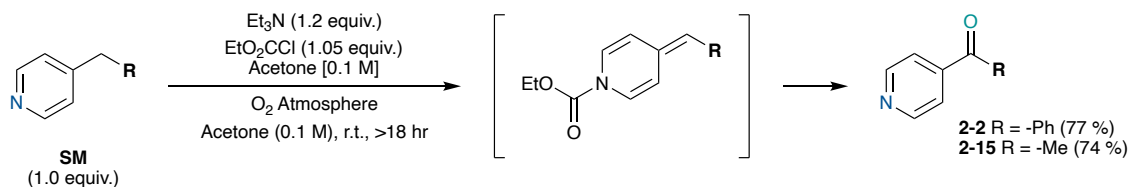


Entry	SM Conv. (%)	EtO ₂ CCl Addition Rate	ADHP (%)	Ketone (%)
1	-Me (92)	~30 s	2-14 (0)	2-15 (54)
2	-Me (92)	0.5 hr	2-14 (0)	2-15 (66)
3	-Me (100)	1 hr	2-14 (0)	2-15 (74)
4	-Ph (100)	~30 s	2-1 (0)	2-2 (77)
5	-Ph (100)	1 hr	2-1 (8)	2-2 (62)

Conditions: **2-1** prepared from 4-benzyl pyridine (50 mg, 0.295 mmol). **2-14** prepared from 4-ethyl pyridine (50 mg, 0.467 mmol). Percentages based on ¹H-NMR qNMR analysis with *p*-anisaldehyde.

2.5 Conclusions and Future Work

Exploiting the electron rich nature of ADHPs, we have established the mild preparation of 4-pyridylic ketones from 4-alkyl pyridines via ADHPs (scheme 2.21). This oxidation demonstrates excellent chemoselectivity in the presence of competing benzylic and pyridylic positions. Due to the inability to form the ADHP with 2-substituted alkyl pyridines, this oxidation cannot be applied to 2-alkyl pyridines or 2-substituted 4-alkyl pyridines. In addition, we have simplified the ADHP oxidation to a 1-pot protocol, noting a difference in ADHP oxidation between 4-ethyl pyridine and 4-benzyl pyridine. With optimized conditions established, we will perform a substrate scope to further investigate reaction chemoselectivity and utility.

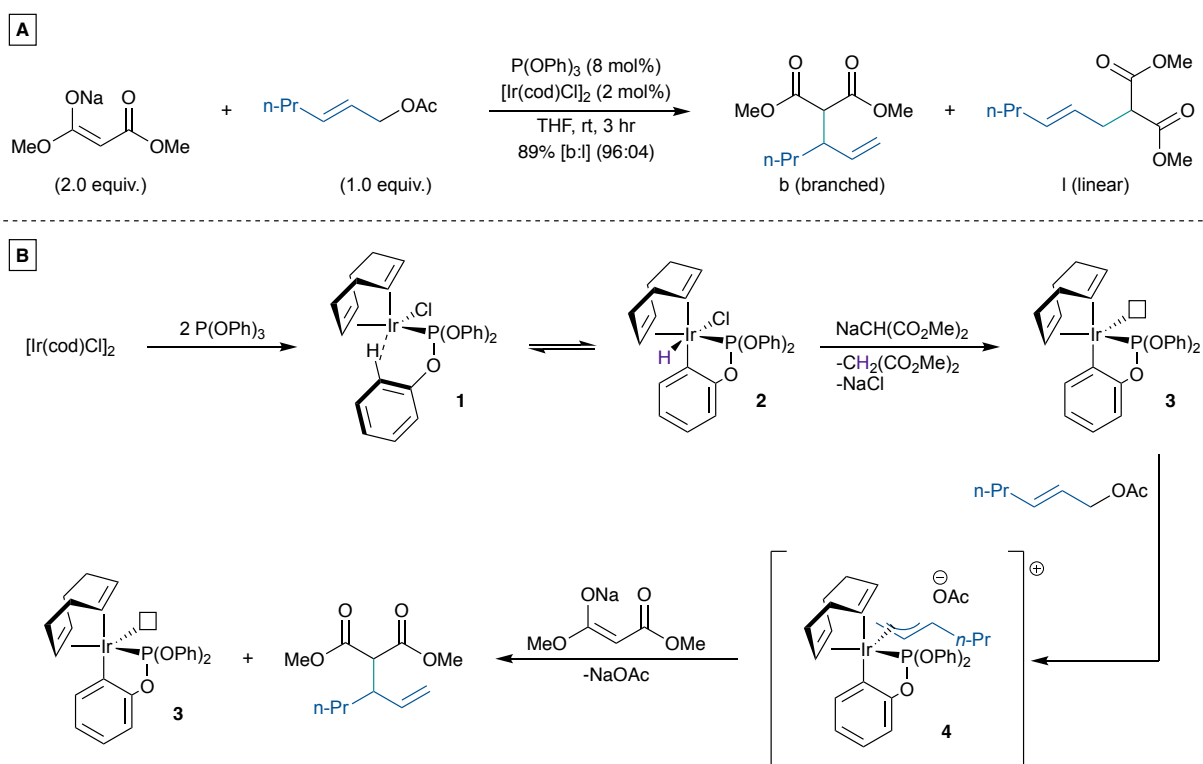


Scheme 2.21 1-Pot oxidation of 4-alkyl pyridines to 4-acetyl pyridines.

Chapter III: Development of the Iridium-Catalyzed Alkylation of 4-Methyl Pyridines

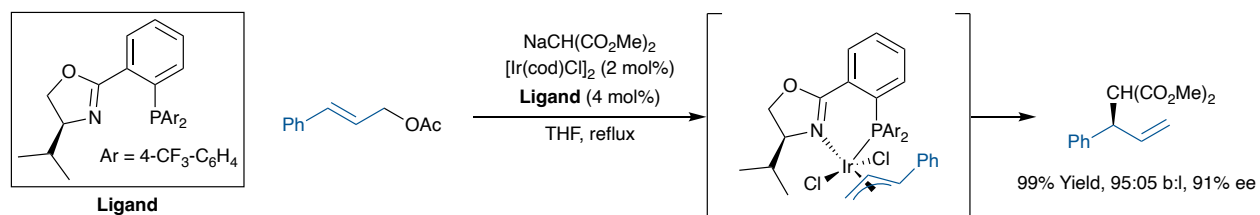
3.1 Iridium-Catalyzed Asymmetric-Alkylation

In 1997, Kashio and Takeuchi reported the first iridium-catalyzed allylic alkylation reaction (scheme 3.1, A).^[32] Mechanistic studies by Helmchen and co-workers established an iridacyclic complex as the active catalyst (scheme 3.1, B, 3).^[33] The complex is formed by reversible ortho C-H oxidative-addition of the phosphite ligand, driven forward by base assisted reductive-elimination by sodium malonate (scheme 3.1, B, 1 to 3). Coordination and oxidative-addition of allyl acetate by complex 3 forms the cationic allyl-iridium (III) 4, intercepted by sodium malonate to form the branched allylated product.

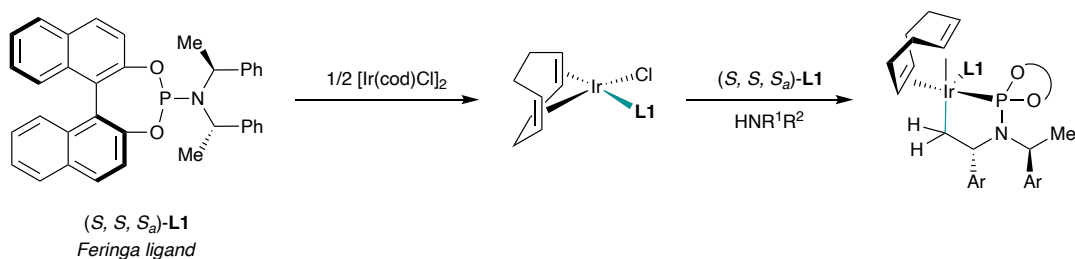


Scheme 3.1 A) First reported Ir-catalyzed allylic alkylation by Kashio and Takeuchi. B) Mechanism determined by Helmchen.

Shortly after Kashio and Takeuchi's report, the first enantioselective variant was reported by Helmchen and Jansen (scheme 3.2).^[34] Further advancements in iridacyclic catalyst systems would be made, with major contributions from the application of Feringa-type phosphoramidites by Hartwig (scheme 3.3).^[35]

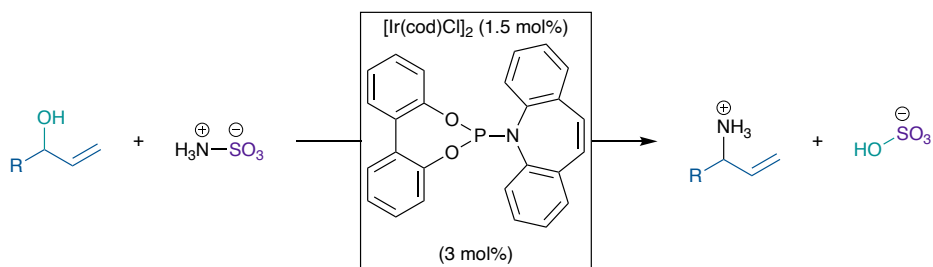


Scheme 3.2 First enantioselective iridium-catalyzed allylation by Helmchen and Jansen.

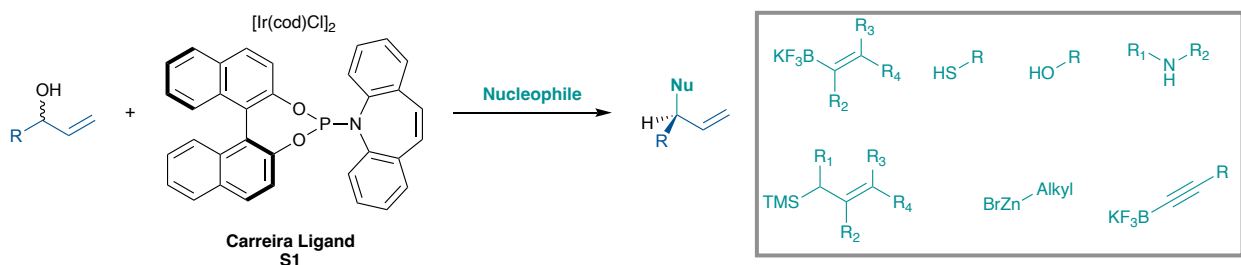


Scheme 3.3 Hartwig's synthesis of Feringa ligand based iridacyclic complex.

In 2007, Carreira reported the application of P-olefin phosphoramidite ligands (dubbed Carreira ligand) in the iridium-catalyzed synthesis of primary allylic amines from allylic alcohols (scheme 3.4).^[36] Years since this report, a rich library of nucleophiles have been applied in Carreira-iridium catalyzed asymmetric alkylations (scheme 3.5).^[37]

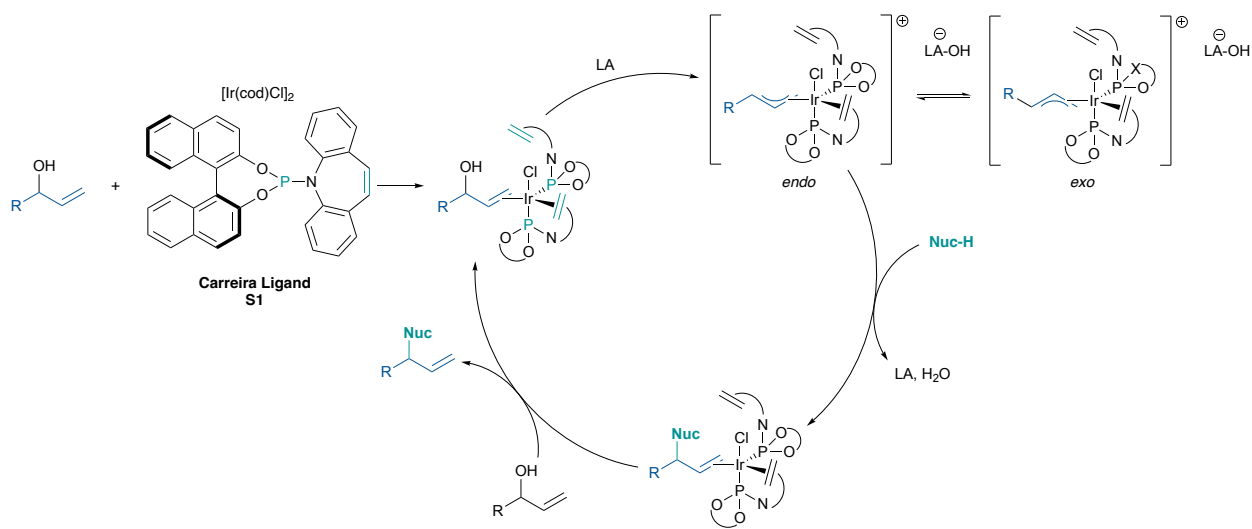


Scheme 3.4 Carreira's iridium-catalyzed synthesis of primary allylic amines.



Scheme 3.5 Survey of nucleophiles applied in Carreira's iridium-catalyzed asymmetric alkylation.

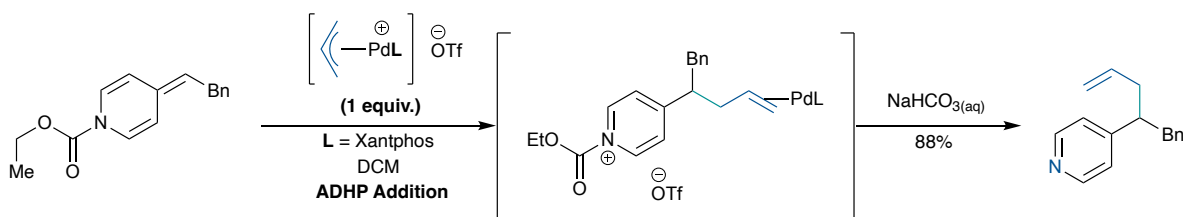
Mechanistic studies by Carreira established the formation of a cationic allyl-iridium complex by Lewis acid promoted oxidative-addition of α -allyl benzylic alcohol (scheme 3.6).^[36] The cationic allyl-iridium complex is in equilibrium between *exo* and *endo* diastereomers. In one mechanistic proposal, the *endo* diastereomer is intercepted by a nucleophile at the benzylic allyl terminus through an outer-sphere approach, forming the branched allylated nucleophile. From X-ray crystal analysis of the cationic allyl-iridium diastereomers, the researchers observed a longer carbon-iridium bond at the benzylic allyl carbon compared to the terminal allyl carbon.^[38] This difference in carbon-iridium bond length is postulated to be from a *trans* influence by the phosphorus atom of the ligand, resulting in the benzylic position as the favorable site of nucleophilic attack.^[38]



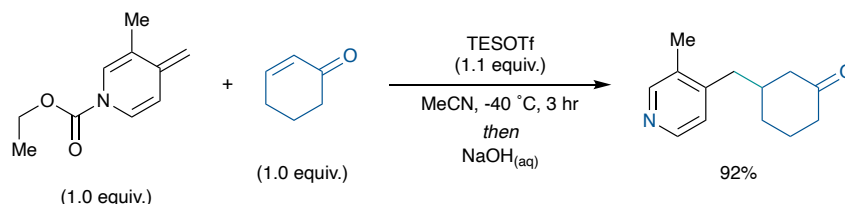
Scheme 3.6 Proposed mechanism of Carreira's Ir-catalyzed asymmetric allylation method.

3.2 Iridium-Catalyzed Allylation of Alkylidene Dihydropyridines

Previously, we established ADHPs as competent nucleophiles against cationic allyl-palladium complexes (scheme 3.7). Exploiting this reactivity, we recently demonstrated ADHPs as soft nucleophiles, capable of forming 1,4-conjugated addition products with α,β -unsaturated ketones (scheme 3.8).^[9]

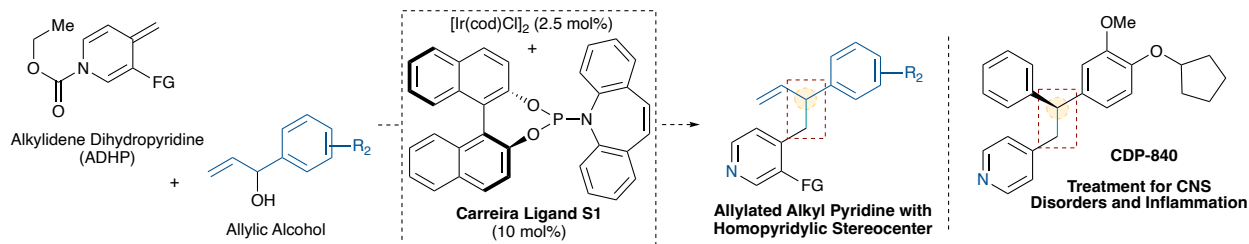


Scheme 3.7 ADHP addition to cationic allyl-palladium.



Scheme 3.8 ADHP as soft nucleophiles.

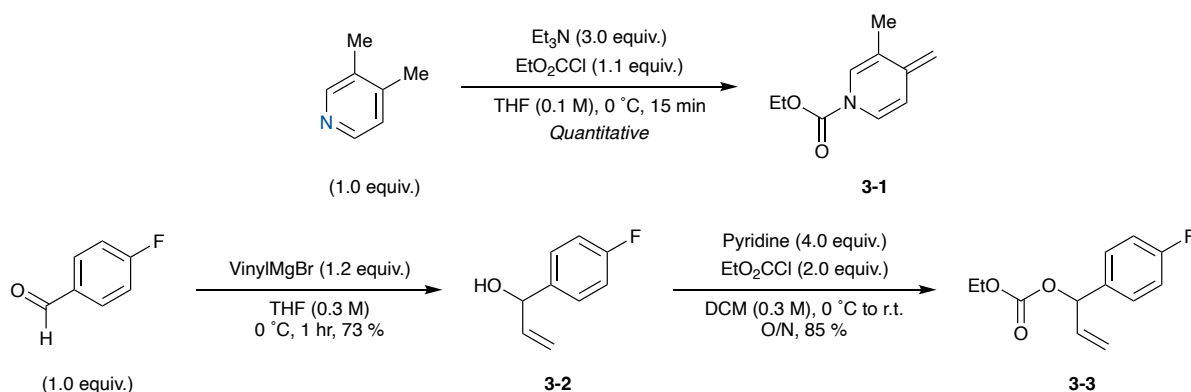
We speculated that ADHPs should also be capable of intercepting cationic allyl-iridium complexes to form branched allylated 4-alkyl pyridines, bearing new a homopyridylic stereogenic center (scheme 3.9).^[39] Alkylpyridines with stereogenic centres at the pyridylic or homopyridylic positions are privileged motifs in medicinal chemistry.^[10] Existing methods to prepare these motifs use strongly basic or Lewis acidic reagents,^[40] limiting functional group compatibility. By exploiting the nucleophilicity of alkyldiene dihydropyridines and their mild preparation,^[5] we can establish structurally complex pyridine scaffolds under accessible conditions.



Scheme 3.9 ADHPs as nucleophiles in Carreira's iridium-catalyzed allylation protocol.

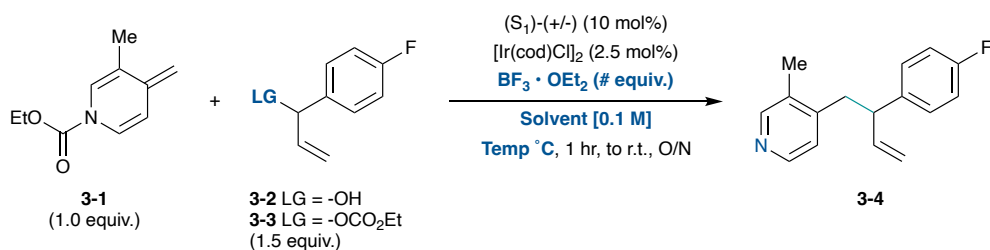
3.3 Proof of Concept

Preliminary experiments used ADHP **3-1** and *para*-fluorinated α -allyl benzylic partners **3-2** and **3-3** (scheme 3.10). Fluorine tagged allyl electrophiles were used to determine branched and linear product ratios by ^{19}F -NMR. Reactivity was observed using the ethylcarbonate ester leaving group on the allyl partner, and stoichiometric $\text{BF}_3\cdot\text{OEt}_2$, giving the branch allylated product **3-4** exclusively (confirmed by ^1H -NMR) in 58% isolated yield (table 3.1, entry 7). The reaction gave only trace amounts of branched product when catalytic $\text{BF}_3\cdot\text{OEt}_2$ was used (entry 9), and in the absence of the Carreira ligand or catalyst system, we observed only trace amount of branched product (entry 10 & 11). These results suggest that the allylation is mediated by the Carreira-iridium catalyst and requires stoichiometric $\text{BF}_3\cdot\text{OEt}_2$ for reaction productivity.



Scheme 3.10 Synthesis of ADHP **3-1** and branched allyl partners **3-2**, **3-3**.

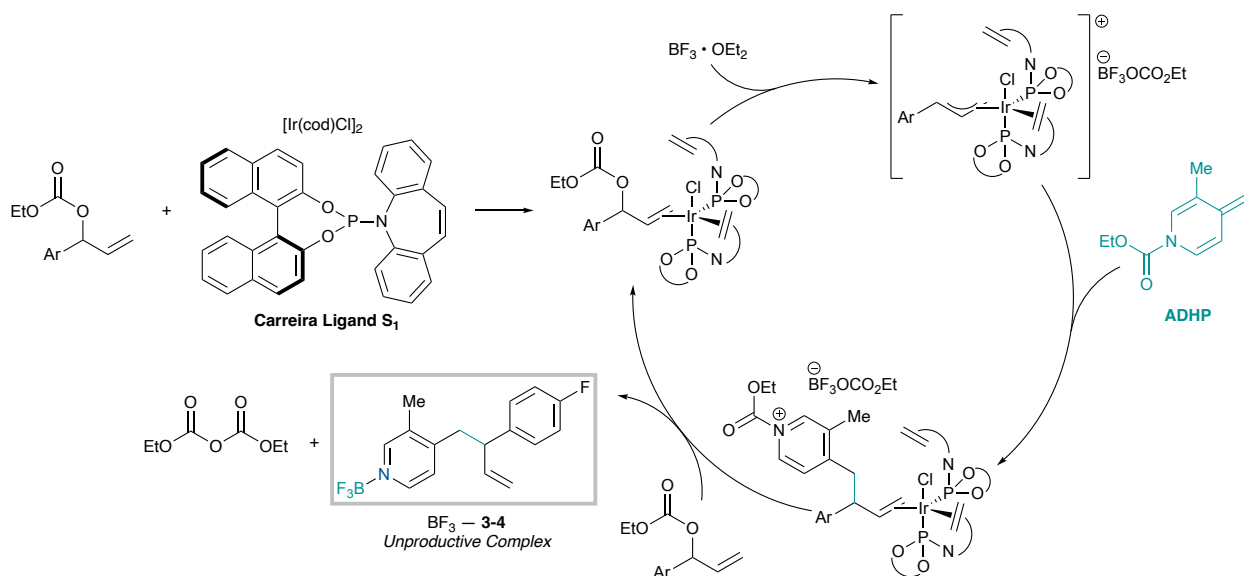
Table 3.1 Proof of concept reactions summary.



Entry	Leaving group LG, (equiv.)	BF ₃ · OEt ₂ (equiv.)	Temperature (°C)	Solvent [0.1 M]	Conv. 3-1 (%)	Product Yield 3-4 (%)
1	3-2	0.3	50	MeCN	100	Trace
2	3-2	1.0	rt	1,2-DCE	100	Trace
3	3-2	2.5	0	DCM	100	0
4	3-2	1.0	0	DCM	100	Trace
6	3-2	0.3	0	DCM	100	0
7	3-3	1.15	0	THF	100	58
8	3-3	0	0	THF	100	Trace
9	3-3	0.3	0	THF	100	Trace
10 ^a	3-3	1.15	0	THF	100	0
11 ^b	3-3	1.15	0	THF	100	Trace

Conditions: **3-1** prepared from 3,4-lutidine (100 mg, 0.932 mmol). Isolated yields. [a] No catalyst. [b] No Carreira ligand.

Based on Carreira's mechanistic work,^[38] the iridium-catalyzed allylation of ADHPs could proceed through a similar mechanism (scheme 3.11). After addition of the ADHP to the cationic allyl-iridium complex, diethyl pyrocarbonate and a BF_3 – **3-4** adduct could form as reaction by-products. The poor reaction productivity observed with catalytic $\text{BF}_3 \cdot \text{OEt}_2$ could be caused by the formation of the unproductive BF_3 – **3-4** complex.

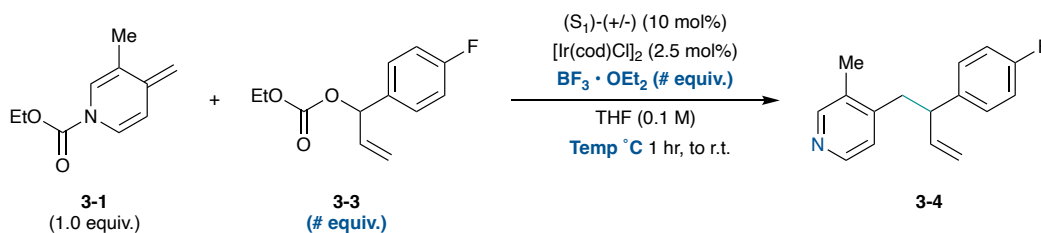


Scheme 3.11 Proposed mechanism for the iridium-catalyzed allylation of ADHPs.

3.4 Reaction Optimization

During reactivity screening experiments, we found that the order of ADHP **3-1** addition to the reaction gave different outcomes in product yield. By adding ADHP last to the reaction mixture, **3-4** was isolated in an improved 68% yield with 80% ee (table 3.2, entry 1). To improve enantioselectivity, we found that reducing the reaction temperature from 0 °C to -40 °C during ADHP addition gave the best results, providing 55% yield and 99% ee (entry 3). At -40 °C, increasing the equivalents of allyl carbonate and $\text{BF}_3 \cdot \text{OEt}_2$ gave branched product **3-4** in an improved 77% isolated yield and 98% ee (entry 5).

Table 3.2 Summary of optimization experiments.

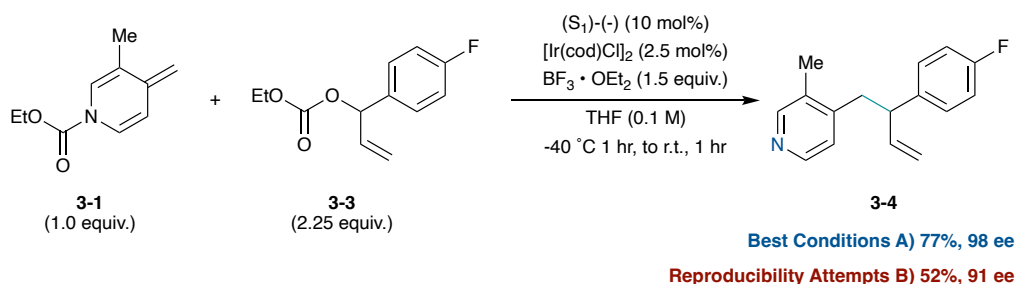


Entry	Allyl Carbonate (equiv.)	$\text{BF}_3 \cdot \text{OEt}_2$ (equiv.)	Temp (°C)	Conv. 3-1 (%)	3-4 (%) ^[a]	3-4 ee (%)
1 ^[b]	1.5	1.05	0	100	68	80
2	1.5	1.05	-20	100	68	90
3	1.5	1.05	-40	100	55	99
4	1.5	1.5	-40	100	69	95
5	2.25	1.5	-40	100	77	98

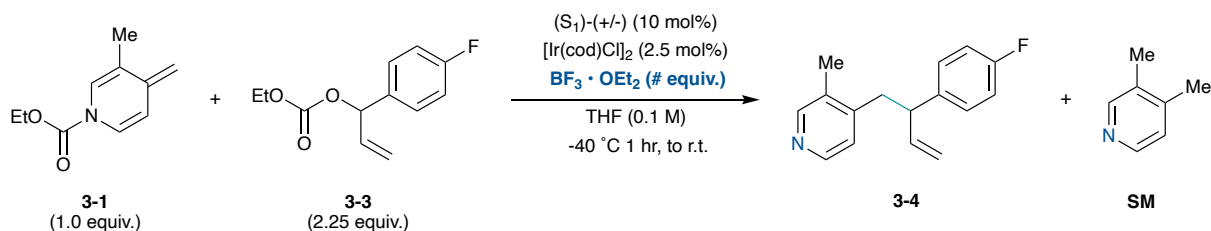
Conditions: **3-1** prepared from 3,4-lutidine (50 mg, 0.467 mmol). [a] Isolated yields. [b] ADHP added last.

3.5 Method Reproducibility

During our optimization experiments, efforts to reproduce our best result of 77% isolated yield and 98% ee were unsuccessful, as multiple attempts consistently gave 52% isolated yield and 91% ee (scheme 3.12, A & B). After a thorough investigation, we found that the quality of $\text{BF}_3 \cdot \text{OEt}_2$ used at different points in the optimization contributed to the variance observed in product yield. Summarized in table 3.3, new sources of $\text{BF}_3 \cdot \text{OEt}_2$ used in later reproducibility experiments gave lower product yield (entry 1 & 2) compared to the older source of $\text{BF}_3 \cdot \text{OEt}_2$ (entry 3). This older source of $\text{BF}_3 \cdot \text{OEt}_2$ was used extensively in early optimization experiments. We speculated that the older source of $\text{BF}_3 \cdot \text{OEt}_2$ lost Et_2O overtime, increasing the concentration of BF_3 relative to Et_2O . Following this idea, we found that using 3.0 equivalents of new $\text{BF}_3 \cdot \text{OEt}_2$ gave a similar yield compared to 1.5 equivalents of the older $\text{BF}_3 \cdot \text{OEt}_2$ source (entry 4 vs 3).



Scheme 3.12 A) Best optimization conditions B) Best reproduced results.

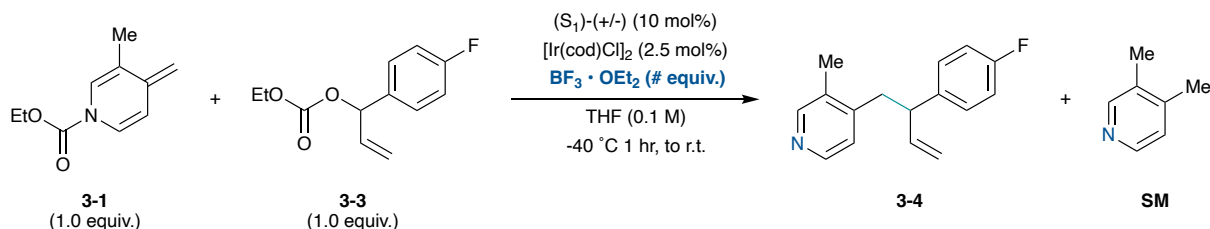
Table 3.3 Impact of $\text{BF}_3 \cdot \text{OEt}_2$ quality on product yield.

Entry	$\text{BF}_3 \cdot \text{OEt}_2$ Quality and (equiv.)	Conv. 3-1 (%)	3-4 (%)	3,4-Lutidine SM (%)
1	New – 01 (1.5)	100	52	-
2	New – 02 (1.5)	100	46	33
3	Old (1.5)	100	61	12
4	New – 01 (3.0)	100	59	15

Conditions: **3-1** prepared from 3,4-lutidine (25 mg, 0.233 mmol). Percentages based on $^1\text{H-NMR}$ qNMR analysis with *p*-anisaldehyde.

3.6 Effect of Boron Trifluoride Etherate

Investigating further, we found that a super stoichiometric excess of $\text{BF}_3 \cdot \text{OEt}_2$ greatly improved reaction productivity without the need for excess carbonate (table 3.4, entry 4). At excess equivalents of $\text{BF}_3 \cdot \text{OEt}_2$, pyridylic allylation of ADHP **3-1** could be occurring in the absence of catalyst. However, when the allylation was conducted without catalyst present, only trace amounts of branched product were observed (entry 5), suggesting that a non-catalyzed allylation pathway is not dominant.

Table 3.4 Effect of $\text{BF}_3 \cdot \text{OEt}_2$ on product yield.

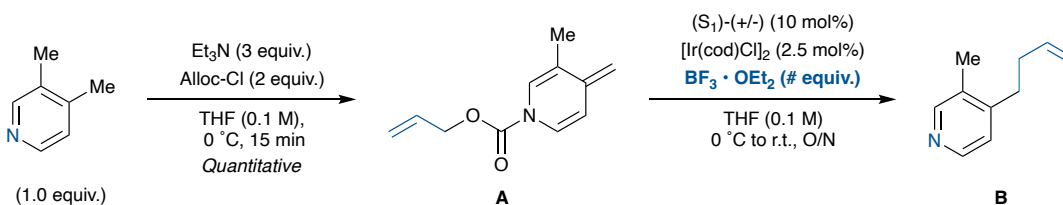
Entry	$\text{BF}_3 \cdot \text{OEt}_2$ (equiv.)	Conv. 3-1 (%)	3-4 (%)	3,4-Lutidine SM (%)
1	1	100	40	11
2	2	100	56	26
3	3	100	51	20
4	4	100	70	20
5 ^[a]	4	100	trace	80

Conditions: **3-1** prepared from 3,4-lutidine (25 mg, 0.233 mmol). Percentages based on $^1\text{H-NMR}$ qNMR analysis with *p*-anisaldehyde. [a] No catalyst.

3.7 Alternative ADHP Allylation Strategies

From our previous work, we established that ADHPs prepared with allyl-chloroformate can form allylated 4-alkyl pyridines when treated with a Xantphos-palladium catalyst system (scheme 1.2, A).^[7] We speculated that these ADHPs could be suitable substrates in iridium-catalyzed asymmetric alkylations with the Carreira catalyst system. From our proof of concept, a modest amount of allylated product **B** was formed when ADHP **A** treated with the Carreira iridium-catalyst system (table 3.5).

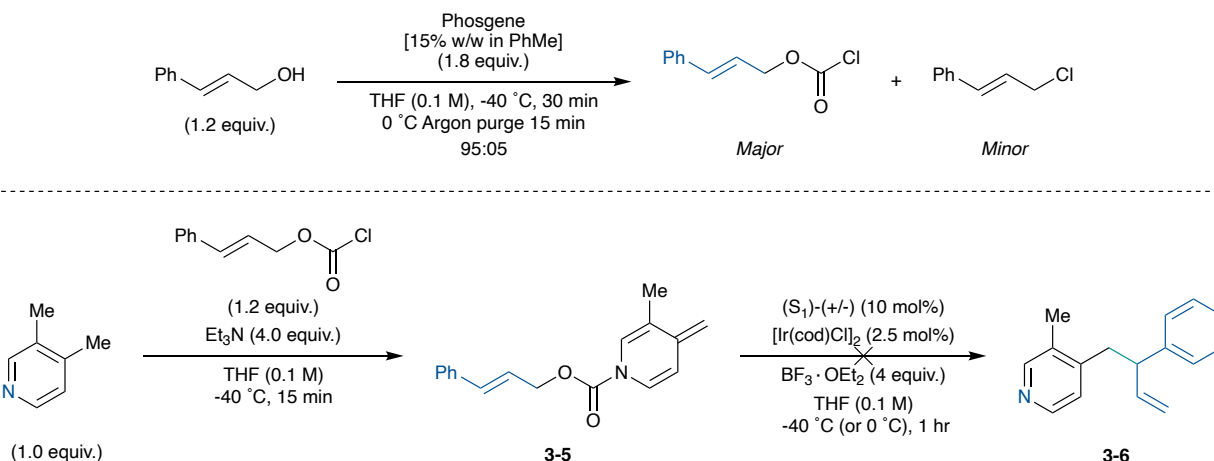
Table 3.5 Iridium-catalyzed allylation of allyl-ADHPs, proof of concept.



Entry	BF ₃ · OEt ₂ (equiv.)	Conv. A (%)	B (%)
1	0	100	17
2	4	100	22

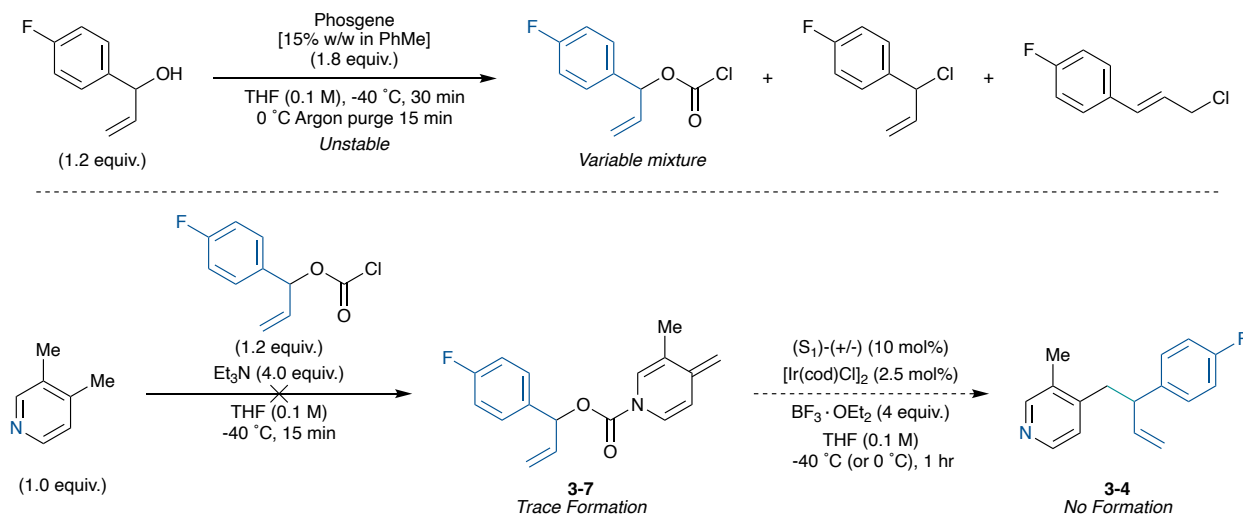
Conditions: **A** prepared from 3,4-lutidine (50 mg, 0.467 mmol). Percentages based on ¹H-NMR qNMR analysis with *p*-anisaldehyde.

From this preliminary result, we believed that a cinnamyl-ADHP could provide the branched allylated alkyl-pyridine (scheme 3.13). However, when the cinnamyl-ADHP **3-5** was treated with the iridium-catalyst and BF₃·OEt₂, we did not observe any formation of product **3-6** by ¹H-NMR.



Scheme 3.13 Unsuccessful allylation of **3-6**.

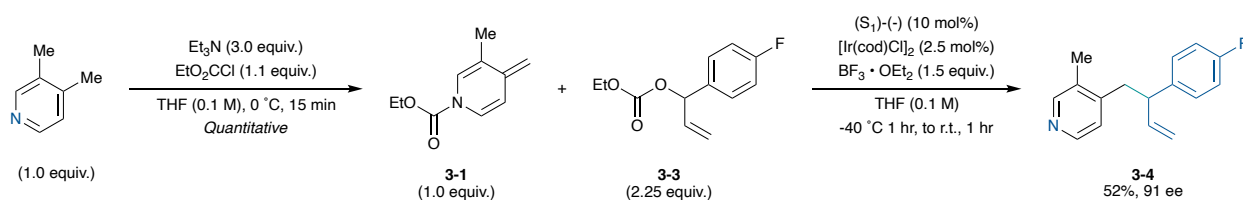
To improve reactivity, we believed that the branched cinnamyl-ADHP would accelerate oxidative addition at the α -allylic benzylic carbon-oxygen by the iridium catalyst (scheme 3.14). However, attempts to prepare the branched ADHP **3-7** were unsuccessful due to the poor stability of the branched cinnamyl-chloroformate and ADHP **3-7**.



Scheme 3.14 Unsuccessful synthesis of ADHP **3-7**.

3.8 Conclusions and Future Work

Exploiting the nucleophilicity of ADHPs, we have established the iridium-catalyzed enantioselective allylation of 4-alkyl pyridines via ADHPs (scheme 3.15). Early optimization experiments showed excess α -allyl benzylic carbonate, stoichiometric $\text{BF}_3 \cdot \text{OEt}_2$, and low reaction temperatures are necessary for reaction productivity and enantioselectivity. Variance of product yield in method reproducibility experiments was highly dependent on the quality of $\text{BF}_3 \cdot \text{OEt}_2$. Further investigation found that stoichiometric α -allyl benzylic carbonate and super stoichiometric $\text{BF}_3 \cdot \text{OEt}_2$ improved product yield. Future optimization experiments will investigate the impact of excess $\text{BF}_3 \cdot \text{OEt}_2$ on reaction enantioselectivity and viability.



Scheme 3.15 Iridium-catalyzed enantioselective allylation of 4-alkyl pyridines via ADHPs.

4.0 Experimental

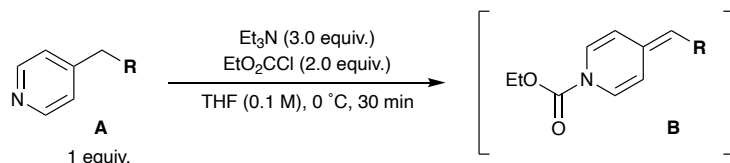
4.1.1 Chapter 2 Experimental

General Considerations

All reactions were conducted in flame- or oven-dried glassware under an atmosphere of argon using anhydrous solvents unless specified otherwise. Tetrahydrofuran (THF) and acetonitrile (MeCN) were dried using an INERT® PureSolv solvent purification system. Commercial 4-alkyl pyridines were used as received. Thin-layer chromatography was performed on SiliCycle® silica gel 60 F254 plates. Visualization was carried out using UV light (254 nm) and/or KMnO₄. Auto-flash column chromatography was carried out using a Buchi Pure C-810 Flash Pure Chromatography System. ¹H-NMR and ¹³C-NMR spectra were recorded on a Bruker 400 AV or Bruker 300 AV spectrometer in chloroform-d (99.8% deuterated). *p*-Anisaldehyde was used as internal standard for quantitative ¹H NMR analysis (d1 30s). All alkylidene dihydropyridines were prepared and verified following our previous procedures.^[7,9,41] Spectra recorded using chloroform were calibrated to 7.26 ppm ¹H and 77.16 ppm ¹³C. Chemical shifts (δ) are reported in ppm and multiplicities are indicated by s (singlet), d (doublet), t (triplet), q (quartet), m (multiplet) and br (broad). Coupling constants *J* are reported in Hertz (Hz).

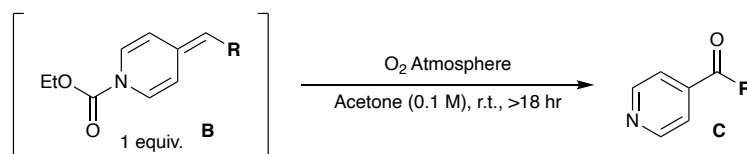
4.1.2 Chapter 2 General Procedures

General Procedure 1: Alkylidene Dihydropyridine Synthesis from 4-Alkyl Pyridines



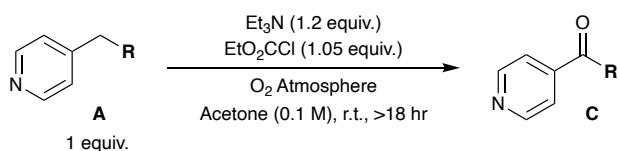
Following our modified procedure,^[8] under argon atmosphere, a 25 mL round-bottom flask equipped with a 1 cm stir-bar was charged with 4-Alkyl Pyridine **A** (1 eq), triethyl amine (3.0 eq), and anhydrous THF ([0.1 M] w.r.t. **A**). After stirring at $0\text{ }^\circ\text{C}$ for 5 minutes, neat ethyl chloroformate (2.0 eq) was added dropwise, and the solution was stirred at temperature for 30 minutes. The heterogeneous yellow mixture was warmed to room temperature and concentrated *in vacuo* to remove solvent and excess reagents. The concentrate was diluted with ACS grade hexanes and filtered through a cotton plug into a 100 mL round-bottom flask. Concentration of the filtrate *in vacuo* furnished crude alkylidene dihydropyridine **B** which was used immediately without further purification.

General Procedure 2: Mild ADHP Oxidation to Pyridylic Ketones



A 25 mL round-bottom flask equipped with a 1 cm stir-bar was purged with an oxygen balloon for 5 minutes, followed by addition of crude alkylidene dihydropyridine **B** in ACS grade acetone ([0.1 M] w.r.t. **A**). The solution was stirred at room temperature overnight (>18 hr) under oxygen atmosphere. After overnight stirring, the mixture was concentrated *in vacuo* to give crude pyridylic ketone **C**. The crude ketone was dry loaded on to silica (500 mg) and purified by auto-flash chromatography (12g FlashPure EcoFlex, EtOAc/Hexanes, 0 – 100% over 12 column volumes) to give pyridylic ketone **C**.

General Procedure 3: Mild 1-Pot Oxidation of 4-Alkyl Pyridines

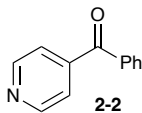


3.1 Slow chloroformate addition: Under oxygen atmosphere, a 25 mL round-bottom flask equipped with a 1 cm stir-bar was charged with 4-Alkyl Pyridine **A** (1 eq), triethyl amine (1.2 eq) and ACS grade acetone ([0.1 M] w.r.t. **A**). Concurrently, ethyl chloroformate (1.05 eq) was weighed into a 20 mL vial and diluted with ACS grade acetone ([0.1 M] w.r.t. **A**). To the room temperature alkyl pyridine mixture, the dilute chloroformate solution was added dropwise over 60 minutes using a syringe pump or addition funnel. After the addition was complete, the heterogenous solution was stirred at room temperature overnight (> 18 hr). After overnight stirring, the mixture is diluted with ethyl acetate and filtered through a cotton plug into a 100 mL round-bottom flask. The filtrate was concentrated *in vacuo* to give crude pyridylic ketone **C**. The crude ketone was dry loaded on to silica (500 mg) and purified by auto-flash chromatography (12g FlashPure EcoFlex, EtOAc/Hexanes, 0 – 100% over 12 column volumes) to give pyridylic ketone **C**.

3.2 Fast chloroformate addition: Under oxygen atmosphere, a 25 mL round-bottom flask equipped with a 1 cm stir-bar was charged with 4-Alkyl Pyridine **A** (1 eq), triethyl amine (1.2 eq) and ACS grade acetone ([0.1 M] w.r.t. **A**). Ethyl chloroformate (1.05 eq) was added to the room temperature alkyl pyridine mixture dropwise, rinsing with ACS grade acetone ([0.3 M] w.r.t. **A**). After the addition was complete, the heterogenous solution was stirred at room temperature overnight (> 18 hr). After overnight stirring, the mixture is diluted with ethyl acetate and filtered through a cotton plug into a 100 mL round-bottom flask. The filtrate was concentrated *in vacuo* to give crude pyridylic ketone **C**. The crude ketone was dry loaded on to silica (500 mg) and purified by auto-flash chromatography (12g FlashPure EcoFlex, EtOAc/Hexanes, 0 – 100% over 12 column volumes) to give pyridylic ketone **C**.

4.1.3 Pyridylic Ketones (2-2, 2-4, 2-15)

Synthesis of 2-2 (4-Benzoyl Pyridine):



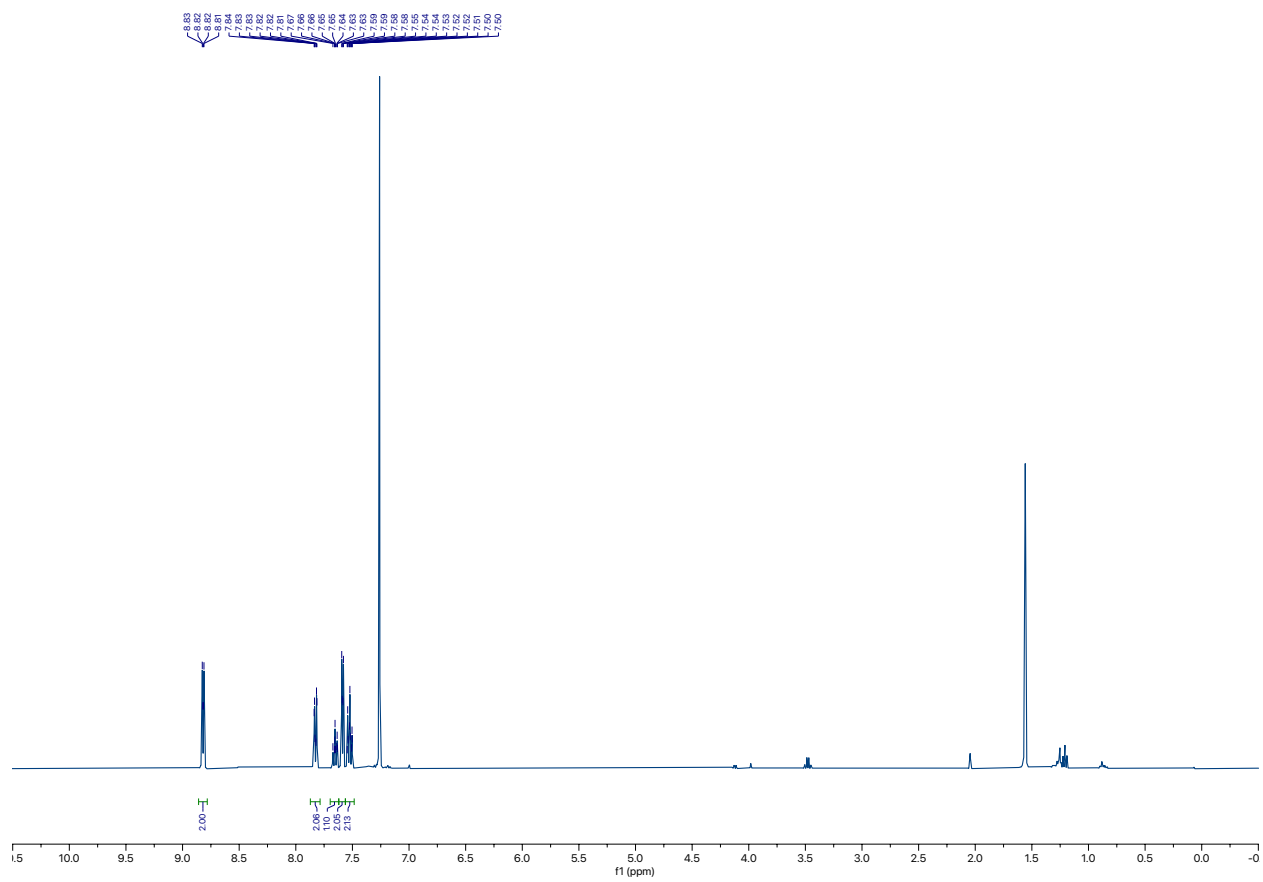
Following general procedure **3.2 (fast addition)**, oxidation of 4-benzyl pyridine (100 mg, 0.591 mmol) gave 4-benzoyl pyridine **2-2** as a white solid (78%, 84 mg, 0.461 mmol) and is consistent with reported data.²⁵

Data for **2-2**

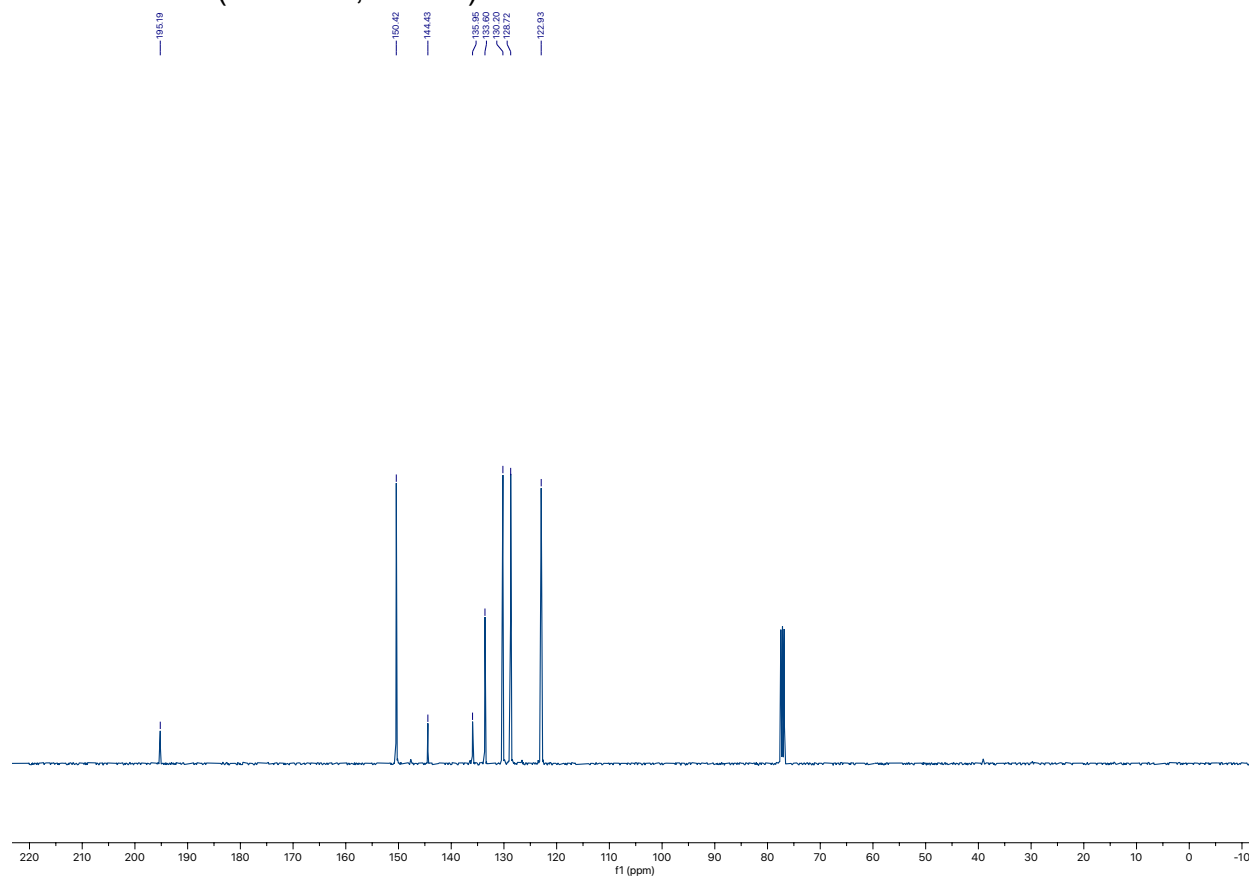
¹H NMR (400 MHz, CDCl₃) δ 8.85 – 8.79 (m, 2H), 7.86 – 7.79 (m, 2H), 7.70 – 7.48 (m, 5H).

¹³C NMR (101 MHz, CDCl₃) δ 195.19, 150.42, 144.43, 135.95, 133.60, 130.20, 128.72, 122.93.

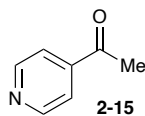
2-2 1H NMR (400 MHz, CDCl3)



2-2 ¹³C NMR (101 MHz, CDCl₃)



Synthesis of 2-15 (4-Acetyl Pyridine):

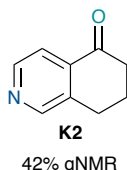


Following general procedure **3.1 (slow addition)**, oxidation of 4-ethyl pyridine (50 mg, 0.591 mmol) gave 4-acetyl pyridine **2-15** in 77% qNMR yield and is consistent with reported data.²⁵

Data for **2-15**

¹H NMR (400 MHz, CDCl₃) δ 8.82 (d, J = 6.1 Hz, 2H), 7.73 (d, J = 6.1 Hz, 2H),
2.63 (s, 3H).

Identification of 2-4:

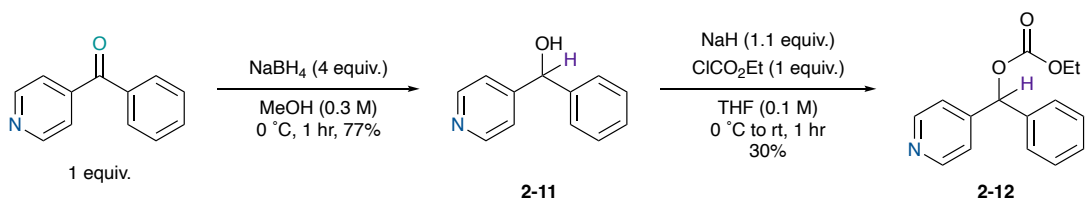


Appearance of **2-4** in quantitative ¹H-NMR (scheme **2.12**) is consistent with reported data.²⁶

Data for **2-4**

¹H NMR (300 MHz, CDCl₃) δ 8.64 (s, 1H), 8.59 (d, J = 5.0 Hz, 1H), 7.72 (d, J =
5.0 Hz, 1H), 2.95 (t, J = 6.1 Hz, 2H), 2.68 (dd, J = 7.3,
5.7 Hz, 2H), 2.17 (m, J = 6.3 Hz, 2H).

4.1.4 By-Product Synthesis (2-11, 2-12, 2-13)



Synthesis of 2-11

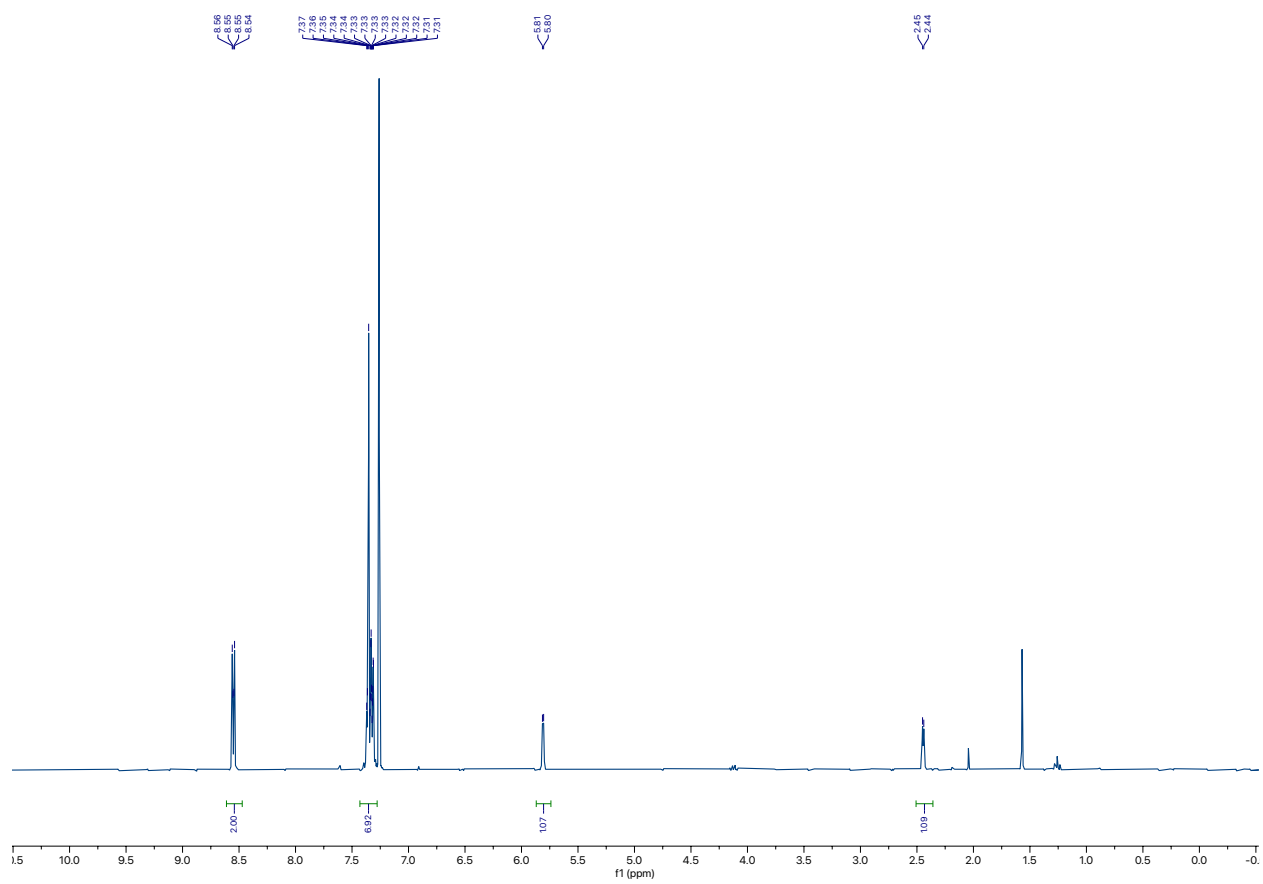
Under open atmosphere, a 100 mL round-bottom flask equipped with a 3 cm stir-bar was charged with 4-benzoyl pyridine (1 eq, 500 mg, 2.73 mmol) and methanol (9 mL, [0.3 M] w.r.t. 4-benzoyl pyridine). After cooling the solution to 0 °C, sodium borohydride (4 eq, 413 mg, 10.9 mmol) was added in portions over 3 minutes and stirred at temperature for 1 hour. The reaction was quenched with 10 mL of saturated NH₄Cl_(aq) and stirred for 15 minutes. The heterogeneous mixture was diluted with EtOAc (15 mL), and the aqueous phase was extracted with EtOAc (x2 10 mL). The organic phases were dried over Na₂SO₄ and concentrated *in vacuo*. The crude alcohol was dry loaded on silica (1 g) and purified by auto-flash chromatography (12g FlashPure EcoFlex, MeOH/EtOAc, 0 – 100% over 6 column volumes) to give **2-11** as a white solid (386 mg, 77%) found to be consistent with reported literature.^[42]

Data for 2-11

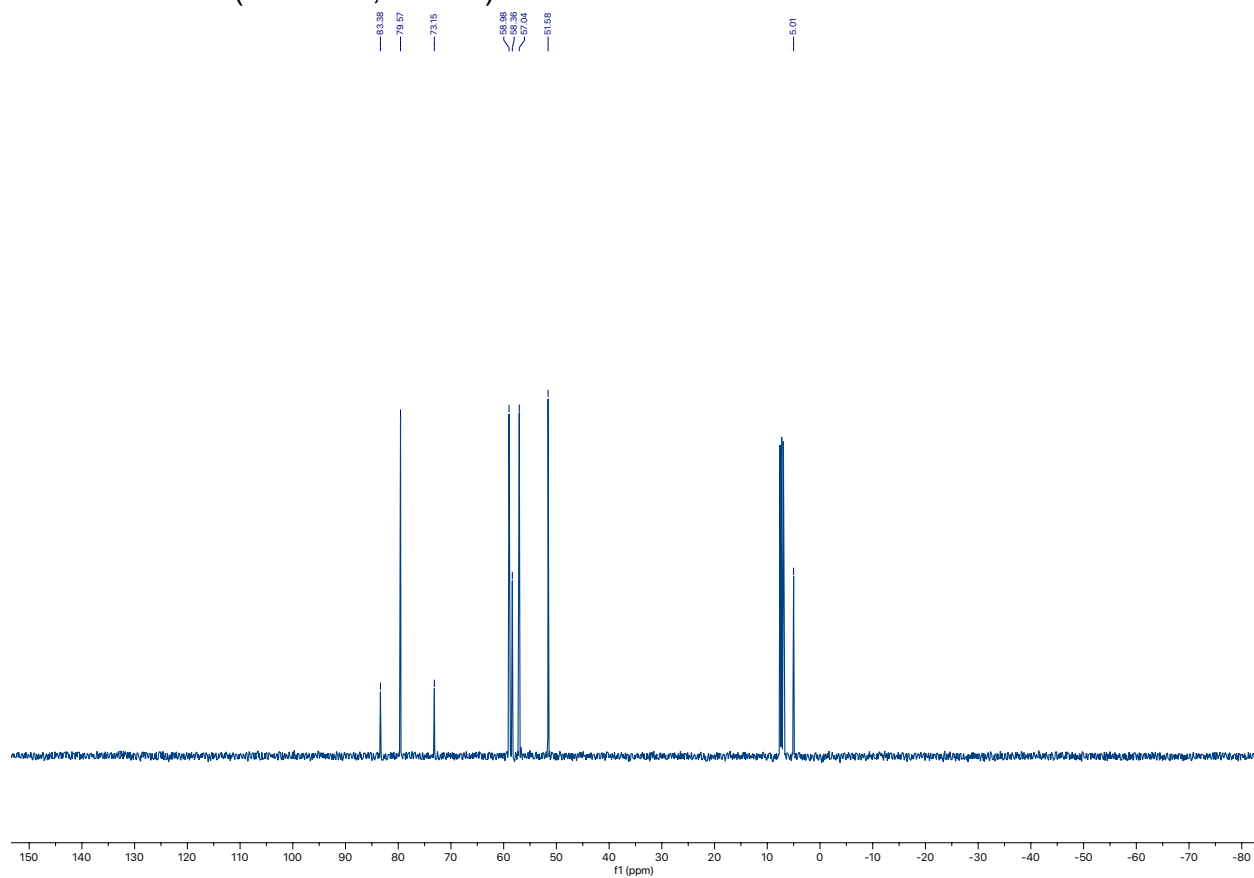
¹H NMR (300 MHz, CDCl₃) δ 8.62 – 8.47 (m, 2H), 7.45 – 7.28 (m, 7H), 5.81 (d, J = 3.22 Hz, 1H), 2.44 (d, J = 3.22 Hz, 1H).

¹³C NMR (101 MHz, CDCl₃) δ 153.28, 149.47, 143.05, 128.89, 128.26, 126.95, 121.48, 74.91.

2-11 1H NMR (300 MHz, CDCl3)



2-11 ¹³C NMR (101 MHz, CDCl₃)



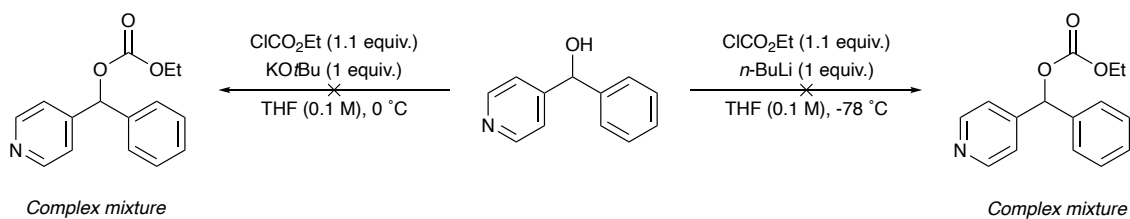
Synthesis of **2-12**

In an atmosphere-controlled glove box, a 20 mL vial equipped with a 1 cm stir-bar was charged with NaH (1.1 eq, 11 mg, 0.439 mmol) and sealed with a septum. The vial was removed from the glove box and purged with argon. A solution of **2-11** (74 mg, 1 eq, 0.399 mmol) in anhydrous THF (4 mL, [0.1 M] w.r.t. **2-11**) was added to the vial slowly at room temperature and stirred for 30 minutes. The solution was cooled to 0 °C, after which, neat ethyl chloroformate (1 eq, 0.04 mL, 0.399 mmol) was added dropwise. The solution was warmed to room temperature and stirred for an additional 30 minutes before being quenched with distilled water (10 mL). The mixture was diluted with EtOAc (10 mL) and the aqueous phase was extracted with EtOAc (x2 5 mL). The organic phases were dried over Na₂SO₄ and concentrated *in vacuo*. The crude carbonate ester was dry loaded on silica (300 mg) and purified by auto-flash chromatography (4g FlashPure EcoFlex, EtOAc/Hexanes, 0 – 60% over 12 column volumes) to give an inseparable mixture of **2-12** and 4-benzoyl pyridine (30% mass).

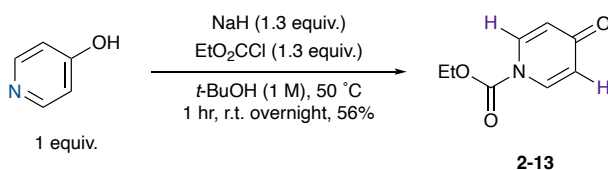
Data for **2-12**

¹H NMR (300 MHz, CDCl₃) δ 8.66 – 8.45 (m, 2H), 7.40 – 7.31 (m, 5H), 7.31 – 7.26 (m, 2H), 6.63 (s, 1H), 4.22 (d, J = 7.14 Hz, 2H), 1.32 (t, J = 7.14 Hz, 3H).

Unsuccessful attempts to synthesize pure **2-12**



Synthesis of **2-13**



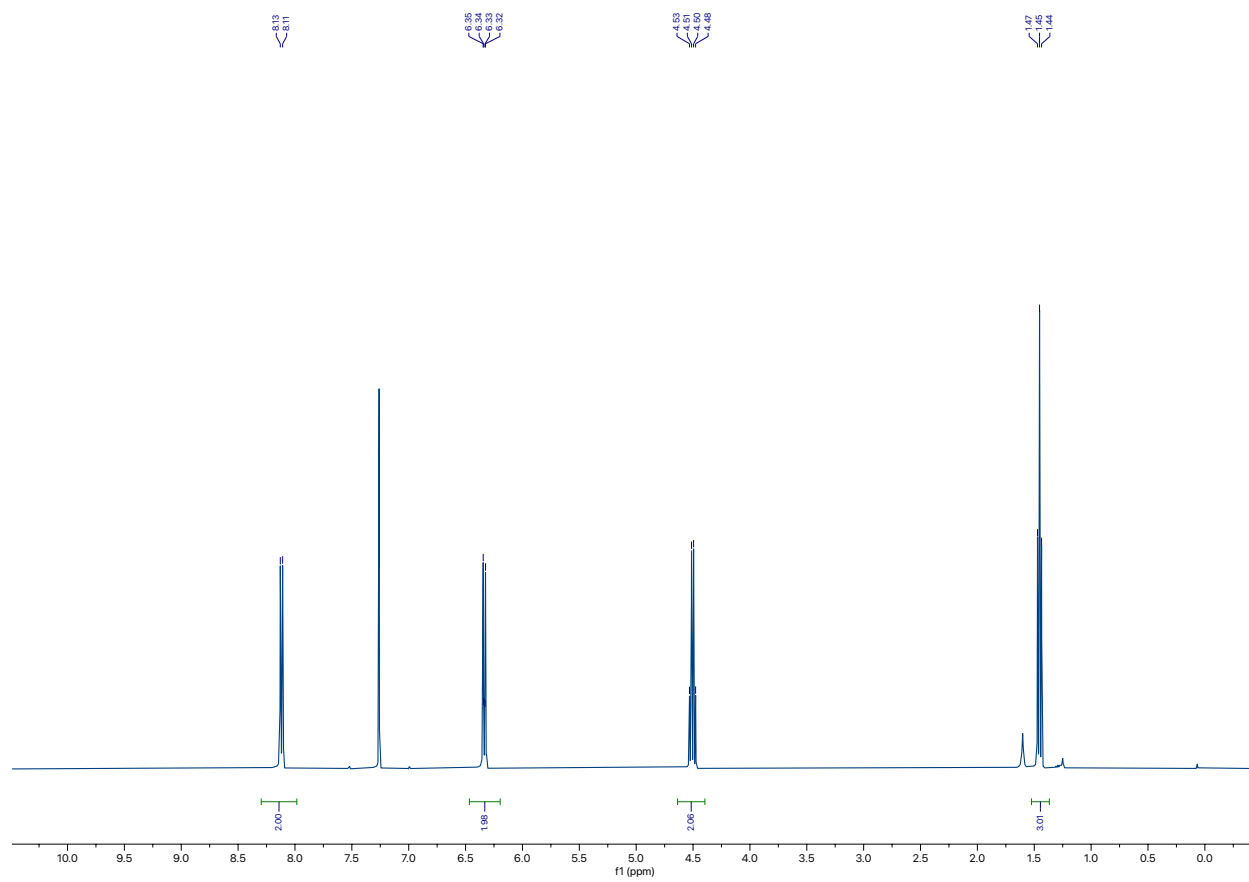
In an atmosphere-controlled glove box, a 20 mL vial equipped with a 1 cm stir-bar was charged with NaH (1.3 eq, 93 mg, 3.88 mmol) and sealed with a septum. The vial was removed from the glove box and purged with argon. A solution of 4-hydroxy pyridine (284 mg, 1.0 eq, 2.99 mmol) in *t*-butanol (3 mL, [1 M] w.r.t. 4-hydroxy pyridine) was added to the vial slowly at room temperature and stirred for 10 minutes. The solution was warmed to 50 °C and stirred for 15 minutes, after which, neat ethyl chloroformate (1.3 eq, 0.37 mL, 3.8 mmol) was added dropwise. The solution was stirred at temperature for 1 hour and left to cool to room temperature overnight. The mixture was quenched with distilled water (5 mL) and diluted with EtOAc (15 mL). The aqueous phase was extracted with EtOAc (x2 10 mL). The organic phases were dried over Na₂SO₄ and concentrated *in vacuo*. The crude carbamate dry loaded on silica (1 g) and purified by auto-flash chromatography (12g FlashPure EcoFlex, MeOH/EtOAc, 0 – 100% over 6 column volumes) to give **2-13** as an off-white solid (56%, 280 mg) found to be consistent with reported literature.^[43]

Data for **2-13**

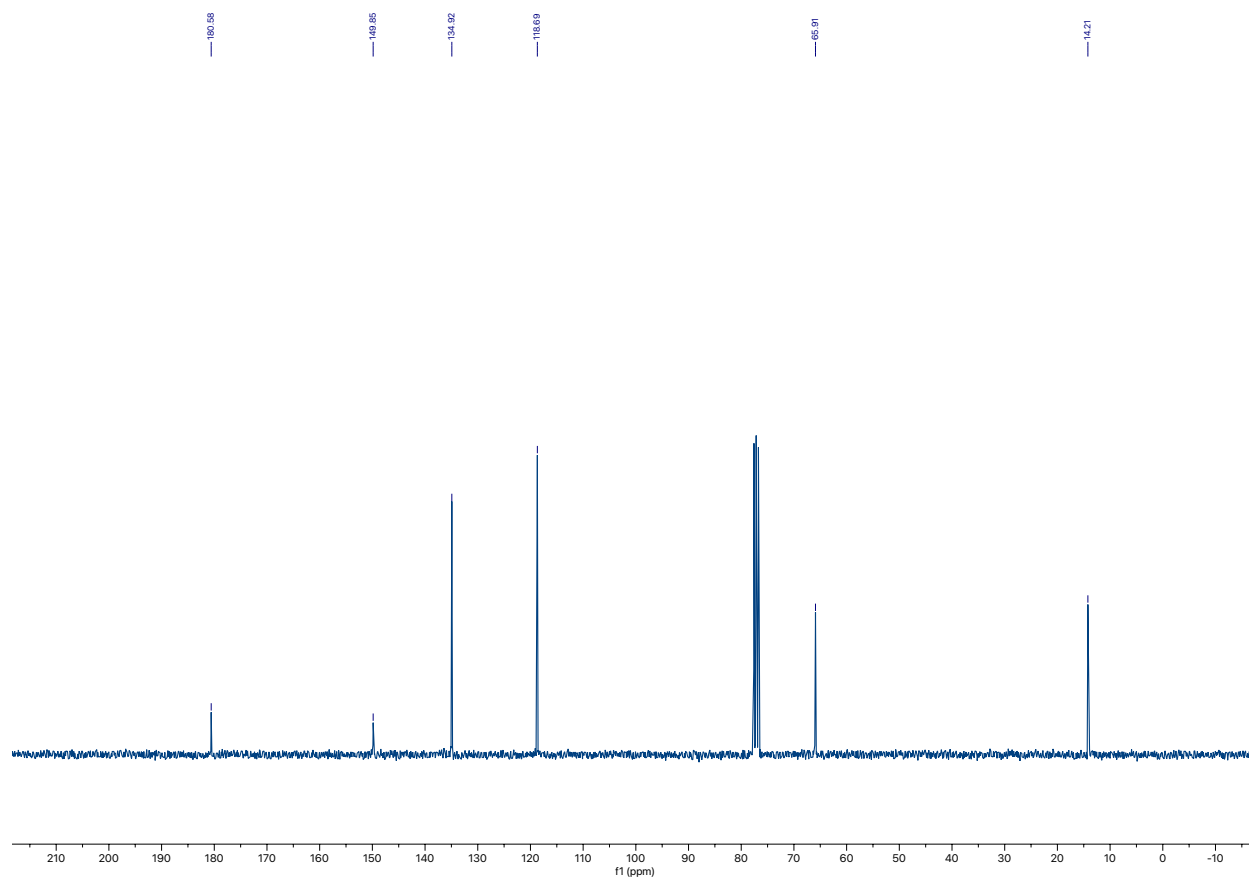
¹H NMR (400 MHz, CDCl₃) δ 8.16 – 8.08 (m, 2H), 6.38 – 6.29 (m, 2H), 4.50 (q, J = 7.13 Hz, 2H), 1.45 (t, J = 7.13 Hz, 3H).

¹³C NMR (75 MHz, CDCl₃) δ 180.58, 149.85, 134.92, 118.69, 65.91, 14.21.

2-13 1H NMR (400 MHz, CDCl3)



2-13 13C NMR (75 MHz, CDCl3)



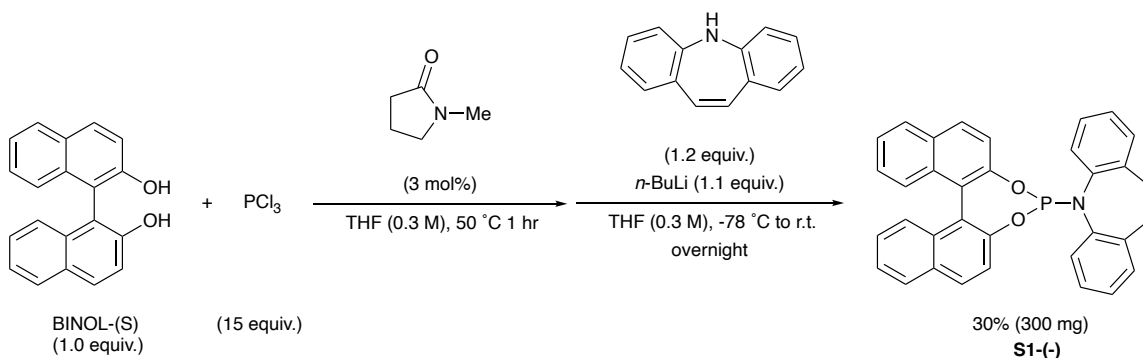
4.2.1 Chapter 3 Experimental

General Considerations

All reactions were conducted in flame- or oven-dried glassware under an atmosphere of argon using anhydrous solvents unless specified otherwise. Tetrahydrofuran (THF) and diethylether (Et₂O) were dried using an INERT® PureSolv solvent purification system. Commercial reagents were used as received. Thin-layer chromatography was performed on SiliCycle® silica gel 60 F254 plates. Visualization was carried out using UV light (254 nm) and/or KMnO₄. Flash column chromatography was carried out using SiliCycle® SiliaFlash® silica gel (230-400 mesh, 40- 63 μ, 60 Å pore size). Hexanes (ACS grade), Toluene (ACS grade) and ethyl acetate (ACS grade) were used as received. ¹H-NMR and ¹³C-NMR spectra were recorded on a Bruker 400 AV or Bruker 300 AV spectrometer in chloroform-d (99.8% deuterated). Spectra recorded using chloroform were calibrated to 7.26 ppm ¹H and 77.16 ppm ¹³C. *p*-Anisaldehyde was used as internal standard for quantitative ¹H NMR analysis (d1 30s). Chemical shifts (δ) are reported in ppm and multiplicities are indicated by s (singlet), d (doublet), t (triplet), q (quartet), p (quintet), sext (sextet), sept (septet), dd (doublet of doublets), dt (doublet of triplets), td (triplet of doublets), tt (triplet of triplets), qd (quartet of doublets), ddd (doublet of doublet of doublets), tdd (triplet of doublet of doublets), dddd (doublet of doublet of doublet of doublets), m (multiplet) and br (broad). Coupling constants J are reported in Hertz (Hz).

4.2.2 Starting Material Synthesis (S1, 3-1, 3-2, 3-3)

Synthesis of Carreira Ligand **S1** (+/-) or (-)



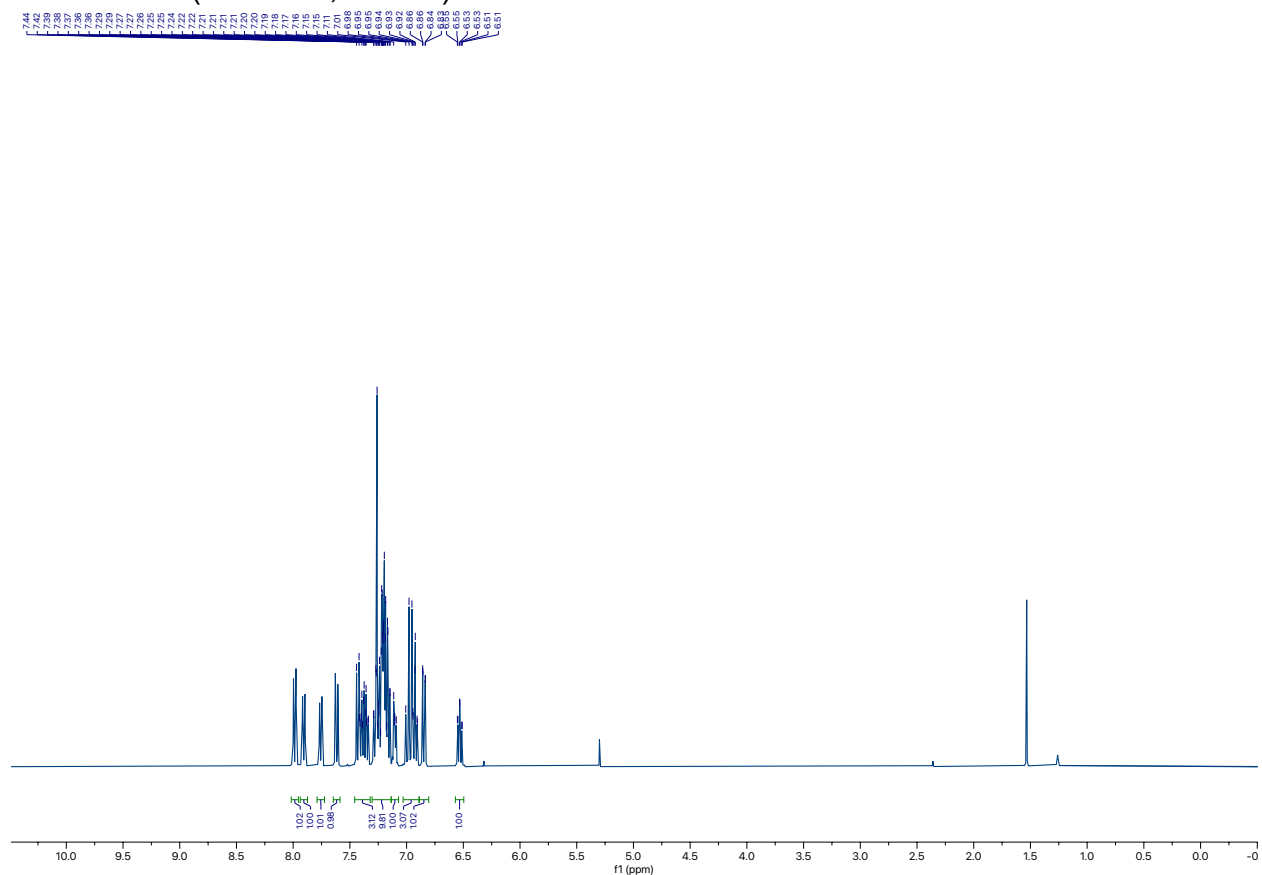
To a 100 mL round-bottom flask equipped with a stir bar, BINOL-(S or S/R) (564 mg, 1.97 mmol), NMP (9.8 mg, 0.0985 mmol) was dissolved in 5 mL of anhydrous THF. The flask was vented with argon at which point PCl₃ (2.6 mL, 29.5 mmol) was added dropwise. The reaction was heated to 50 °C for 1 hr, after which the mixture was concentrated *in vacuo* to remove excess PCl₃. Concurrently, to a 100 mL round-bottom flask equipped with a stir bar, iminostilbene (457 mg, 2.36 mmol) was dissolved in 10 mL of anhydrous THF and cooled to -78 °C. After stirring at -78 °C for 5 minutes, *n*-BuLi (1.35 mL, 2.16 mmol, 1.6 M) was added dropwise to form an intensely dark colored solution and stirred at temperature for 30 minutes. Crude BINOL phosphorus chloride was dissolved in 10 mL of anhydrous THF and added dropwise to the lithiated iminostilbene at -78 °C and stirred at temperature for 30 minutes. The mixture is warmed to room temperature overnight and concentrated *in vacuo* crude foamy solid which was dry loaded on to 1500 mg of silica. The dry load was purified by flash-column chromatography (30:70, Toluene:Hexanes) to give **S1**(-) or (+/-) as an off white solid (30%, 300 mg, 0.591 mmol), found to be consistent with reported literature.^[36]

Data for S1

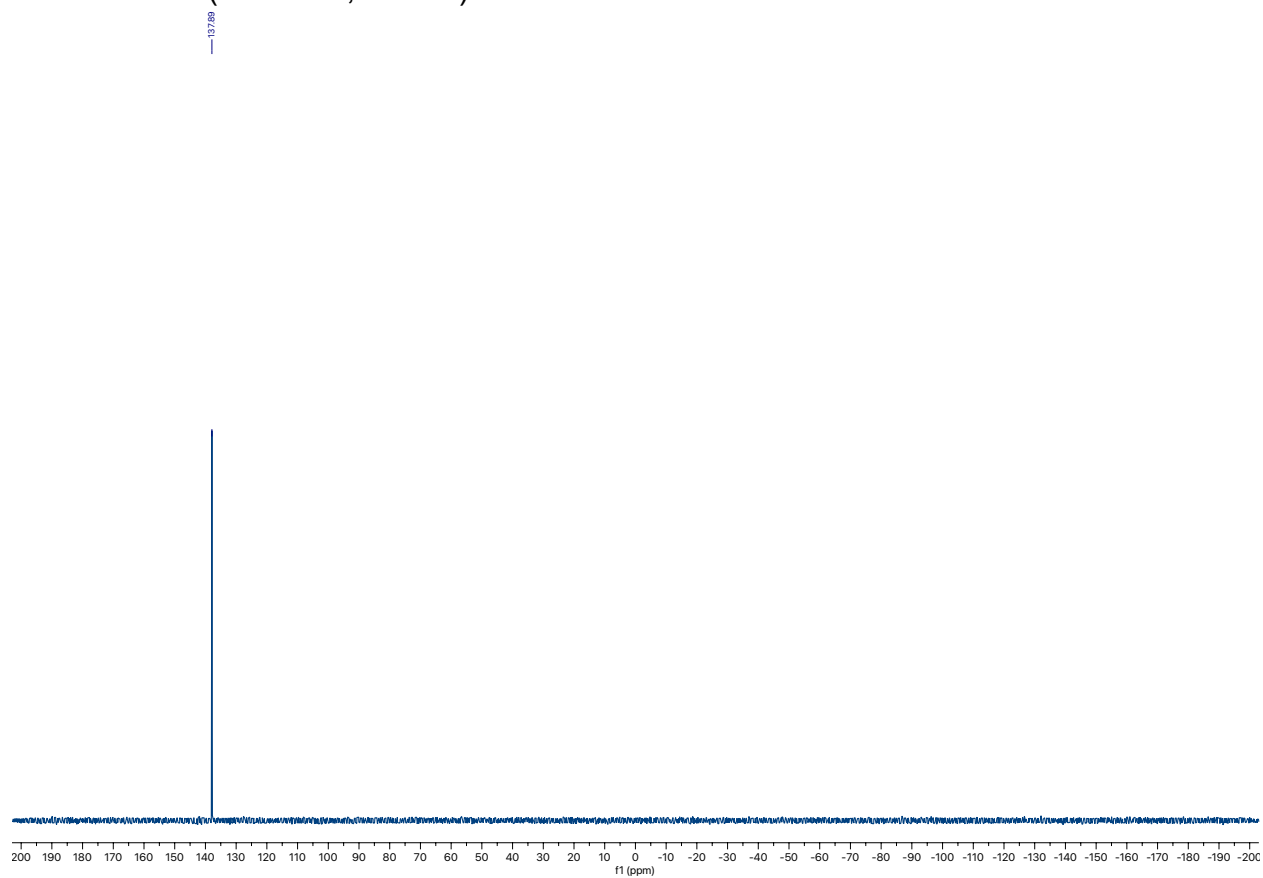
^1H NMR (400 MHz, CDCl_3) δ 7.99 (d, $J = 8.8$ Hz, 1H), 7.91 (dd, $J = 8.1, 1.2$ Hz, 1H), 7.76 (dt, $J = 8.1, 0.9$ Hz, 1H), 7.62 (dd, $J = 8.8, 0.9$ Hz, 1H), 7.46 – 7.32 (m, 3H), 7.30 – 7.14 (m, 10H), 7.14 – 7.07 (m, 1H), 7.03 – 6.89 (m, 3H), 6.85 (dd, $J = 8.8, 0.8$ Hz, 1H), 6.53 (td, $J = 7.7, 1.6$ Hz, 1H).

^{31}P NMR (162 MHz, CDCl_3) δ 137.89.

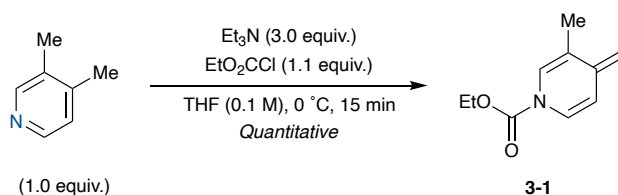
S1 ^1H NMR (400 MHz, CDCl_3)



S1 31P NMR (162 MHz, CDCl3)



Synthesis of ADHP **3-1**



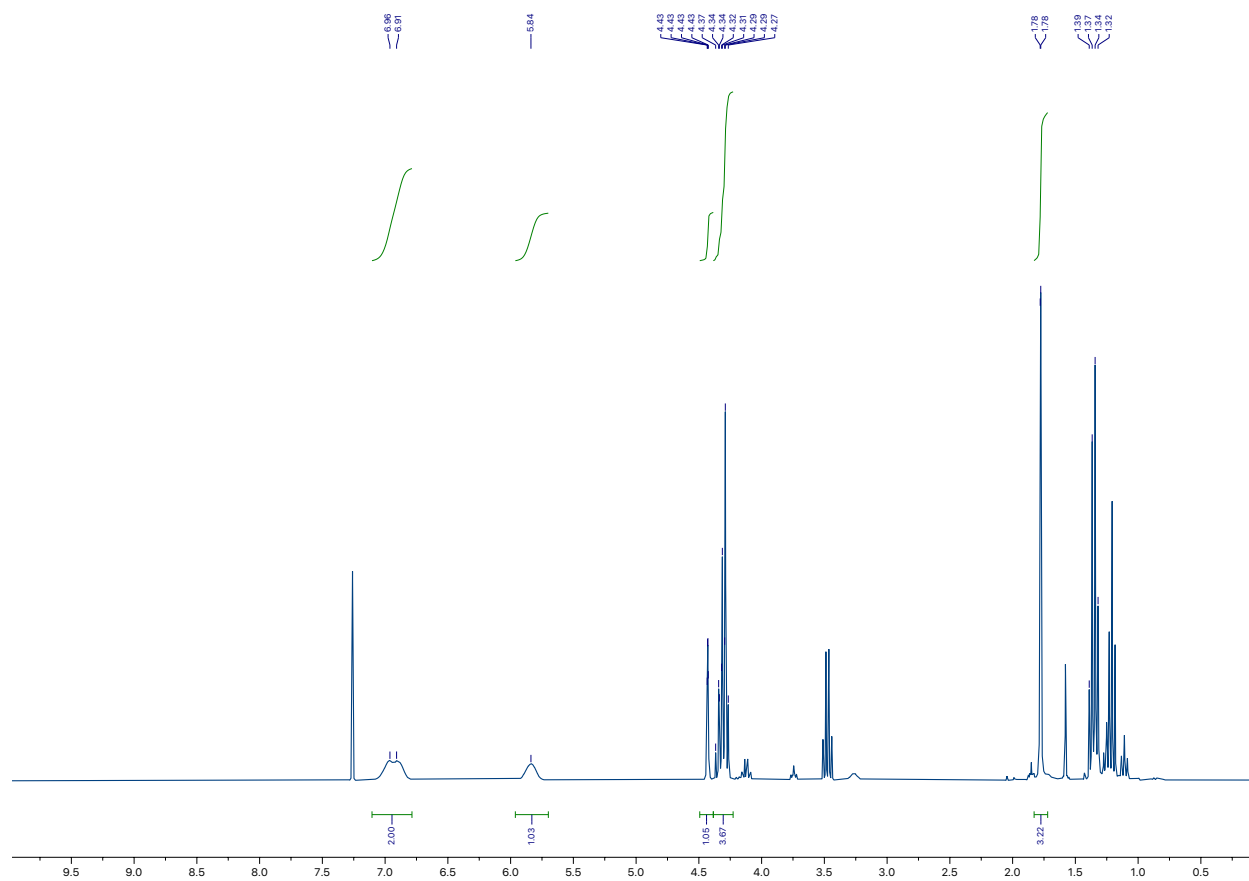
Following our general procedure for ADHP synthesis,^[7] A round-bottom flask (25 mL) was charged with 3,4-Lutidine (50 mg, 0.47 mmol, 1 equiv.), THF (4.7 mL) and triethyl amine (0.20 mL, 1.4 mmol, 3 equiv.). The flask was cooled with an ice bath for 5 minutes, followed by drop wise addition of ethyl chloroformate (0.05 mL, 0.5 mmol, 1.1 equiv.). After 15 minutes, the mixture was concentrated *in vacuo* and triturated with ether (15 mL). Ether was removed *in vacuo* to give the crude ADHP (**3-1**) as a yellow oil and used immediately without further purification.

Data for **3-1**

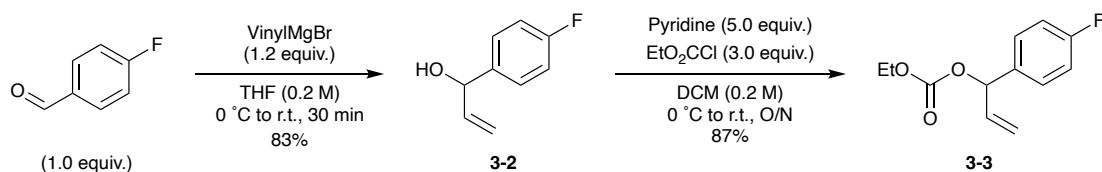
$^1\text{H-NMR}$ (300 MHz, CDCl_3)

δ 6.9 (br d, 2H), 5.8 (br s, 1H), 4.4 (s, 1H), 4.3 – 4.2 (m, 3H), 1.7 (s, 3H), 1.4 – 1.3 (m, 3H).

3-1 ¹H NMR (300 MHz, CDCl₃)



Synthesis of **3-2**



To a 200 mL round bottom flask equipped with a stir bar, 4-fluoro benzaldehyde (2.44 g, 19.66 mmol) was dissolved in anhydrous THF (100 mL) and cooled to 0 °C. VinylMgBr (23.6 mmol, 23.6 mL, 1M in THF) was added dropwise over 5 minutes and the reaction was warmed to room temperature to stir for 30 minutes. After checking with TLC, 50 mL of saturated aqueous NH₄Cl was added and the aqueous phase is extracted with EtOAc (3x 40 mL). The organics were collected and dried over Na₂SO₄ and concentrated *in vacuo* to give crude **3-2**. The crude alcohol was purified by flash-column chromatography (20:80 EtOAc:Hexanes) to give **3-2** as a pale yellow oil (83%, 2.48 g, 16.32 mmol) that is consistent with reported literature.^[44]

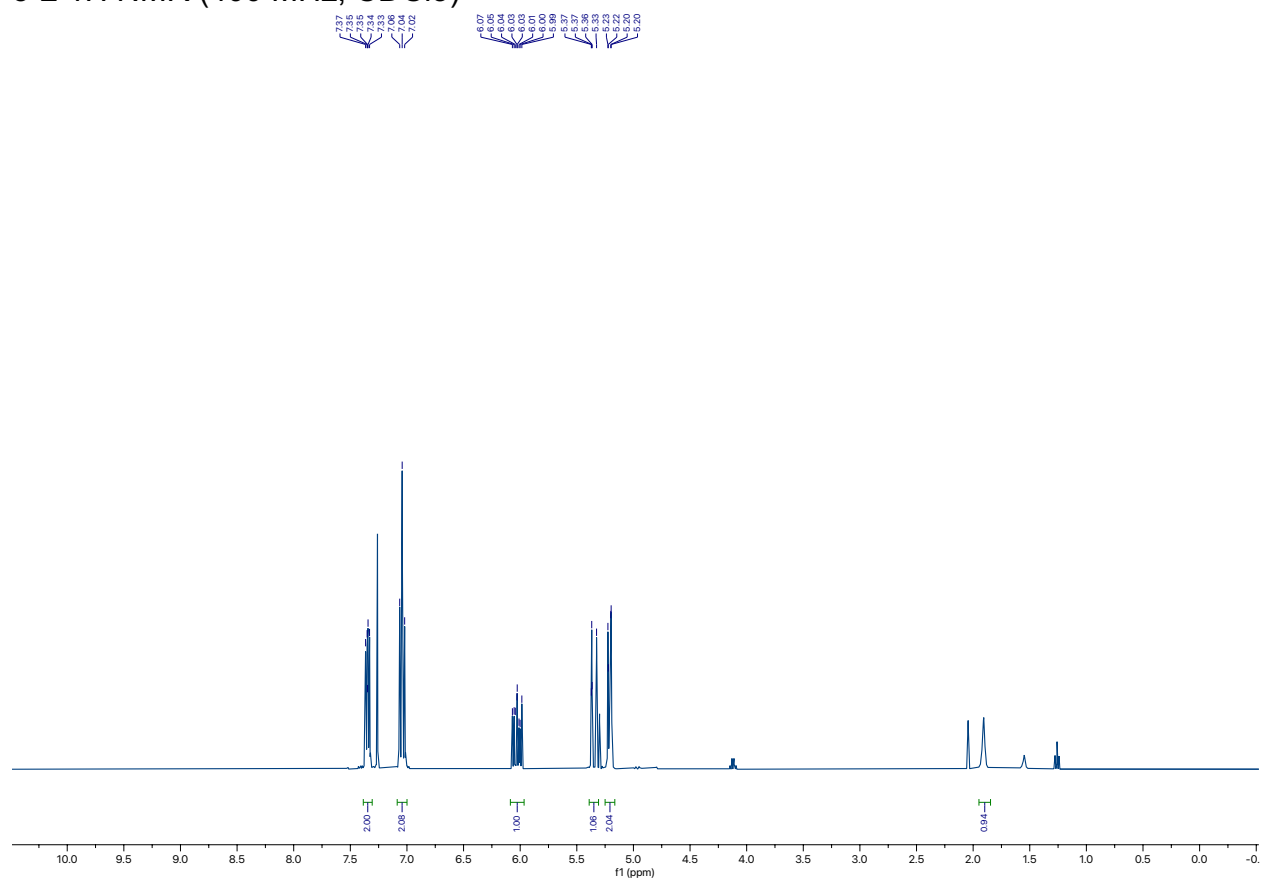
Data for **3-2**

¹H NMR (400 MHz, CDCl₃) δ 7.39 – 7.31 (m, 2H), 7.04 (t, J = 8.7 Hz, 2H), 6.03 (ddd, J = 17.2, 10.1, 6.1 Hz, 1H), 5.39 – 5.31 (m, 1H), 5.25 – 5.16 (m, 2H), 1.91 (bs, 1H).

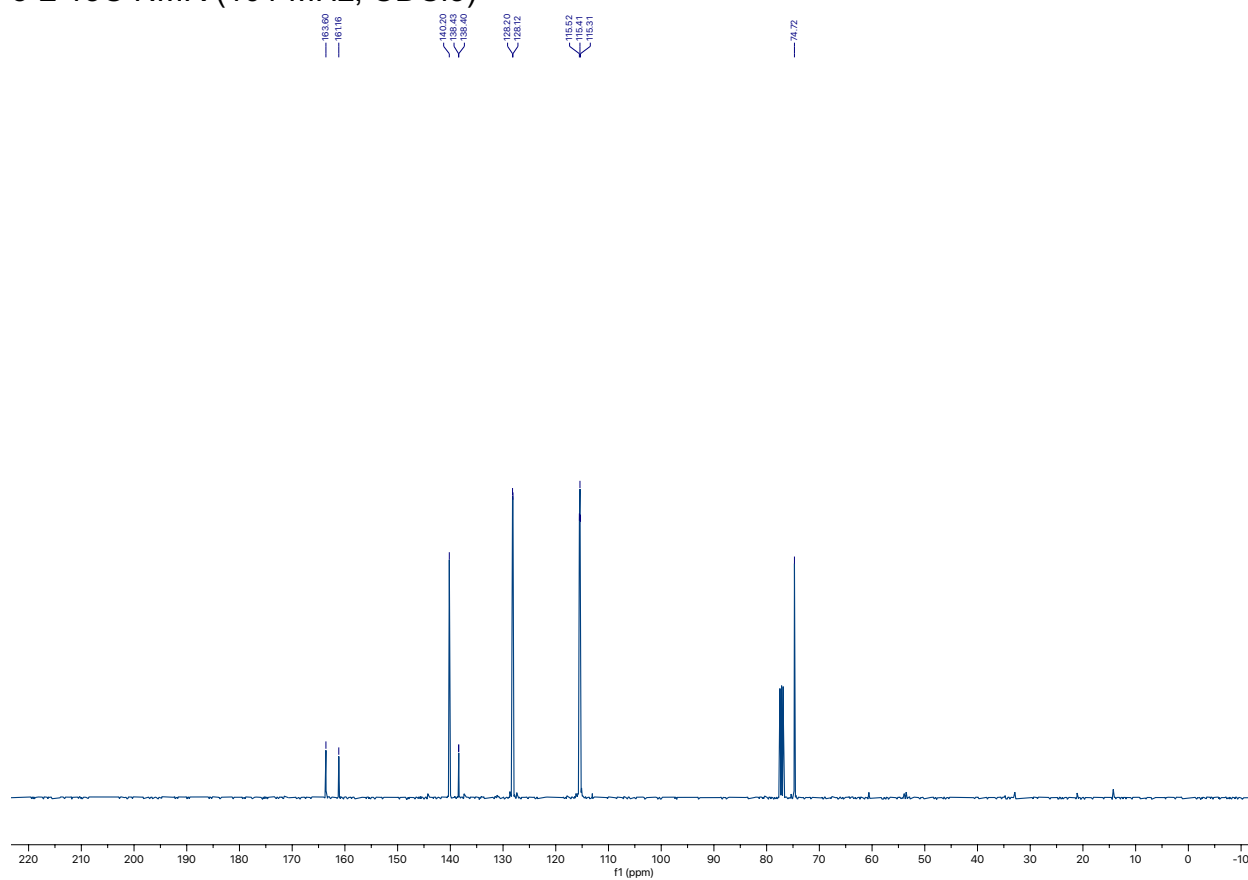
¹³C NMR (101 MHz, CDCl₃) δ 163.60, 161.16, 140.20, 138.43, 138.40, 128.20, 128.12, 115.52, 115.41, 115.31, 74.72.

¹⁹F NMR (377 MHz, CDCl₃) δ -114.83.

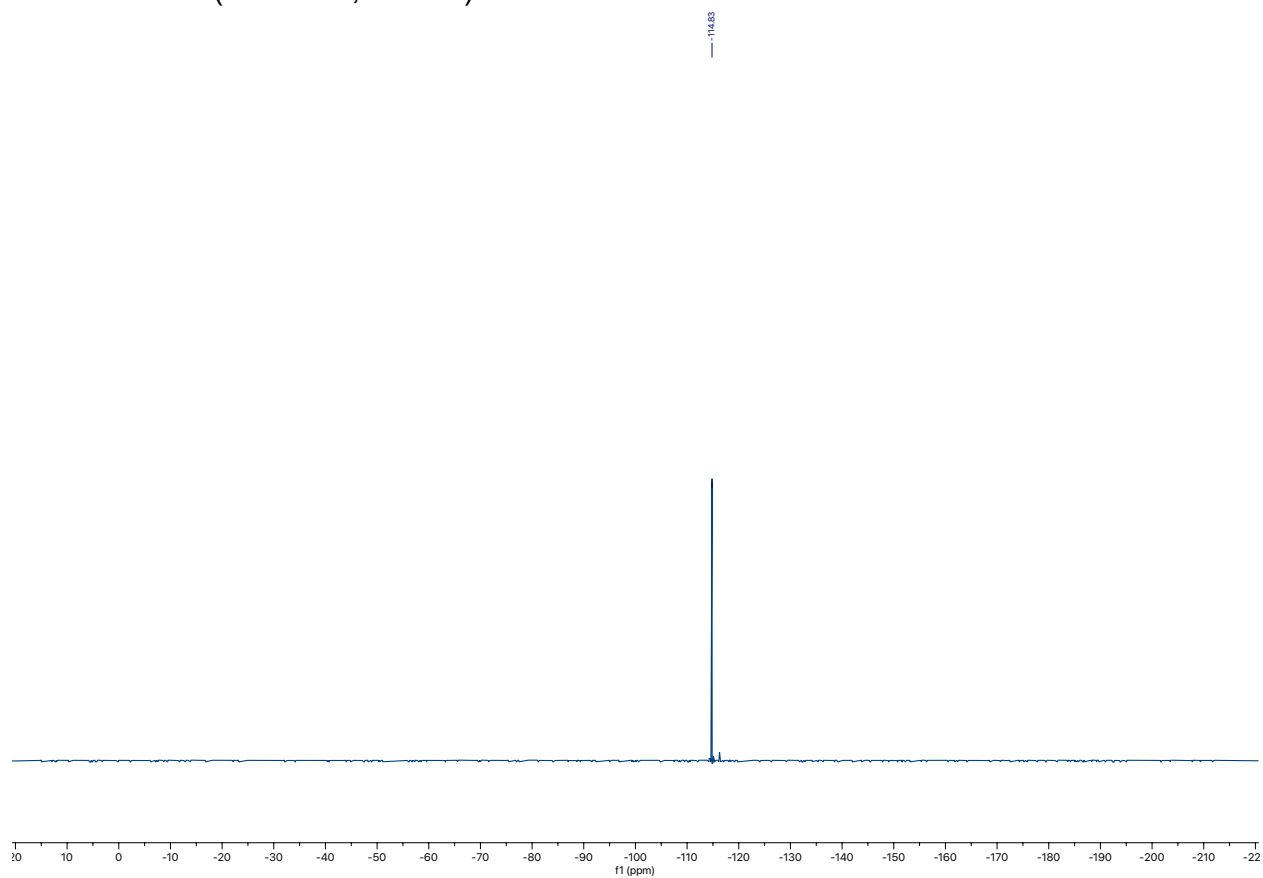
3-2 1H NMR (400 MHz, CDCl3)



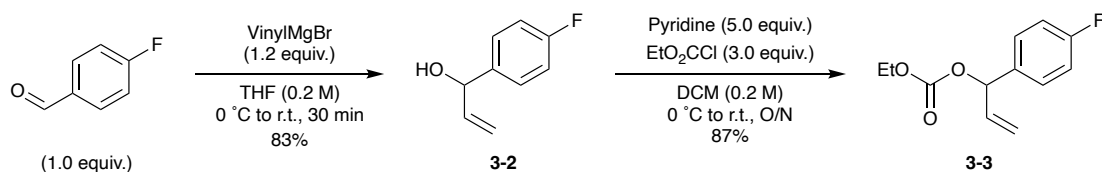
3-2 ¹³C NMR (101 MHz, CDCl₃)



3-2 ¹⁹F NMR (377 MHz, CDCl₃)



Synthesis of **3-3**



To a 100 mL round bottom flask equipped with a stir bar, **3-2** (1.45 g, 9.54 mmol) and pyridine (3.8 mL, 47.7 mmol) was dissolved in anhydrous DCM (48 mL) and cooled to 0 °C. Ethyl chloroformate (28.6 mmol, 2.74 mL) was added dropwise over 3 minutes and the reaction was warmed to room temperature to stir overnight. After checking with TLC, 100 mL of distilled water was added, and organic phase was extracted with distilled water (3x 50 mL). The organic layer was dried over Na₂SO₄ and concentrated *in vacuo* to give crude **3-3**. The crude carbonate was purified by flash-column chromatography (05:95 EtOAc:Hexanes) to give **3-3** as a clear oil (87%, 1.85 g, 8.31 mmol) that is consistent with reported literature.^[45]

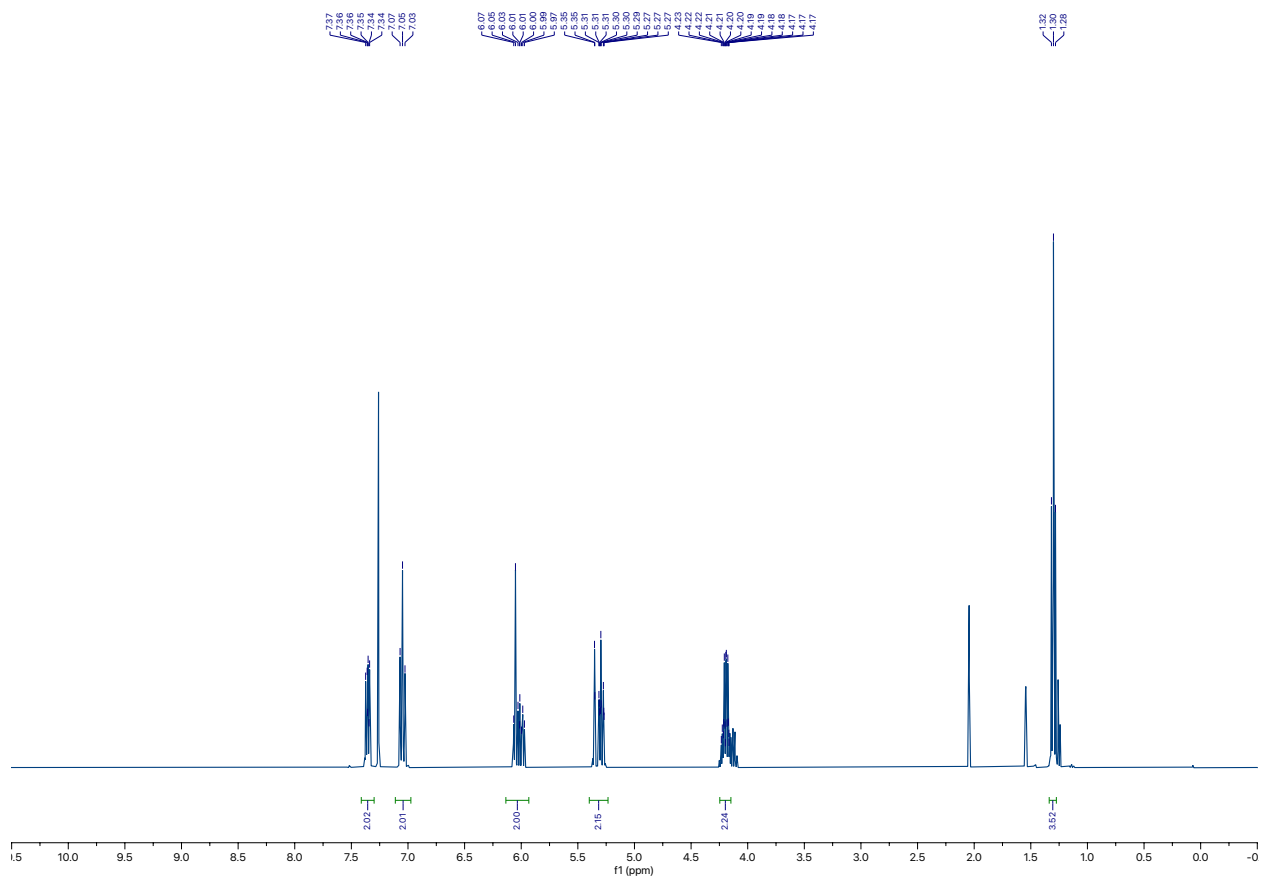
Data for **3-3**

¹H NMR (400 MHz, CDCl₃) δ 7.41 – 7.30 (m, 2H), 7.11 – 6.97 (m, 2H), 6.14 – 5.93 (m, 2H), 5.40 – 5.23 (m, 2H), 4.25 – 4.15 (m, 2H), 1.34 – 1.27 (m, 3H).

¹³C NMR (101 MHz, CDCl₃) δ 163.95, 161.50, 154.39, 135.76, 134.34, 134.31, 129.15, 129.06, 117.54, 115.67, 115.46, 79.21, 64.19, 14.25.

¹⁹F NMR (377 MHz, CDCl₃) δ -113.51.

3-3 1H NMR

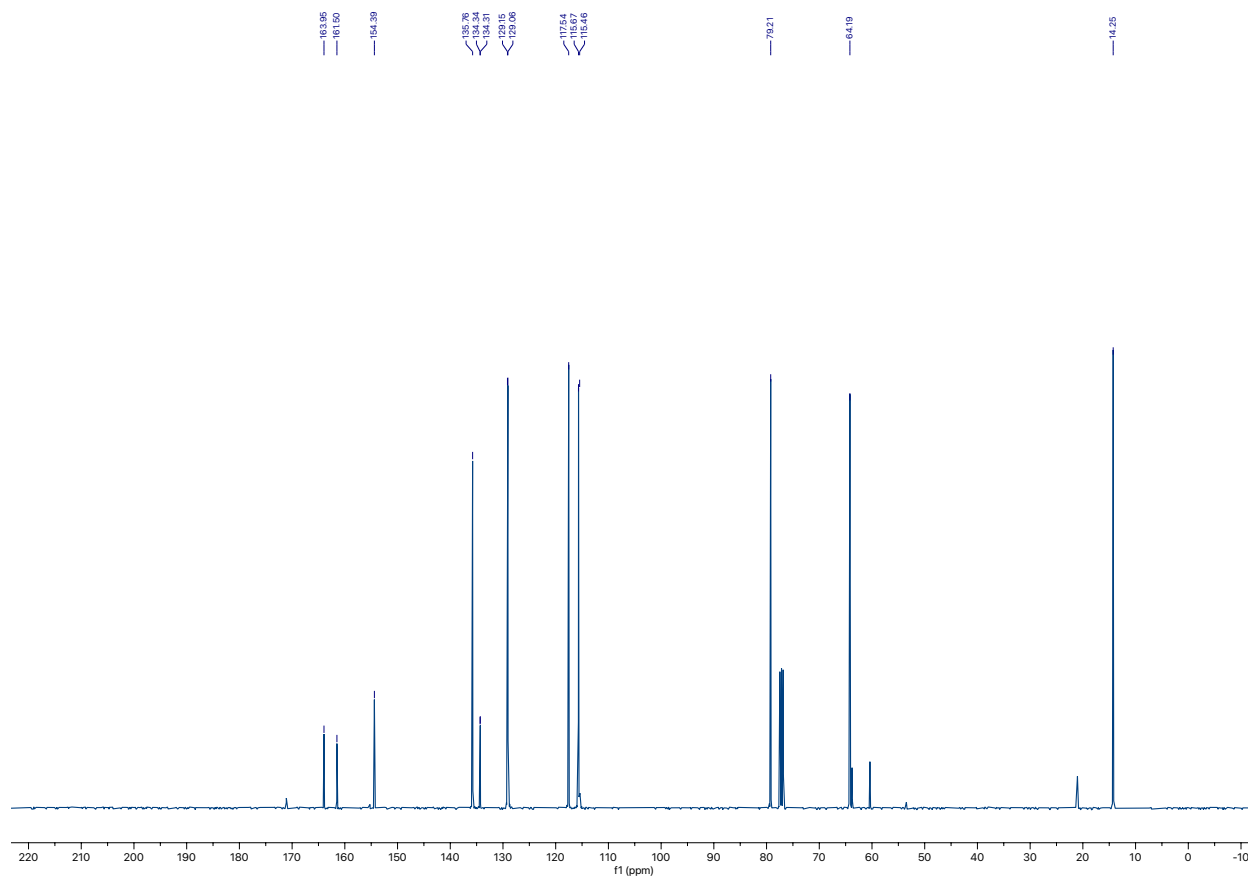


Ethyl acetate Impurity: 1H NMR (400 MHz, CDCl₃) δ 4.13-4.09, 2.04, 1.26-1.24.

1H NMR (400 MHz, CDCl₃)

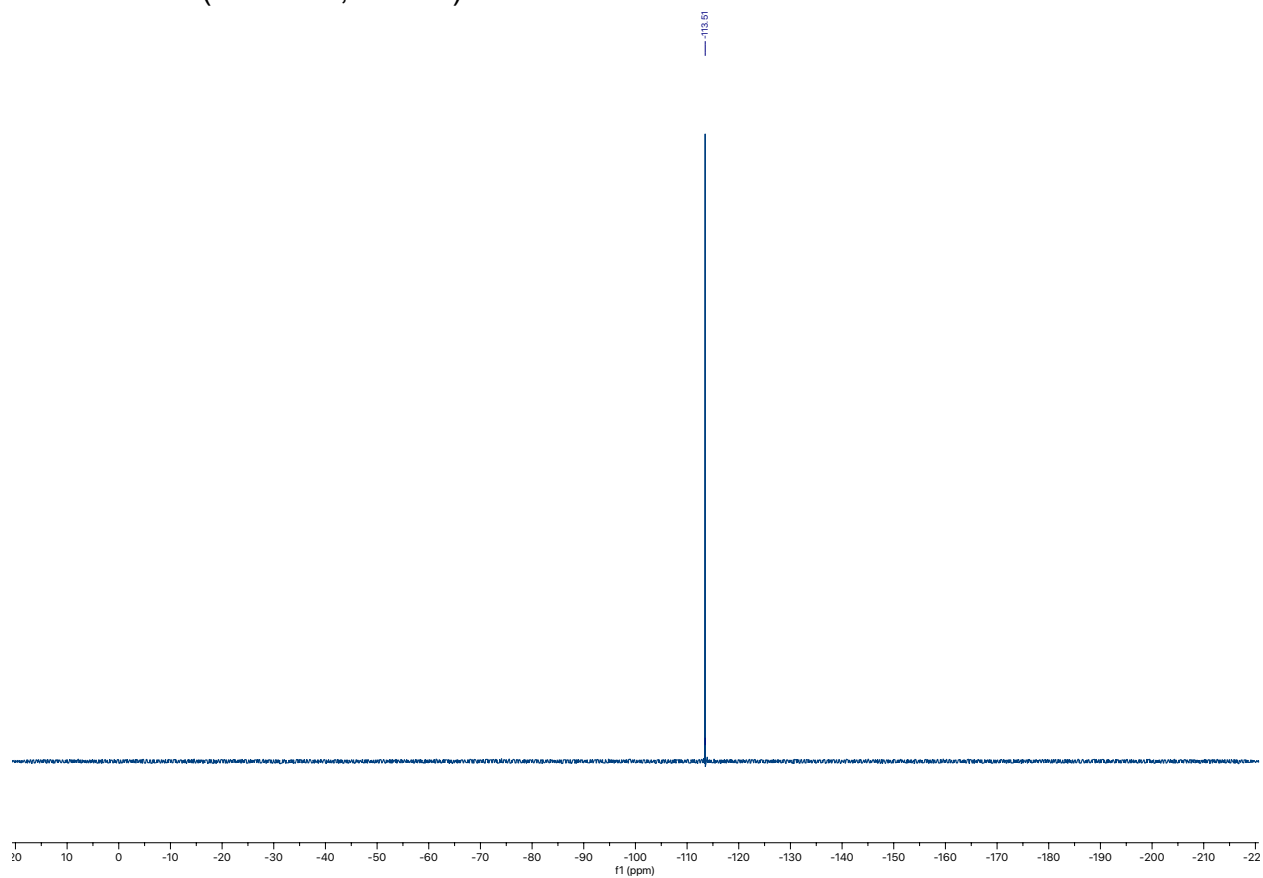
δ 7.41 – 7.30 (m, 2H), 7.11 – 6.97 (m, 2H), 6.14 – 5.93 (m, 2H), 5.40 – 5.23 (m, 2H), 4.25 – 4.15 (m, 2H), 1.34 – 1.27 (m, 3H).

3-3 ¹³C NMR



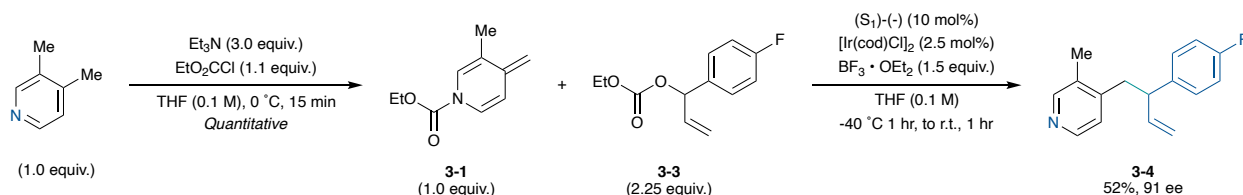
Ethyl acetate Impurity: ¹³C NMR (101 MHz, CDCl₃) δ 171.10, 63.78, 60.39, 21.02.

3-3 ^{19}F NMR (377 MHz, CDCl_3) δ -113.51.



4.2.3 Iridium-catalyzed Allylation of ADHPs General Procedure

Synthesis of **3-4**



Alongside the preparation of ADHP (**3-1**, 0.467 mmol), $[\text{Ir}(\text{cod})\text{Cl}]_2$ (7.8 mg, 0.0117 mmol, 2.5 mol%) and Carreira Ligand **S1** (*S*)-(-)-99% (23.7 mg, 0.0467 mmol, 10 mol%) is weighed into a round-bottom flask (10 mL) under a blanket of argon. Allyl carbonate **3-3** (235.6 mg, 1.05 mmol, 2.25 equiv.) was added as a solution in THF (2.5 mL), and the bright orange solution was stirred for 20 minutes, at which point turned clear yellow. The reaction was cooled to -40°C with acetonitrile/dry ice or ethylene glycol/ethanol/dry ice bath for 5 minutes. $\text{BF}_3 \cdot \text{OEt}_2$ (0.09 mL, 0.7 mmol, 1.5 equiv.) was added drop wise to the reaction and stirred for 15 minutes. Freshly prepared ADHP (**3-1**) was added dropwise to the reaction in a solution of THF (2 mL), resulting in a slow change in color to orange. The reaction was stirred at -40°C for 1 hr and left to warm up to room temperature over 1 hour. The reaction was quenched with 4 mL of aqueous NH_3 solution (28% w/w). The reaction mixture was extracted with DCM (3 x 5 mL) and the collected organic extracts are dried over sodium sulphate. After filtration and concentration *in vacuo*, the crude mixture was dry loaded on to 2.5 mL of silica and purified by flash column chromatography (20:80 EtOAc:Toluene) to give the branched allylated product (**3-4**, 87 mg, 0.36 mmol, Yield 52 %, 91 ee).

Data for **3-4**

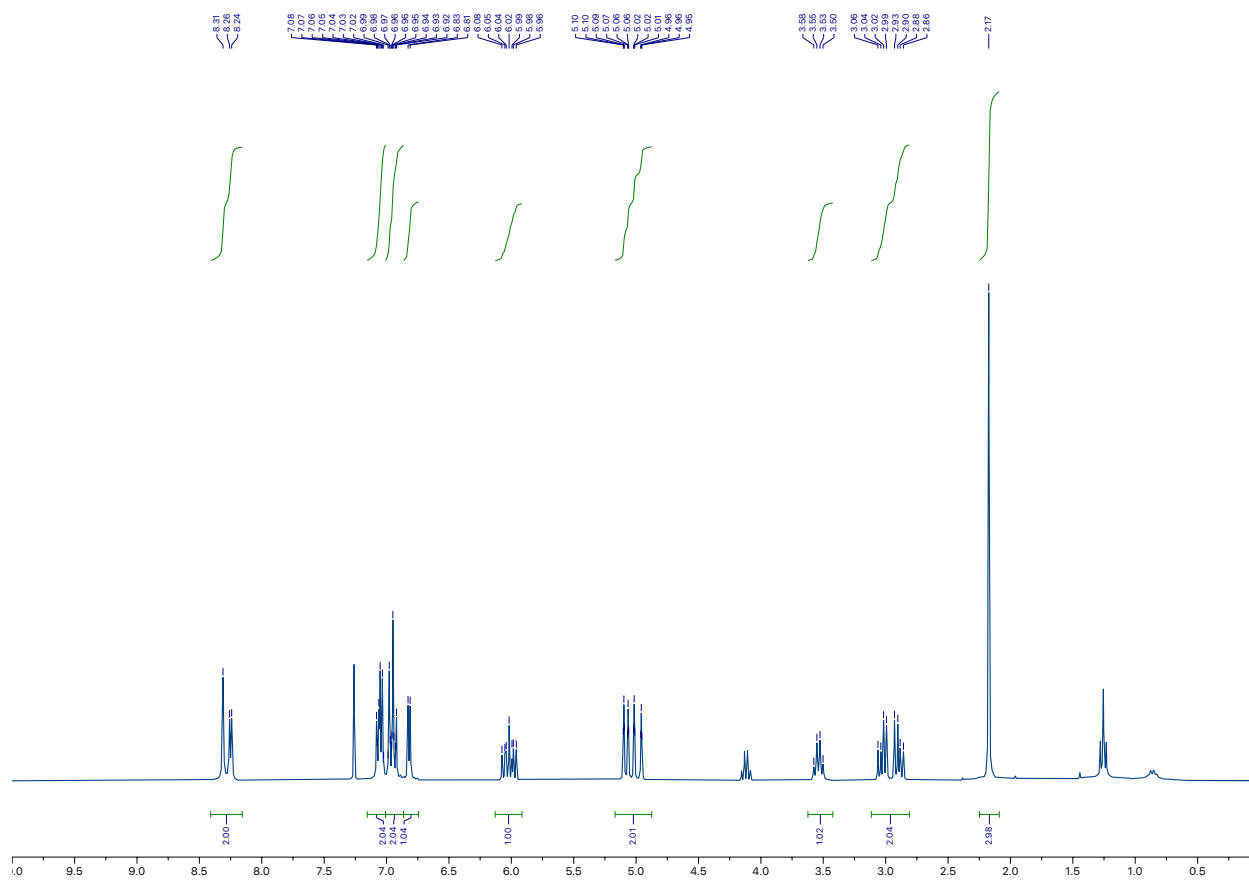
$^1\text{H-NMR}$ (300 MHz, CDCl_3) δ 8.4 – 8.2 (m, 2H), 7.1 (ddd, $J = 8.4, 5.4, 2.6$ Hz, 2H), 7.0 – 6.9 (m, 2H), 6.8 (d, $J = 5.0$ Hz, 1H), 6.0 (ddd, $J = 17.3, 10.3, 7.1$ Hz, 1H), 5.2 – 4.9 (m, 2H), 3.5 (q, $J = 7.4$ Hz, 1H), 3.1 – 2.8 (m, 2H), 2.17 (s, 3H).

$^{13}\text{C-NMR}$ (75 MHz, CDCl_3) δ 163.3, 160.1, 150.9, 147.3, 146.9, 140.4, 138.5,

138.5, 131.9, 129.2, 129.1, 124.5, 115.5 -115.2 (m),
48.8, 38.6, 16.2.

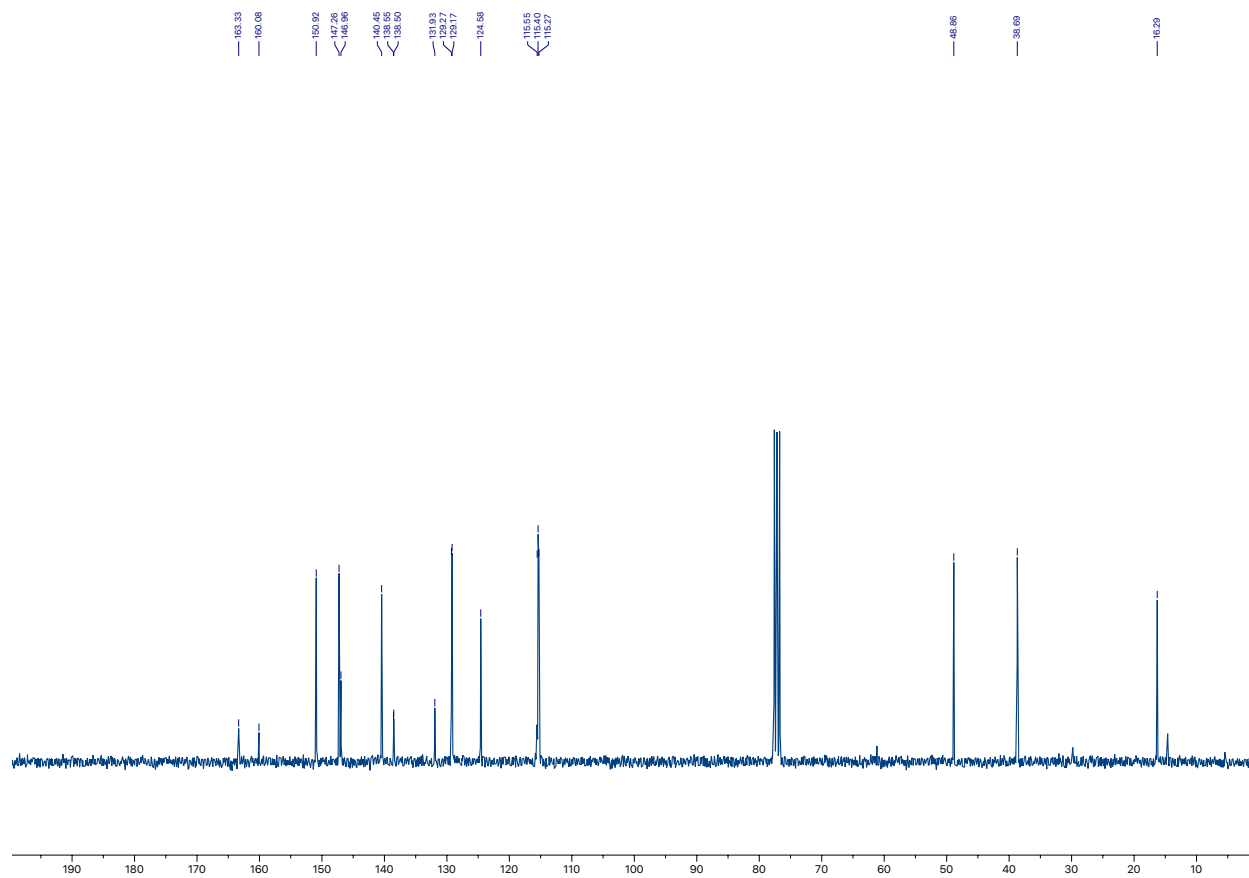
¹⁹F-NMR (282 MHz, CDCl₃) δ -116.2 ppm.

3-4 ¹H NMR (300 MHz, CDCl₃)

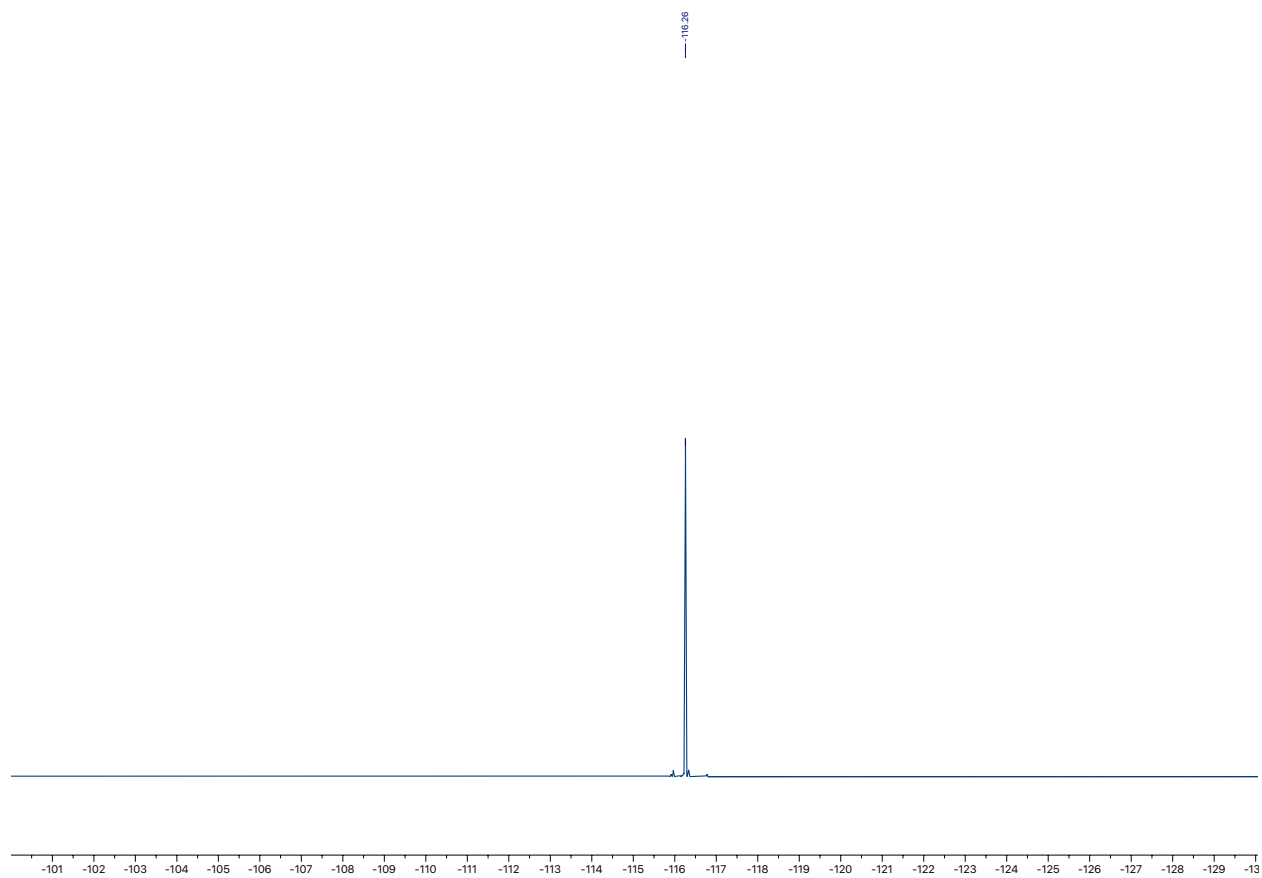


Unknown Impurity: ¹H NMR (400 MHz, CDCl₃) δ 4.13-4.09, 1.26-1.24.

3-4 ^{13}C NMR (75 MHz, CDCl_3)



3-4 ^{19}F NMR (282 MHz, CDCl_3)



^{19}F -NMR (282 MHz, CDCl_3)

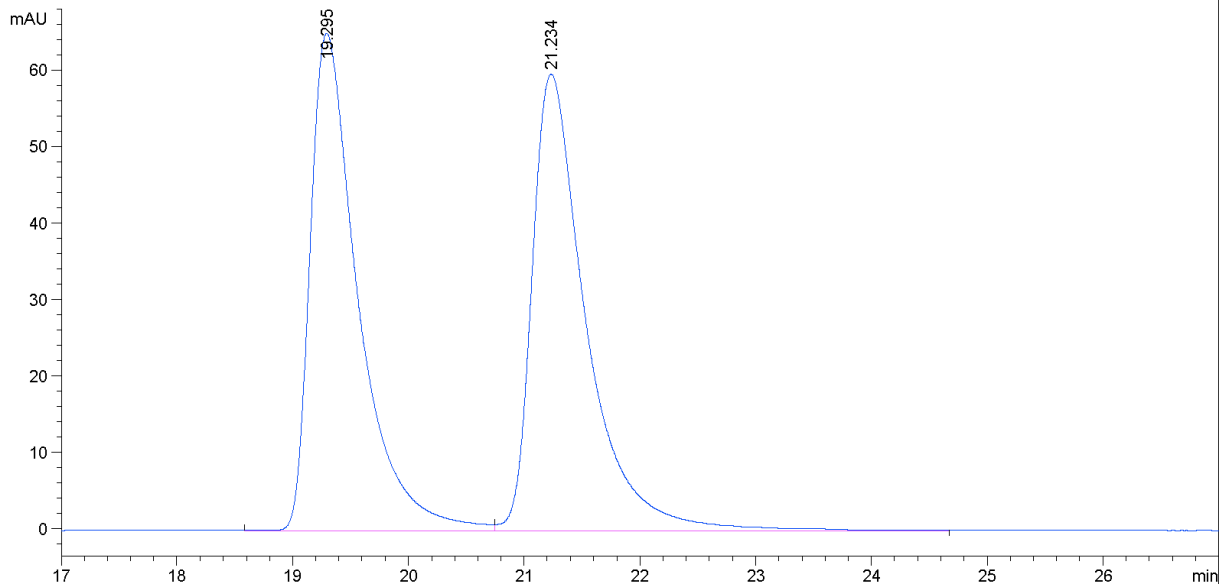
$\delta -116.2$ ppm.

4.2.4 Optimization Experiments HPLC Trace

General HPLC Method

Enantiomer resolution was performed with an Agilent 1200 series HPLC and chiral resolution column is a Daicel CHIRALPAK-IC, with Internal diameter 4.6 mm, length 180 mm and particle size 3.0 μm . Ideal flow rate and solvent composition for enantiomer resolution at 0.750mL/min 90% Heptane (HPLC Grade), 10% Isopropyl Alcohol (HPLC Grade). HPLC samples are diluted to 1mg/mL in HPLC grade Heptane: Isopropanol (90:10) with a 5.0 μL injection volume.

3-4 RACEMIC



Data File C:\CHEM32\..._01_2021-IC-90_10-HEPT_IPROH 2021-04-01 11-50-35\BD-05-57-RACEMIC.D
Sample Name: BD-05-57-Racemic

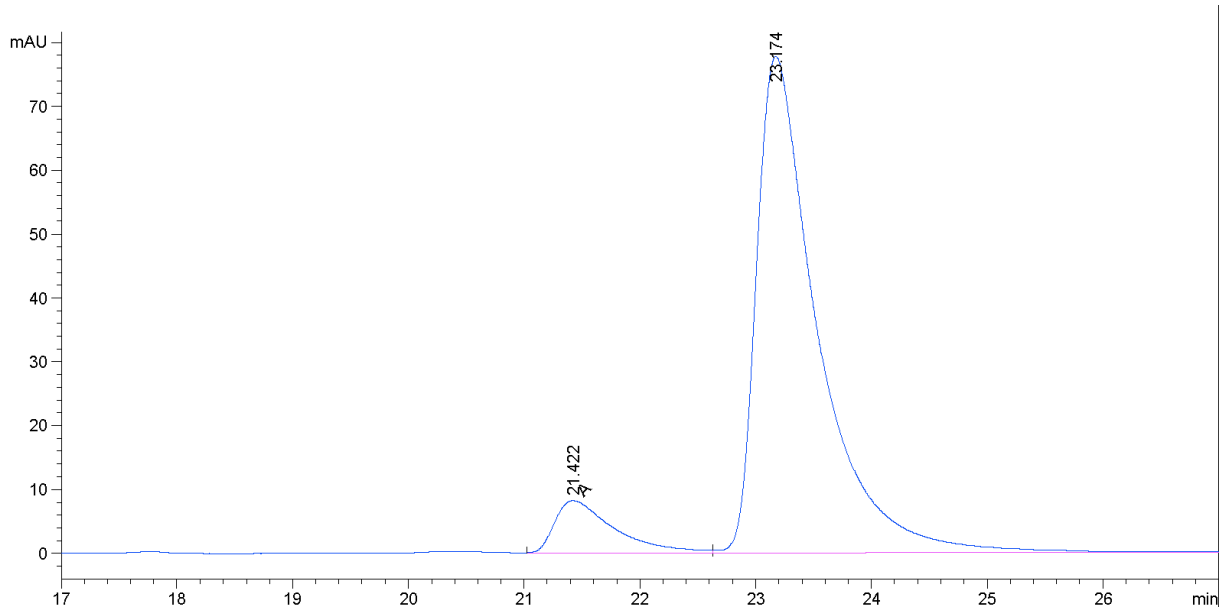
Signal 1: DAD1 A, Sig=254,4 Ref=360,100

Peak #	RetTime [min]	Type	Width [min]	Area [mAU*s]	Height [mAU]	Area %
1	19.295	MF	0.4801	1873.98438	65.05532	49.1596
2	21.234	FM	0.5406	1938.05396	59.74950	50.8404

Totals : 3812.03833 124.80482

=====
*** End of Report ***

Table 3.2, Entry 1.



Data File C:\CHEM32\...H_08_2021-IC-90_10-HEPT_IPROH 2021-03-08 14-50-53\BD-05-57-02-THF.D
Sample Name: BD-05-57-02-THF

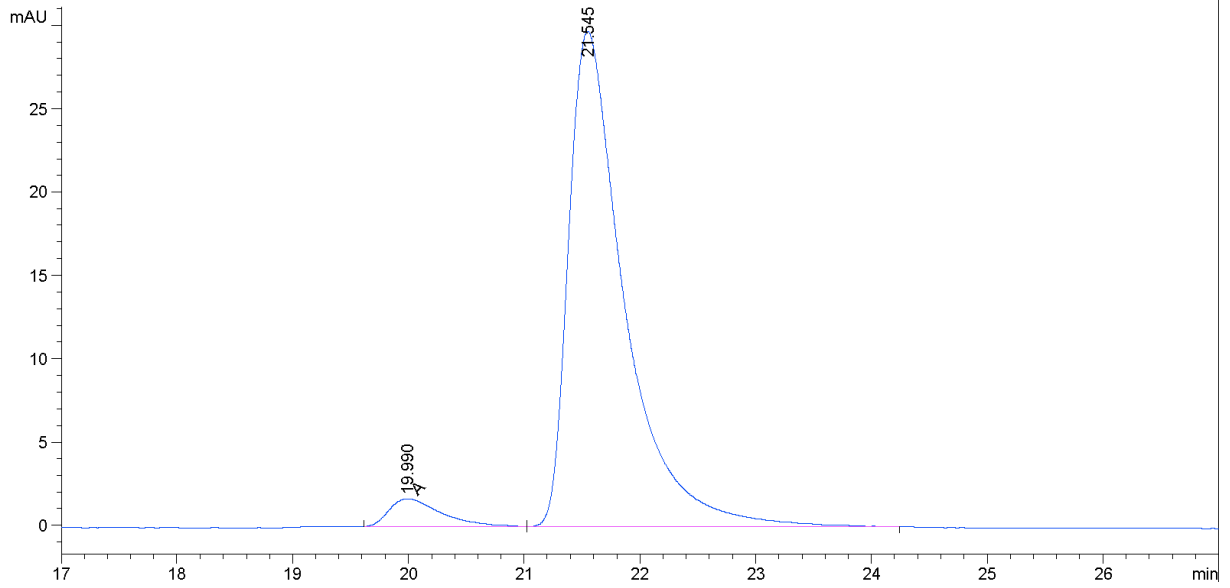
Signal 1: DAD1 A, Sig=254,4 Ref=360,100

Peak #	RetTime [min]	Type	Width [min]	Area [mAU*s]	Height [mAU]	Area %
1	21.422	MF	0.5890	288.81683	8.17191	9.1851
2	23.174	FM	0.6125	2855.60498	77.70459	90.8149

Totals : 3144.42181 85.87650

=====
*** End of Report ***

Table 3.2, Entry 2.



Data File C:\CHEM32\...1-IC-90_10-HEPT_IPROH 2021-04-01 11-50-35\BD-05-67-02-05-MINUS 20.D
Sample Name: BD-05-67-02-05-minus 20

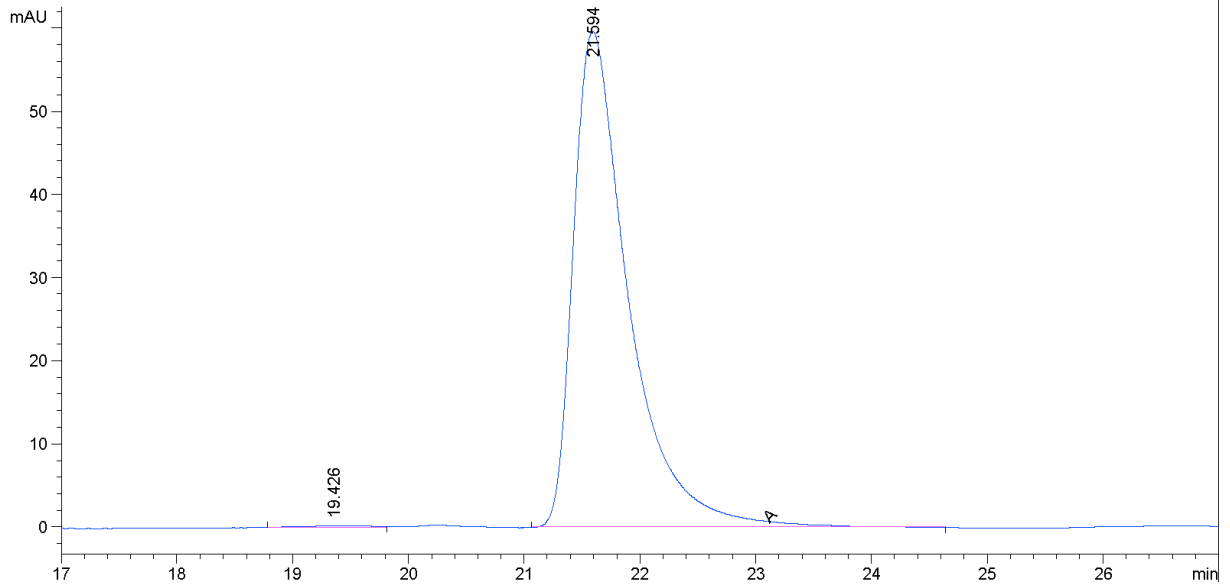
Signal 1: DAD1 A, Sig=254,4 Ref=360,100

Peak #	RetTime [min]	Type	Width [min]	Area [mAU*s]	Height [mAU]	Area %
1	19.990	MF	0.5251	52.69646	1.67254	4.9982
2	21.545	FM	0.5618	1001.60828	29.71511	95.0018

Totals : 1054.30473 31.38764

=====
*** End of Report ***

Table 3.2, Entry 3.



Data File C:\CHEM32\...1-IC-90_10-HEPT_IPROH 2021-04-01 11-50-35\BD-05-67-02-03-MINUS 40.D
Sample Name: BD-05-67-02-03-minus 40

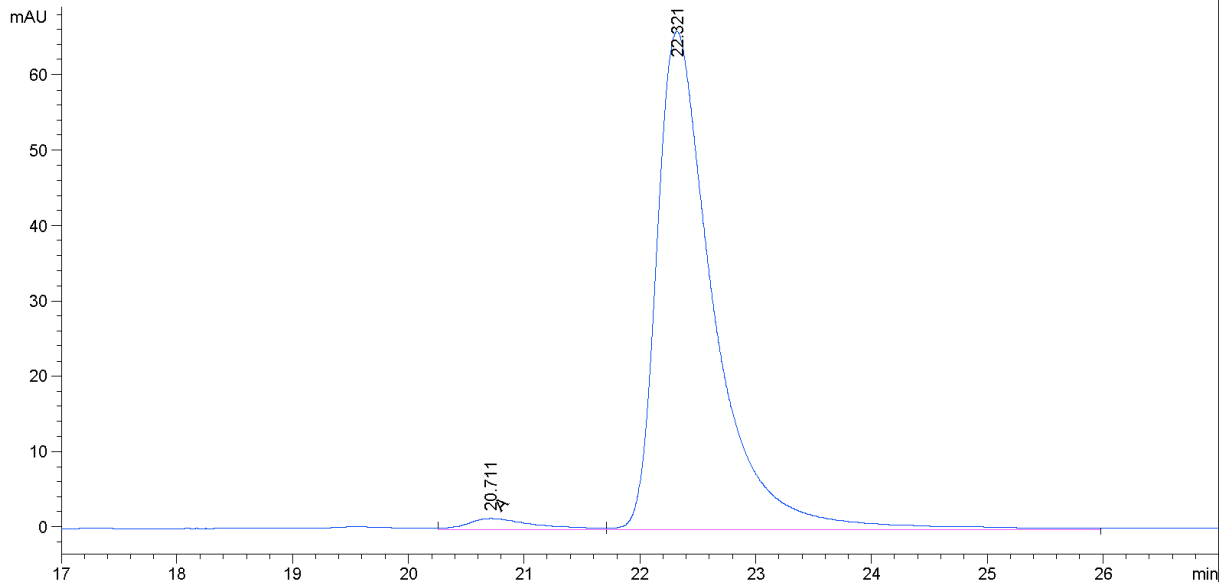
Signal 1: DAD1 A, Sig=254,4 Ref=360,100

Peak #	RetTime [min]	Type	Width [min]	Area [mAU*s]	Height [mAU]	Area %
1	19.426	MM	0.7053	9.64356	2.27879e-1	0.4885
2	21.594	MM	0.5499	1964.51282	59.54066	99.5115

Totals : 1974.15637 59.76854

=====
*** End of Report ***

Table 3.2, Entry 4.



Data File C:\CHEM32\...90_10-HEPT_IPROH 2021-04-14 12-38-38\BD-05-71-02-1P5 ELECTROPHILE.D
 Sample Name: BD-05-71-02-1.5 ELECTROPHILE

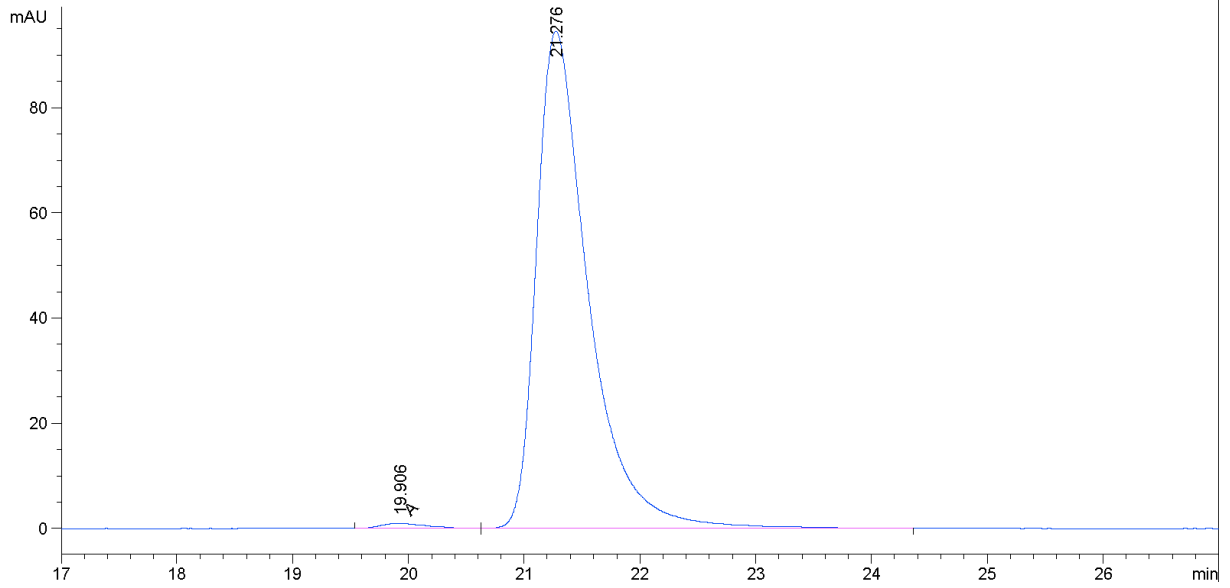
Signal 1: DAD1 A, Sig=254,4 Ref=360,100

Peak #	RetTime [min]	Type	Width [min]	Area [mAU*s]	Height [mAU]	Area %
1	20.711	MF	0.6549	56.85460	1.44684	2.4477
2	22.321	FM	0.5714	2265.90088	66.09464	97.5523

Totals : 2322.75548 67.54148

=====
 *** End of Report ***

Table 3.2, Entry 5.



Data File C:\CHEM32\...IC-90_10-DUPLICATES 2021-04-16 12-14-19\BD-05-71-01-R2-HPLC-02-P1.D
 Sample Name: BD-05-71-01-R2-HPLC-02-P1

Signal 1: DAD1 A, Sig=254,4 Ref=360,100

Peak #	RetTime [min]	Type	Width [min]	Area [mAU*s]	Height [mAU]	Area %
1	19.906	MF	0.4761	25.83721	9.04425e-1	0.8689
2	21.276	FM	0.5199	2947.74414	94.50058	99.1311

Totals : 2973.58135 95.40500

=====
 *** End of Report ***

References

- (1) Vitaku, E.; Smith, D. T.; Njardarson, J. T. Analysis of the Structural Diversity, Substitution Patterns, and Frequency of Nitrogen Heterocycles among U.S. FDA Approved Pharmaceuticals. *J. Med. Chem.* **2014**, *57* (24), 10257–10274. <https://doi.org/10.1021/jm501100b>.
- (2) Blakemore, D. C.; Castro, L.; Churcher, I.; Rees, D. C.; Thomas, A. W.; Wilson, D. M.; Wood, A. Organic Synthesis Provides Opportunities to Transform Drug Discovery. *Nature Chemistry.* **2018**, pp 383–394. <https://doi.org/10.1038/s41557-018-0021-z>.
- (3) Zhang, Z.; Collum, D. B. Evans Enolates: Structures and Mechanisms Underlying the Aldol Addition of Oxazolidinone-Derived Boron Enolates. *J. Org. Chem.* **2017**, *82* (14), 7595–7601. <https://doi.org/10.1021/acs.joc.7b01365>.
- (4) Joshi, M. S.; Pigge, F. C. Dearomatized Alkylidene Dihydropyridines as Substrates for Mizoroki-Heck Cyclizations. *ACS Catal.* **2016**, *6* (7), 4465–4469. <https://doi.org/10.1021/acscatal.6b01151>.
- (5) Lansakara, A. I.; Mariappan, S. V. S.; Pigge, F. C. Alkylidene Dihydropyridines As Synthetic Intermediates: Model Studies toward the Synthesis of the Bis(Piperidine) Alkaloid Xestoproxamine C. *J. Org. Chem.* **2016**, *81* (21), 10266–10278. <https://doi.org/10.1021/acs.joc.6b01269>.
- (6) Joshi, M. S.; Pigge, F. C. Construction of 1,2,4-Triazole Derivatives via Cyclocondensation of Alkylidene Dihydropyridines and Aryldiazonium Salts. *Org. Lett.* **2016**, *18* (22), 5916–5919. <https://doi.org/10.1021/acs.orglett.6b03019>.
- (7) Wasfy, N.; Rasheed, F.; Robidas, R.; Hunter, I.; Shi, J.; Doan, B.; Legault, C. Y.; Fishlock, D.; Orellana, A. Pyridylic Anions Are Soft Nucleophiles in the Palladium-Catalyzed C(Sp³)-H Allylation of 4-Alkylpyridines. *Chem. Sci.* **2021**, *12* (4), 1503–1512. <https://doi.org/10.1039/d0sc03304a>.
- (8) Wasfy, N.; Doan, B.; Rasheed, F.; Fishlock, D.; Orellana, A. Palladium-Catalyzed, Mild Dehydrogenation of 4-Alkylpyridines. *ACS Catal.* **2021**, *11* (6), 3251–3256. <https://doi.org/10.1021/acscatal.0c05209>.
- (9) Shi, J.; Sayyad, A.; Fishlock, D.; Orellana, A. Alkylidene Dihydropyridines Are Surrogates for Pyridylic Anions in the Conjugate Addition to α,β -Unsaturated

- Ketones. *Org. Lett.* **2022**, *24* (1), 48–52.
<https://doi.org/10.1021/acs.orglett.1c03615>.
- (10) Roughley, S. D.; Jordan, A. M. The Medicinal Chemist's Toolbox: An Analysis of Reactions Used in the Pursuit of Drug Candidates. *Journal of Medicinal Chemistry*. 2011, pp 3451–3479. <https://doi.org/10.1021/jm200187y>.
- (11) Lynch, J. E.; Choi, W. B.; Churchill, H. R. O.; Volante, R. P.; Reamer, R. A.; Ball, R. G. Asymmetric Synthesis of CDP840 by Jacobsen Epoxidation. An Unusual Syn Selective Reduction of an Epoxide. *J. Org. Chem.* **1997**, *62* (26), 9223–9228. <https://doi.org/10.1021/jo971476c>.
- (12) Lessa, J. A.; Mendes, I. C.; Da Silva, P. R. O.; Soares, M. A.; Dos Santos, R. G.; Speziali, N. L.; Romeiro, N. C.; Barreiro, E. J.; Beraldo, H. 2-Acetylpyridine Thiosemicarbazones: Cytotoxic Activity in Nanomolar Doses against Malignant Gliomas. *Eur. J. Med. Chem.* **2010**, *45* (12), 5671–5677. <https://doi.org/10.1016/j.ejmech.2010.09.021>.
- (13) Reis, D. C.; Pinto, M. C. X.; Souza-Fagundes, E. M.; Wardell, S. M. S. V.; Wardell, J. L.; Beraldo, H. Antimony(III) Complexes with 2-Benzoylpyridine-Derived Thiosemicarbazones: Cytotoxicity against Human Leukemia Cell Lines. *Eur. J. Med. Chem.* **2010**, *45* (9), 3904–3910. <https://doi.org/10.1016/j.ejmech.2010.05.044>.
- (14) Cheng, Q.; Tu, H. F.; Zheng, C.; Qu, J. P.; Helmchen, G.; You, S. L. Iridium-Catalyzed Asymmetric Allylic Substitution Reactions. *Chem. Rev.* **2019**, No. 119, 1855–1969. <https://doi.org/10.1021/acs.chemrev.8b00506>.
- (15) Wang, J.; Zhang, C.; Ye, X. Q.; Du, W.; Zeng, S.; Xu, J. H.; Yin, H. An Efficient and Practical Aerobic Oxidation of Benzylic Methylenes by Recyclable: N - Hydroxyimide. *RSC Adv.* **2021**, *11* (5), 3003–3011. <https://doi.org/10.1039/d0ra10475b>.
- (16) Nicolaou, K. C.; Montagnon, T.; Baran, P. S.; Zhong, Y. L. Iodine(V) Reagents in Organic Synthesis. Part 4. o-Iodoxybenzoic Acid as a Chemospecific Tool for Single Electron Transfer-Based Oxidation Processes. *J. Am. Chem. Soc.* **2002**, *124* (10), 2245–2258. <https://doi.org/10.1021/ja012127+>.
- (17) Nicolaou, K. C.; Baran, P. S.; Zhong, Y. L. Selective Oxidation at Carbon Adjacent

- to Aromatic Systems with IBX. *J. Am. Chem. Soc.* **2001**, *123* (13), 3183–3185.
<https://doi.org/10.1021/ja004218x>.
- (18) Dunn, P. J. The Importance of Green Chemistry in Process Research and Development. *Chem. Soc. Rev.* **2012**, *41* (4), 1452–1461.
<https://doi.org/10.1039/c1cs15041c>.
- (19) Ren, L.; Wang, L.; Lv, Y.; Li, G.; Gao, S. Synergistic H₄Ni-AcOH Catalyzed Oxidation of the Csp³-H Bonds of Benzylpyridines with Molecular Oxygen. *Org. Lett.* **2015**, *17* (9), 2078–2081. <https://doi.org/10.1021/acs.orglett.5b00602>.
- (20) Urgoitia, G.; Sanmartin, R.; Herrero, M. T.; Domínguez, E. An Outstanding Catalyst for the Oxygen-Mediated Oxidation of Arylcarbinols, Arylmethylene and Arylacetylene Compounds. *Chem. Commun.* **2015**, *51* (23), 4799–4802.
<https://doi.org/10.1039/c5cc00750j>.
- (21) Hruszkewycz, D. P.; Miles, K. C.; Thiel, O. R.; Stahl, S. S. Co/NHPI-Mediated Aerobic Oxygenation of Benzylic C-H Bonds in Pharmaceutically Relevant Molecules. *Chem. Sci.* **2017**, *8* (2), 1282–1287.
<https://doi.org/10.1039/c6sc03831j>.
- (22) Wang, H.; Liu, J.; Qu, J. P.; Kang, Y. B. Overcoming Electron-Withdrawing and Product-Inhibition Effects by Organocatalytic Aerobic Oxidation of Alkylpyridines and Related Alkylheteroarenes to Ketones. *J. Org. Chem.* **2020**, *85* (5), 3942–3948. <https://doi.org/10.1021/acs.joc.9b03205>.
- (23) De Houwer, J.; Abbaspour Tehrani, K.; Maes, B. U. W. Synthesis of Aryl(Di)Azinyl Ketones through Copper- and Iron-Catalyzed Oxidation of the Methylene Group of Aryl(Di)Azinylmethanes. *Angew. Chemie - Int. Ed.* **2012**, *51* (11), 2745–2748.
<https://doi.org/10.1002/anie.201108540>.
- (24) Sterckx, H.; De Houwer, J.; Mensch, C.; Caretti, I.; Tehrani, K. A.; Herrebout, W. A.; Van Doorslaer, S.; Maes, B. U. W. Mechanism of the Cu II -Catalyzed Benzylic Oxygenation of (Aryl)(Heteroaryl)Methanes with Oxygen. *Chem. Sci.* **2016**, *7* (1), 346–357. <https://doi.org/10.1039/c5sc03530a>.
- (25) Liu, J.; Zhang, X.; Yi, H.; Liu, C.; Liu, R.; Zhang, H.; Zhuo, K.; Lei, A. Chloroacetate-Promoted Selective Oxidation of Heterobenzylic Methylenes under Copper Catalysis. *Angew. Chemie - Int. Ed.* **2015**, *54* (4), 1261–1265.

- <https://doi.org/10.1002/anie.201409580>.
- (26) Cooper, J. C.; Luo, C.; Kameyama, R.; Van Humbeck, J. F. Combined Iron/Hydroxytriazole Dual Catalytic System for Site Selective Oxidation Adjacent to Azaheterocycles. *J. Am. Chem. Soc.* **2018**, *140* (4), 1243–1246.
<https://doi.org/10.1021/jacs.7b12864>.
- (27) Gao, X.; Han, S.; Zheng, M.; Liang, A.; Li, J.; Zou, D.; Wu, Y.; Wu, Y. Transition-Metal-Free Oxidation of Benzylic C-H Bonds of Six-Membered N-Heteroaromatic Compounds. *J. Org. Chem.* **2019**, *84* (7), 4040–4049.
<https://doi.org/10.1021/acs.joc.9b00035>.
- (28) Recupero, F.; Punta, C. Free Radical Functionalization of Organic Compounds Catalyzed by N-Hydroxyphthalimide. *Chem. Rev.* **2007**, *107* (9), 3800–3842.
<https://doi.org/10.1021/cr040170k>.
- (29) Konya, K. G.; Paul, T.; Lin, S.; Luszyk, J.; Ingold, K. U. Laser Flash Photolysis Studies on the First Superoxide Thermal Source. First Direct Measurements of the Rates of Solvent-Assisted 1,2-Hydrogen Atom Shifts and a Proposed New Mechanism for This Unusual Rearrangement. *J. Am. Chem. Soc.* **2000**, *122* (31), 7518–7527. <https://doi.org/10.1021/ja993570b>.
- (30) Su, Y.; Zhang, L.; Jiao, N. Utilization of Natural Sunlight and Air in the Aerobic Oxidation of Benzyl Halides. *Org. Lett.* **2011**, *13* (9), 2168–2171.
<https://doi.org/10.1021/ol2002013>.
- (31) Wasfy, N.; Doan, B.; Rasheed, F.; Fishlock, D.; Orellana, A. Palladium-Catalyzed, Mild Dehydrogenation of 4-Alkylpyridines. *ACS Catal.* **2021**, *11* (6), 3251–3256.
<https://doi.org/10.1021/acscatal.0c05209>.
- (32) Takeuchi, R.; Kashio, M. Highly Selective Allylic Alkylation with a Carbon Nucleophile at the More Substituted Allylic Terminus Catalyzed by an Iridium Complex: An Efficient Method for Constructing Quaternary Carbon Centers. *Angew. Chemie (International Ed. English)* **1997**, *36* (3), 263–265.
<https://doi.org/10.1002/anie.199702631>.
- (33) Bartels, B.; García-Yebra, C.; Rominger, F.; Helmchen, G. Iridium-Catalysed Allylic Substitution: Stereochemical Aspects and Isolation of Ir(III) Complexes Related to the Catalytic Cycle. *Eur. J. Inorg. Chem.* **2002**, No. 10, 2569–2586.

[https://doi.org/10.1002/1099-0682\(200210\)2002:10<2569::AID-EJIC2569>3.0.CO;2-5](https://doi.org/10.1002/1099-0682(200210)2002:10<2569::AID-EJIC2569>3.0.CO;2-5).

- (34) Janssen, J. P.; Helmchen, G. First Enantioselective Alkylations of Monosubstituted Allylic Acetates Catalyzed by Chiral Iridium Complexes. *Tetrahedron Lett.* **1997**, *38* (46), 8025–8026. [https://doi.org/10.1016/S0040-4039\(97\)10220-9](https://doi.org/10.1016/S0040-4039(97)10220-9).
- (35) Kiener, C. A.; Shu, C.; Incarvito, C.; Hartwig, J. F. Identification of an Activated Catalyst in the Iridium-Catalyzed Allylic Amination and Etherification. Increased Rates, Scope, and Selectivity. *J. Am. Chem. Soc.* **2003**, *125* (47), 14272–14273. <https://doi.org/10.1021/ja038319h>.
- (36) Defieber, C.; Ariger, M. A.; Moriel, P.; Carreira, E. M. Iridium-Catalyzed Synthesis of Primary Allylic Amines from Allylic Alcohols: Sulfamic Acid as Ammonia Equivalent. *Angew. Chemie - Int. Ed.* **2007**, *46* (17), 3139–3143. <https://doi.org/10.1002/anie.200700159>.
- (37) Rössler, S. L.; Petrone, D. A.; Carreira, E. M. Iridium-Catalyzed Asymmetric Synthesis of Functionally Rich Molecules Enabled by (Phosphoramidite, Olefin) Ligands. *Acc. Chem. Res.* **2019**, *52* (9), 2657–2672. <https://doi.org/10.1021/acs.accounts.9b00209>.
- (38) Rössler, S. L.; Krautwald, S.; Carreira, E. M. Study of Intermediates in Iridium-(Phosphoramidite, Olefin)-Catalyzed Enantioselective Allylic Substitution. *J. Am. Chem. Soc.* **2017**, *139* (10), 3603–3606. <https://doi.org/10.1021/jacs.6b12421>.
- (39) Ma, Z.; Lin, D. C. H.; Sharma, R.; Liu, J.; Zhu, L.; Li, A. R.; Kohn, T.; Wang, Y.; Liu, J.; Bartberger, M. D.; Medina, J. C.; Zhuang, R.; Li, F.; Zhang, J.; Luo, J.; Wong, S.; Tonn, G. R.; Houze, J. B. Discovery of the Imidazole-Derived GPR40 Agonist AM-3189. *Bioorganic Med. Chem. Lett.* **2016**, *26* (1), 15–20. <https://doi.org/10.1016/j.bmcl.2015.11.050>.
- (40) Trost, B. M.; Thaisrivongs, D. A. Strategy for Employing Unstabilized Nucleophiles in Palladium-Catalyzed Asymmetric Allylic Alkylations. *J. Am. Chem. Soc.* **2008**, *130* (43), 14092–14093. <https://doi.org/10.1021/ja806781u>.
- (41) Wasfy, Nour; Doan, Brian; Fishlock, Dan; Orellana, A. Palladium-Catalyzed, Mild Dehydrogenation of 4-Alkylpyridines. *ACS Catal.* **2020**, *Submitted*.

- (42) Zhang, X.; Yang, C.; Gao, H.; Wang, L.; Guo, L.; Xia, W. Reductive Arylation of Aliphatic and Aromatic Aldehydes with Cyanoarenes by Electrolysis for the Synthesis of Alcohols. *Org. Lett.* **2021**, *23* (9), 3472–3476. <https://doi.org/10.1021/acs.orglett.1c00920>.
- (43) Guo, F.; Dhakal, R. C.; Dieter, R. K. Conjugate Addition Reactions of N - Carbamoyl-4-Pyridones and 2,3-Dihydropyridones with Grignard Reagents in the Absence of Cu(I) Salts. *J. Org. Chem.* **2013**, *78* (17), 8451–8464. <https://doi.org/10.1021/jo400936z>.
- (44) Yang, J.; Liu, J.; Ge, Y.; Huang, W.; Neumann, H.; Jackstell, R.; Beller, M. Direct and Selective Synthesis of Adipic and Other Dicarboxylic Acids by Palladium-Catalyzed Carbonylation of Allylic Alcohols. *Angew. Chemie - Int. Ed.* **2020**, *59* (46), 20394–20398. <https://doi.org/10.1002/anie.202008916>.
- (45) Soheili, A.; Tambar, U. K. Tandem Catalytic Allylic Amination and [2,3]-Stevens Rearrangement of Tertiary Amines. *J. Am. Chem. Soc.* **2011**, *133* (33), 12956–12959. <https://doi.org/10.1021/ja204717b>.